Radiochemical Studies Relevant to Cyclotron Production of the Radionuclides ^{71,72}As, ^{68}Ge/^{68}Ga and ^{76,77,80m}Br

Inaugural – Dissertation

zur

Erlangung des Doktorgrades

der Mathematisch-Naturwissenschaftlichen Fakultät

der Universität zu Köln

vorgelegt von

Mohamed Mostafa Mostafa Shehata

aus Kairo, Ägypten

Druckerei der Forschungszentrum Jülich GmbH

2011

Berichterstatter: Prof. Dr. Dr. h.c. mult. S. M. Qaim

Prof. Dr. Heinz H. Coenen

Tag der mündlichen Prüfung: 26.05.2011

Die vorliegende Arbeit wurde in der Zeit von April 2007 bis März 2011 am Institut für Neurowissenschaften und Medizin, INM-5: Nuklearchemie, der Forschungszentrum Jülich GmbH, unter der Anleitung von Herrn Prof. Dr. Dr. h.c. mult. S. M. Qaim durchgeführt.

Abstract

The radionuclides ^{71,72,73,74}As, ^{68}Ge/^{68}Ga and ^{76,77,80m}Br are gaining considerable interest in nuclear medicine. A method for the separation of no-carrier-added arsenic radionuclides from the bulk amount of proton-irradiated GeO_2 target as well as from coproduced radiogallium was developed. The extraction of radioarsenic by different organic solvents from acid solutions containing alkali iodide was studied and optimized. The influence of the concentration of various acids (HCl, $HClO_4$, HNO_3, HBr, H_2SO_4) as well as of KI was studied using cyclohexane. The practical application of the optimized procedure in the production of ^{71}As and ^{72}As is demonstrated. The batch yields achieved were in the range of 75–84% of the theoretical values.

The radiochemical separation of radiogallium from radiogermanium was studied using ion exchange chromatography (Amberlite IR-120) and solvent extraction (Aliquat 336 in o-xylene). At first optimized methods for the separation of no-carrier-added ^{68}Ge/^{69}Ge formed via the ^{nat}Ga(p,xn)^{69}Ge process in a Ga_2O_3 target and for n.c.a. ^{67}Ga formed via the ^{nat}Zn(p,xn)^{67}Ga reaction in a Zn target were developed. Using those radionuclides as tracers several factors affecting the separation of radiogallium from radiogermanium were studied and for each procedure the optimum conditions were determined. The solvent extraction using Aliquat 336 was found to be more suitable and was adapted to the separation of n.c.a. ^{68}Ga from its parent n.c.a. ^{68}Ge. The quality of the product thus obtained is discussed.

The separation of no-carrier-added radiobromine and no-carrier-added radiogallium from proton irradiated ZnSe target was studied in detail. The adsorption behaviour of n.c.a. radiobromine, n.c.a. radiogallium, zinc and selenium towards the cation-exchange resin Amberlyst 15, in H^+ form, and towards the anion-exchange resin Dowex 1X10 in Cl^- and OH^- forms, was investigated. The elution of n.c.a. radiobromine and n.c.a. radiogallium was studied using different solvents. Additionally separation of n.c.a. radiobromine was also done via solvent extraction using TOA in o-xylene. Finally an optimized procedure applicable to the production of ^{77}Br and ^{67}Ga was developed, and the quality control of the products was done.

The nuclear reaction cross section of the Auger electron emitting radionuclide ^{80m}Br ($T_{1/2}$ =4.4 h), was determined for its production using enriched ^{80}Se targets. Thin ^{80}Se samples were irradiated with incident protons of energies up to 18 MeV and the induced radioactivity was measured *via* nondestructive γ-ray spectrometery, allowing the determination and extension of the excitation function of the ^{80}Se(p,n)^{80m}Br reaction. The possible thick target yield was calculated and the energy range for production is discussed, especially with regard to the yield and radionuclidic purity of the produced radionuclide.

Kurzzusammenfassung

Die Radionuklide ^{71,72,73,74}As, ^{68}Ge/^{68}Ga und ^{76,77,80m}Br gewinnen großes Interesse in der Nuklearmedizin. Ein Verfahren zur Abtrennung von nicht-geträgerten Arsen-Radionukliden aus den großen Mengen des mit Protonenbestrahlte GeO_2-Targets sowie aus koproduzierten Radiogalliumisotopen wurde entwickelt. Die Gewinnung von Radioarsen mittels verschiedener organischer Lösungsmitteln aus sauren Lösungen unter Zusatz von Alkalijodid wurde untersucht und optimiert. Der Einfluss der Konzentration verschiedener Säuren (HCl, $HClO_4$, HNO_3, HBr, H_2SO_4) sowie des KI wurde auf die Extraktion mit Cyclohexan untersucht. Die praktische Anwendung des optimierten Verfahrens bei der Produktion von ^{71}As und ^{72}As wurde demonstriert. Die Gesamtausbeuten lagen im Bereich von 75-84% der theoretischen Werte.

Die radiochemische Trennung von Radiogallium aus Radiogermanium wurde mittels Ionenaustausch-Chromatographie (Amberlite IR-120) und Solventextraktion mit Aliquat 336 in o-Xylol untersucht. Dazu wurden zunächst der Radiotracer ^{69}Ge aus einem bestrahlten Ga_2O_3-Target und des ^{67}Ga aus einem Zn-Target abgetrennt. Sie wurden durch die Kernreaktion ^{nat}Ga (p,xn)^{69} Ge bzw ^{nat}Zn (p,xn)^{67}Ga. hergestellt. Mehrere Faktoren, die die Trennung von Radiogallium aus Radiogermanium beeinflussen wurden untersucht und für jedes Verfahren werden die optimalen Bedingungen ermittelt. Die Lösungsmittelextraktion mit Aliquat 336 erwies sich als besser geeignet und wurde deshalb zur Trennung von ^{68}Ga aus dem Mutternuklid ^{68}Ge herangezogen. Die Qualität des so erhaltenen Produkts wird diskutiert.

Die Trennung von nicht-geträgertem Radiobrom und Radiogallium aus dem bestrahlten ZnSe-Target wurde entwickelt. Dazu wurde das Adsorptionsverhalten von Radiobrom, Radiogallium, Zink und von Selen auf dem Kationenaustauscher Amberlyst 15, in H^+ Form sowie dem Anionenaustauscher Dowex 1x10 in Cl^- und OH^- Formen, untersucht. Die Elution des Radiobroms und des Radiogalliums wurde mit Hilfe verschiedener Lösungsmittel verfolgt. Zusätzlich wurde die Trennung von Radiobrom über die Lösungsmittelextraktion mit TOA in o-Xylol durchgeführt. Schließlich wurde ein optimiertes Verfahren zur Herstellung von ^{77}Br und ^{67}Ga entwickelt, und die Qualitätskontrolle der Produkte wurde durchgeführt.

Die Kernreaktionsdaten zur Produktion des Auger-Elektronen-emittierenden Radionuklides ^{80m}Br ($T_{1/2}$ = 4,4 h) wurden unter Anwendung des angereicherten ^{80}Se als Targetmaterial bestimmt. Dünne ^{80}Se- Proben wurden mit einfallenden Protonen mit Energien bis zu 18 MeV bestrahlt und die induzierte Radioaktivität wurde durch zerstörungsfreie γ-Spektroskopie gemessen, so dass die Bestimmung und Erweiterung der Anregungsfunktion der Kernreaktion ^{80}Se(p,n)^{80m}Br erfolgen konnte. Die integrale Ausbeute wurde berechnet und die geeigneten Energiebereiche für die Produktion wurden ermittelt, insbesondere im Hinblick auf die Ausbeute und die radionuklidische Reinheit des produzierten Radionuklids.

Contents

List of Figures

List of Tables

1. Introduction

1.1 Discovery of Radioactivity

Radioactivity is the process of spontaneous decay and transformation of unstable atomic nuclei, which is accompanied by the emission of charged particles and/or electromagnetic radiation. Radioactivity was discovered by Henri Becquerel in 1896 in Paris, while investigating the radiation emitted by uranium minerals, one year after the discovery of X-rays by W.C. Roentgen. He found that photographic plates were blackened in the absence of light, if they were in contact with certain minerals. Two years later (1898), Marie Curie in France and G. C. Schmidt in Germany discovered similar properties in thorium. Marie Curie found differences in the radioactivity of uranium and thorium and concluded that these elements must contain unknown radioactive elements. Together with her husband, Pierre Curie, she discovered polonium in 1898 and radium later in the same year. Radioactivity is a property of matter and for the detection of radioactive substances suitable detectors are needed, e.g. Geiger-Müller counters or photographic emulsions.

The naturally occurring radioactive substances were the only ones available for study until 1934. In January of that, year I. Curie and F. Joliot announced that boron and aluminum could be made radioactive by bombardment with α-ray from polonium. The positron had been discovered only two years earlier by C.D. Anderson as a component of the cosmic radiation. A number of laboratories quickly found that positrons could be produced in light elements by α-ray bombardment. Much earlier in 1919 Rutherford had shown nuclear transmutations by α-particle bombardment, and the new phenomenon of induced radioactivity was therefore quickly understood in terms of the production of new unstable nuclei.

At the time, that artificial radioactivity was discovered several laboratories had developed and put into operation devices for the acceleration of hydrogen ions and helium ions to energies at which nuclear transmutations could occur. Furthermore, the discovery of the neutron in 1932 and the isolation of deuterium in 1933 made available two additional bombarding particles that turned out to be especially useful for the production of induced radioactivity. About the same time, Ernest Lawrence built the first working cyclotron in 1931 capable of accelerating protons, deuterons, or helium ions (alpha particles) to energies which were enough to penetrate atomic nuclei and thereby produce numerous stable and radioactive

isotopes that would find many peaceful applications in improving the wellbeing of humanity all over the world. By 1940 the cyclotron developed by Lawrence and his coworkers would produce artificially as many as 223 radioactive isotopes, many of which would prove to be of immediate and immense value in medicine and studies in the biological sciences. The discovery of nuclear fission by O. Hahn and F. Strassmann gave further strong impetus to the study of new radioactive products. A second major source of artificial radionuclides has become available since the development of the first successful atomic pile chain reactor in 1942. Reactor-produced radionuclides became available for public distribution since 1946. The subsequent development of nuclear reactors opened the way for their widespread applications in such diverse fields as chemistry, physics, biology, medicine, agriculture and engineering. Charts and tabulations of the properties of radioactive species are available. There are many books dealing with the radioactivity and nuclear reactions in detail (Loveland et al., 2006; Choppin et al., 2002; Lieser, 2001).

1.2 Nuclear Reaction

When two nuclei approach each other, there are various possibilities to interact with each other, depending on the kinetic energy of the accelerated nucleus. Those interactions can be divided into scattering processes and nuclear reactions. Generally, the interacting nuclei are classified as the target nucleus and the projectile. If the kinetic energy of the projectile is too low to penetrate the target nucleus, it will be scattered elastically or inelastically, thereby transferring excitation energy to the target nucleus in the latter case. If the energy of the interacting nucleus is high enough, a nuclear reaction may occur resulting in a change of the atomic and/or mass number of the target nucleus. Consider the following reaction (see Fig. 1.1).

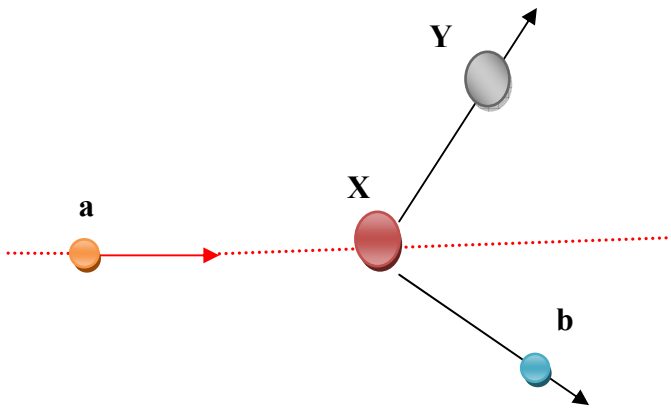

Fig. 1.1: Schematic representation of a nuclear reaction.

$$ {}^{A}_{Z}X + a \rightarrow {}^{A^{\#}}_{Z^{\#}}Y + b + Q \qquad 1.1 $$

where X is the stable target nuclide (at rest), a is an accelerated particle (projectile), Y is the product radionuclide, b is the particle or photon emitted, and Q is the energy released or absorbed. Two important characteristics of nuclear reactions are:

- The minimum projectile energy required to induce such a nuclear reaction
- The probability that a reaction will proceed

As the projectile is slowed down when traversing the matter, the latter characteristic should be known as a function of the projectile energy.

1.2.1 Q-Value and Threshold Energy

As mentioned above, the Q-value is the energy released or absorbed by one single nuclear reaction. It is related to the difference between the resting masses of the reactants and products as given in Eq. (1.2).

$$ Q = [(M_X + m_a) - (M_Y + m_b)]c^2 \qquad 1.2 $$

where M_x is the mass of the target nuclide (at rest), m_a the mass of the projectile, M_Y the mass of the radionuclide formed and m_b the mass of the particle emitted.

A nuclear reaction can be exoergic (Q > 0), i.e. accompanied by liberation of energy or endoergic (Q < 0), i.e. absorption of energy is needed to start it. For an endoergic reaction (Q < 0) the bombarding particle should have a minimum energy value which is slightly higher than -Q. This is characterized by the threshold energy, which is the minimum kinetic energy of the colliding particles above which the reaction becomes possible from the energy point of view. Note that the threshold energy, E_{thr}, always exceeds the reaction energy Q, where it is given by the following equation:

$$ E_{thr} = -|Q| \left(1 + \frac{m_a}{M_x}\right) \qquad 1.3 $$

1.2.2 Coulomb Barrier

The Coulomb barrier determines the minimum energy needed for a charged particle to induce a nuclear reaction. The Coulombic repulsive force between the target nucleus and the charged particle dominates at large distances and increases when the charged particle approaches the target nucleus. At some particular distance, the attractive nuclear force balances the Coulomb repulsive force. Due to the Coulomb potential between the projectile and the target nucleus, additional energy should be added to the projectile energy, namely E_c. This energy depends on the charge of the projectile ($Z_a e$) and of the target nucleus ($Z_x e$)

$$E_c = \frac{Z_a Z_x e^2}{R_o(A_a^{1/3} + A_x^{1/3})} \quad 1.4$$

where R_o=1.2 x 10^{-13} cm, and A is the mass number

There is a certain probability that the incident charged particle is able to penetrate the Coulomb barrier even if $E_a < E_c$. This phenomenon is called *tunneling effect* and is explained by quantum mechanics. In general, a reaction with Q < 0 occurs if the bombarding particle has at least a starting energy E_{thr} or E_c, whichever is higher in the laboratory system.

1.2.3 Nuclear Reaction Cross Section

The nuclear reaction cross section represents the probability with which a projectile and a target nucleus interact according to a specific reaction channel, and is comparable with the rate constant of a bimolecular chemical reaction. To derive simple formula of the reaction cross-section, consider the general equation for a binuclear reaction

$$A + x \rightarrow B + y \quad 1.5$$

The production rate of the nuclide B is given by

$$\frac{dN_B}{dt} = \sigma \quad \Phi \quad N_A \quad 1.6$$

where σ is the cross-section of the reaction, Φ is the flux density of the projectiles, and N_A is the number of atoms of the target nuclide A. The cross section is expressed in cm^2 or barns (=$10^{-24}cm^2$). This originates from the simple picture that the probability for a reaction between the target nucleus and the incident projectile particle is proportional to the geometric cross-section that the target nucleus presents to a beam of charge particles. The cross-section strongly depends on the incident particle energy as will be shown later.

1.2.4 Excitation Function

The excitation function indicates the absolute reaction cross-section as a function of the incident energy of the projectile. For charged particle induced reactions, where the projectiles need additional kinetic energy to overcome the potential barrier, the shape of the excitation function normally shows an increasing trend, reaching a maximum and then an asymptotic decline with the increasing energy.

The more commonly used technique for the determination of the excitation function is known as the ‘’ stacked-foil’’ or ‘’stacked-pellet’’ technique (Weinreich et al., 1974; Qaim et al., 1977); in which, a stack of thin target samples with monitor and absorber foils is irradiated, and the samples are measured individually. In Figure 1.2 a schematic view of a

stack of foils used for irradiation can be seen. Cross-section determination requires absolute activity measurement, absolute beam intensity monitoring and absolute energy measurement of the incident charged particles.

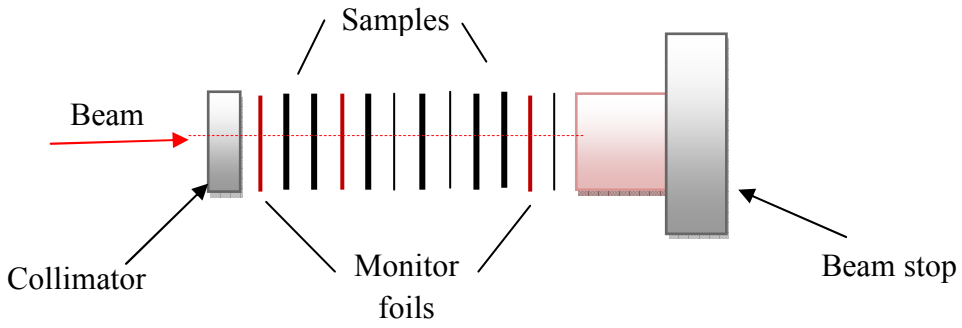

Fig. 1.2 : Irradiation of thin samples via the stacked-foil technique.

The absolute activity is calculated after measuring the count rate of each activated sample. By applying different corrections, (see experimental section) the absolute activity is obtained. From the measured absolute radioactivity, the cross-section is then obtained using the well-known activation formula:

$$\sigma = \frac{A_{EOB}}{\Phi \; N_X \; H \; (1 - e^{-\lambda t_B})} \qquad 1.7$$

where, A_{EOB} is the activity of the produced radionuclide, Φ the flux of the incident particles (number of particles/sec), N_x the number of target atoms/cm^2, H the percentage of target isotope in the element, σ the cross-section of the reaction (cm^2), λ the decay constant of the resulting nuclei (sec^{-1}) and t_B is the irradiation time (sec).

1.2.5 Nuclear Reaction Yield

The yield of a nuclear reaction is defined as the number of the product nuclei formed in the nuclear reaction. It is customary to express the number of radioactive nuclei in terms of the activity, and the number of incident particles in terms of the charge. Thus, the yield can be given as activity per Coulomb, in units of GBq/C.

The differential yield describes the production yield in a thin target, where the energy degradation can be described as an infinitesimal interval dE. In order to calculate the possible production yield in a thick target, the latter is considered to be a sum of thin targets. This way the yield is calculated by integrating the relevant differential yields over the energy range covered in the thick target, leading to the so-called integral yield (Y) of an irradiation

(Eq.1.8).

$$Y = \Phi \frac{N_A H}{M}(1 - e^{-\lambda t}) \int_{E_1}^{E_2} \left(\frac{dE}{dpx} \right)^{-1} \sigma(E) dE \qquad 1.8$$

where E_1= incident energy E_2= exit energy

$(dE/d\rho x)^{-1}$ = stopping power

1.3 Production of Radionuclides

Radionuclides can be produced by various routes, with the most common of these being the bombardment of the starting material or target by either neutrons or charged particles. Neutron bombardments are usually performed in the intense neutron flux inside a nuclear reactor. Charged particle bombardments are usually performed by accelerating ions in an accelerator (e.g. cyclotron) and directing the resulting beam onto a suitable target. The emphasis in this thesis is on cyclotron production of radionuclides.

1.3.1 Production of Radionuclides Using Reactors

In reactor production of radioisotopes, the most commonly used nuclear routes are (n,γ), (n,fission) and (n,charged particles) processes. The (n,γ) reaction has generally a high cross section at thermal neutron energies, so that the yield of the product is rather high (Qaim, 2010). However, a serious drawback of this process is the low specific radioactivity (i.e. the activity per unit mass of the element) which makes the radioisotope less suitable for medical application. Although the specific radioactivity can be improved through various methods (Qaim 2001a), this drawback generally remains. The fission process is a very suitable method to produce a large number of radionuclides in a no-carrier-added form. The chemical process involved, however, is rather extensive. The (n,p) and (n,α) reaction cross-sections are generally low; these processes are therefore used to produce only a few radioisotopes in the light mass element region. Since most therapeutic radionuclides are neutron rich β^--emitters, they are reactor produced.

1.3.2 Production of Radionuclides Using Cyclotrons

The various types of accelerators offer the possibility of applying a great variety of projectiles of different energies. The most frequently used projectiles are protons, deuterons and α-particles. Neutrons may be produced indirectly by nuclear reactions, γ-rays are generated as Bremsstrahlung in electron accelerators, and heavy ions are available in heavy ion accelerators. The most common charged-particle accelerator used for the production of radionuclides is the cyclotron. These machines accelerate light particles at energies that upon striking suitable targets can induce nuclear reactions producing radionuclides with extremely high specific activity (activity per unit mass of the element). Today a large number of cyclotrons are used worldwide for medical radioisotope production. Many small cyclotrons have been installed in hospital environments and are employed extensively for preparation of short-lived radionuclides with very high specific activities for direct use on site. The great advantage of accelerator produced radionuclides is the fact that the primary radionuclide of interest is usually a different element from that of the target, thus allowing for its chemical separation from the target material. This separation leads to a product of high specific activity.

Cyclotrons can be classified according to their maximum energy of acceleration, the type of accelerated particles and, consequently, the type of radionuclides that can be produced. Some terminological classification was given to commercial cyclotrons, etc. Other classification refers to the type of the accelerated charge as negative ion or positive ion machines. Table 1.1 gives categories of cyclotrons used for radionuclide production and their maximum energy of acceleration.

1.3.3 Radionuclide Generators

A radionuclide generator is a device for effective radiochemical separation of a short-lived daughter radionuclide formed by the decay of a long-lived parent radionuclide. The goal is to obtain the daughter in a form having the required radionuclidic and radiochemical purity. For practical reasons, most radionuclide generator systems that are useful for medical applications involve secular equilibrium, where the parent radionuclide has a half-life significantly longer than that of the daughter. Thus, the separation of the short-lived radionuclide can be repeated specifically on a periodic basis.

Table 1.1: Types of accelerators used in radionuclide production. (Qaim, 2001b; Qaim, 2003).

Classification	Characteristics	Energy [MeV]	Major radionuclides produced
Level I	Single particle* (d)	< 4	^{15}O
Level II	Single particle (p)	≤ 11	^{11}C, ^{13}N, ^{15}O,^{18}F
Level III	Single or two particle (p,d)	≤ 20	^{11}C, ^{13}N, ^{15}O,^{18}F (^{123}I, ^{67}Ga, ^{111}In)
Level IV	Single or multiple particle (p, d, ^{3}He,^{4}He)	≤ 40	^{38}K, ^{73}Se, $^{75,77}Br$,^{123}I, ^{81}Rb,(^{81}Kr), ^{67}Ga, ^{111}In, ^{201}Tl, ^{22}Na, ^{57}Co, ^{44}Ti, ^{68}Ge
Level V	Single or multiple particle (p, d, ^{3}He,^{4}He)	≤ 100	^{28}Mg, ^{72}Se (^{72}As), ^{82}Sr(^{82}Rb), ^{117m}Sn,^{123}I
Level VI	Single particle (p)	≤ 200	^{26}Al, ^{32}Si, ^{44}Ti, ^{67}Cu, ^{68}Ge(^{68}Ga), ^{82}Sr(^{82}Rb), ^{109}Cd, ^{95m}Tc, etc

*A small linear two particle accelerator (*p and d*) has also been suggested.

Most commonly used radionuclide generator systems are based on a strong adsorption of the longer-lived parent radionuclide on an immobilized phase under the condition that the formed shorter-lived daughter isotope can easily be removed. As separation basis, column chromatography, liquid-liquid extraction, gas chromatography or other techniques can be applied. Since conventional separation methods are based on differences between chemical properties of the elements, sufficient chemical difference between mother and daughter radionuclides is an essential requirement. Although many parent/daughter pairs have been evaluated as radionuclide generator systems, only a few generators are currently available in routine clinical and research use. These are $^{99}Mo/^{99m}Tc$, $^{90}Sr/^{90}Y$ and $^{188}W/^{188}Re$ in the case of reactor produced systems, while $^{68}Ge/^{68}Ga$ and $^{82}Sr/^{82}Rb$ regarding cyclotron produced systems.

1.4 Radionuclides in Medicine

A large variety of accelerator, reactor and generator produced isotopes are utilized for diagnostic and therapeutic treatments. General requirements of the decay mode of the radionuclides are dictated by the conception of diagnosis or therapy, whereas the adequacy of the half-life depends mainly on the pharmacology of the tracer. Localization and tracking of radiopharmaceuticals *in vivo* is performed by single photon emission computed tomography (SPECT) as well as by positron emission tomography (PET). The nuclear decay data of radionuclides help to decide whether they should be used for therapeutic or diagnostic purposes.

1.4.1 Radiotherapy

Radiation therapy has gained an important place in medicine. It is aimed to deliver the therapeutic doses of ionizing radiation to specific disease sites. This involves the use of external beams of electrons, x-rays, high- energy γ-rays or hadrons (neutrons, protons, heavy ions, etc.). In addition to this external radiation therapy, some radioisotopes are used internally to achieve the therapeutic effect. This involves introducing a radioisotope in a given part of the body (e.g. joints, organ, tumor, etc.). Examples are ^{90}Y, ^{32}P, ^{131}I and ^{192}Ir. For an effective radionuclide therapy a high Linear Energy Transfer (LET) is essential to provide high absorbed dose in specific disease sites, whereas the exposure of the normal tissue remains as low as possible. The most widely used therapeutic radionuclides are β^- emitters. They provide relatively long penetration range depending on the particle energy and are particularly important for solid tumours with a high heterogeneity. The β-emitters yield more homogenous dose distribution even if the tracer is heterogeneously distributed within the target tissue (Zalutsky, 2003).

The introduction of radiation emitters takes place mechanically through injection of conglomerates or colloids or as solids in the form of seeds or stents. This form of therapy is known as *brachytherapy*. The use of biomedical pathways to deliver a therapeutic radioisotope to a specific organ is termed as *endoradiotherapy*. This type of radiotherapy is a unique cancer treatment modality, although there are also several associated problems, such as the exact range of the ionizing radiation, the in vivo stability of the radiotherapeutical, the possibility of immuno chemical changes, etc. (Qaim, 2001c).

1.4.2 Radionuclides in Medical Diagnosis

Radionuclides find manifold application in emission tomography for medical diagnosis. The major criteria for diagnostic use are: (Qaim, 2001b)

- Suitable physical properties, i.e. high detection efficiency for the radionuclide, compatible with the lowest possible radiation dose to the patient
- Suitable biochemical properties, especially organ selectivity and compatibility with the bio-kinetics.

As far as physical properties are concerned, the half-life should be short and match the biochemical process under investigation (between a few minutes and a few hours). In general, the diagnostic radioisotopes are classified into two groups, namely γ-emitters (e.g. ^{67}Ga ($T_{1/2}$= 3.26 d), ^{99m}Tc ($T_{1/2}$= 6.0 h), ^{111}In ($T_{1/2}$= 2.8 d), ^{123}I ($T_{1/2}$= 13.2 h), ^{201}Tl ($T_{1/2}$= 3.06 d), etc.) and β^+ emitters (e.g. ^{11}C ($T_{1/2}$= 20.4 min), ^{13}N ($T_{1/2}$= 10.0 min), ^{15}O ($T_{1/2}$= 2.0 min), ^{18}F ($T_{1/2}$= 109.6 min), ^{82}Rb ($T_{1/2}$= 1.25 min) etc.).

If the radioisotope emits a single γ-ray, it can be applied in Single Photon Emission Computed Tomography (SPECT); in the case of β^+ emitters, the use of Positron Emission Tomography (PET) is very advantageous. The two techniques (SPECT and PET) are often collectively termed as *emission tomography* (Qaim, 2001b). Both techniques are used for imaging tumours and following up metabolisms in human organs. The PET camera is based on the simultaneous detection of the two γ-rays, each of energy 511 keV, resulting from the positron annihilation of the injected radionuclide in the target organ. The SPECT camera detects photons of suitable energy emitted from the injected radionuclide.

In addition to the production and application of the routinely used diagnostic and therapeutic radionuclides, considerable efforts have been devoted in recent years to the development of novel longer-lived positron emitters, e.g. ^{64}Cu ($T_{1/2}$= 12.7 h), ^{73}Se ($T_{1/2}$= 7.15 h), ^{124}I ($T_{1/2}$= 4.17 d), etc. and therapeutic radionuclides like ^{103}Pd ($T_{1/2}$= 16.99 d), ^{186}Re ($T_{1/2}$= 3.7 d), etc. The emphasis in the present thesis is on radiochemical work related to the development of some further diagnostic and therapeutic radionuclides.

1.5 Radiochemical Separation Methods

The processing of activated targets involves various aspects of purification and isolation of radionuclides produced via nuclear reactions. The chemical separation process is designed to permit isolation of the purified radionuclide in a form suitable for its intended application, as well as recovery of the enriched target material for reuse. The radiochemical separation scheme essentially consists of one or more of the conventional chemical separation methods,

such as distillation, precipitation, extraction or chromatography.The speed with which such separations have to be performed depends most importantly upon the half-life of the product radionuclide. Some of the commonly used techniques are discussed below.

1.5.1 Precipitation

Separations, which are based upon precipitation techniques, rely upon the different solubility of the target material and product radionuclide in a selected solvent system. Precipitation is most frequently used at an early step to reduce the total mass of the material, which has to be manipulated in subsequent operations. Most commonly, the target material, which is present in the largest mass, is precipitated and removed by filtration or centrifugation while the product radionuclide remains in solution. While precipitation techniques are quite useful for removing the bulk target material from the small quantities of the product radionuclide, the selectivity of such separations are often inadequate for achieving the required chemical, radiochemical and radionuclidic purities. In addition, the product radionuclide is often adsorbed upon the surface or included within the structure of the precipitate and substantial loss of radioactivity can occur.

1.5.2 Volatilization

Radiochemical processing of activated targets by means of volatilization techniques, such as distillation or sublimation can be used to advantage in situations where the product radionuclide is a volatile at high temperature or when it can be readily converted to a volatile derivative.

1.5.3 Solvent Extraction

Solvent extraction separation is based upon the partitioning of solutes between two immiscible solvent phases. Solvent extraction is a relatively simple and rapid technique which can achieve very high selectivity. The distribution coefficient K_d of the solute is defined as the ratio of the total concentration of the substance in one phase to its total concentration in the other phase, usually measured in equilibrium

$$K_d = [A]_{org} / [A]_{aq} \qquad 1.9$$

The distribution coefficient represents the equilibrium constant of this process. For practical purposes, it is often more popular to use the percentage extraction, (sometimes named the extraction factor % E), which is given by

$$\%E = \frac{100K_d}{1+K_d} \qquad 1.10$$

1.5.4 Chromatography

Chromatographic separation depends upon the different distribution of solutes between two distinct phases, one stationary and the other mobile. Various chromatography systems, e.g. ion exchange, adsorption, reverse phase, etc. have been developed. In this work ion exchange and thin layer chromatography were utilized, and are discussed below in more detail.

1.5.4.1 Principles of ion exchange chromatography

Ion exchange chromatography is a process in which ions, electrostatically bound to functional groups contained within a matrix, exchange with mobile ions from an external solution. Anions are involved in the exchange when the functional groups are positively charged, and conversely, cations are involved when they are negatively charged. By taking advantage of the fact that, under certain conditions, ion exchange medium has a greater affinity for certain ionic species than for others, a separation of these species is possible.
Depending on the type of the functional group, ion exchangers can be divided into several types: weak acidic, weak basic, strong acidic and strong basic. Equilibrium in ion exchange can be described in terms of the following:

Separation Factor

The separation factor α is given by the ratio of the distribution coefficients, K_d^A and K_d^B, of two different elements, A and B, that were determined under the same experimental conditions. It can be defined as follows:

$$\alpha_A^B = \frac{K_d^B}{K_d^A} \qquad 1.11$$

where A and B represent the two different elements of interest in the separation process.

Distribution Coefficient

The distribution coefficient is calculated as the ratio of the concentration of the solute in the stationary phase to the concentration of the solute in the mobile phase. It can be expressed as follows.

$$K_d = \frac{\text{mass of solute per gram of dry solid phase (ion exchange resin)}}{\text{mass of solute per cm}^3 \text{ of mobile phase (solution)}} \quad 1.12$$

The magnitude of K_d is governed by the relative affinity of the solute for the two phases. Those solutes interacting more strongly with the stationary phase will exhibit a larger distribution coefficient and will be retained longer in the chromatographic system.

Ion Exchange Capacity

The term 'ion exchange capacity' describes the total available exchange capacity of a resin, as described by the number of functional groups on it. The value is constant for a given ion exchange material and is generally given as milliequivalents per gram (meq/g), based on the dry weight of the material in a given form (such as H^+ or Cl^-). This number can be used to compare different resins or to calculate the total amount of resin to be added during a batch exchange process. The numbers quoted in the literature vary widely for different resins.

Number of Theoretical Plates

The plate model supposes that the chromatographic column contains a large number of separate layers, called *theoretical plates*. Separate equilibrations of the sample between the stationary and mobile phase occur in these "plates". The solution moves down the column by transfer of equilibrated mobile phase from one plate to the next. They serve as a way of measuring column efficiency, either by stating the number of theoretical plates in a column, *N* (the more plates the better), or by stating the plate height; the *Height Equivalent to a Theoretical Plate* (HETP).

If the length of the column is *L*, then the HETP is

$$\text{HETP} = L / N \quad 1.13$$

The number of theoretical plates that a real column possesses can be found by examining a chromatographic peak after elution;

$$\text{Number of theoretical plates} = 5.55 * (\text{Retention time} / \text{Peak width})^2 \quad 1.14$$

1.5.4.2 Thin layer chromatography

In thin layer chromatography (TLC), the mobile phase is also a solvent, and the stationary phase is a thin layer of finely divided solid, such as silica gel or alumina, supported on glass or aluminum. Thin layer chromatography is similar to paper chromatography in that it involves spotting the mixture on the plate and the solvent (mobile phase) rises up the plate in the chromatography tank. Because the distance travelled by a substance relative to the

distance travelled by the solvent front depends upon the solubility and thus on the molecular structure of the substance, TLC can be used to identify substances as well as to separate them. The relationship between the distance travelled by the solvent front and the substance is usually expressed as the retention factor R_f. Its value can be calculated as:

$$R_f = \frac{\text{distance travelled by substance}}{\text{distance travelled by solvent front}} \qquad 1.15$$

In particular, the various chemical forms of the radionuclide (i.e. speciation) are often characterized by TLC.

1.6 The Radionuclides ^{71,72,73,74}As

1.6.1 Properties and Importance of Arsenic Radionuclides

Arsenic has several radionuclides of interest for medical or environmental application. Its chemical properties are similar to those of nitrogen and phosphorus, both of which are common biologically active molecules (Tolmachev and Lundqvist, 2001). Arsenic forms stable covalent bonds with carbon and sulfur. These favorable biochemical properties enable the synthesis of biologically active molecules (Chattopadhyay et al., 2007). The decay properties of some interesting radioactive arsenic isotopes are summarized in Table 1.2.

The radionuclide ^{71}As decays by 68% through electron capture (see Table 1.2) and has a positron emission rate of 32%. The low energy positron (0.81 MeV) emitted by this radionuclide is very suitable for positron emission tomography while the 175 keV γ-ray is well suited for either planar or tomographic single photon imaging (Beard and Cuninghame, 1965; Billinghurst et al., 1990).

The radionuclide ^{72}As is a positron emitting arsenic isotope, with properties suitable for application in ^{72}As-labelled PET radiopharmaceuticals. It has a positron emission rate of 77 %. Although the positron emission is accompanied by the emission of photons of 834 keV (79.5%), 630 keV (7.9%), 1461 keV (1.1%) and others (< 0.5%), the long physical half-life of 26 hours may render ^{72}As a PET radionuclide of choice for the quantitative imaging of biochemical and physiological processes with longer biological half-lives, e.g. immuno-imaging and receptor mapping (Jennewein et al., 2005). In those cases, the half-life of ^{72}As is commensurate with the radio-pharmacological requirements resulting from the relatively slow localization kinetics of the labelled species.

Table 1.2: Decay properties of some important radioactive arsenic isotopes* and their most relevant production reactions.

Radionuclide	Half- life	Production route	Q- Value [MeV]	Decay mode (%)	γ-ray [keV]	γ-ray (%)
^{71}As	65.28 h	^{72}Ge(p,2n)^{71}As	-13.7	β^+ (32), EC (68)	175	82
		^{73}Ge(p,3n)^{71}As	-20.3			
		^{74}Ge(p,4n)^{71}As	-30.5			
		^{76}Ge(p,6n)^{71}As	- 46.5			
^{72}As	26.01 h	^{72}Ge(p,n)^{72}As	- 5.1	β^+ (77), EC (23)	834	79.5
		^{73}Ge(p,2n)^{72}As	- 11.9		630	7.9
		^{74}Ge(p,3n)^{72}As	- 22.1			
		^{76}Ge(p,5n)^{72}As	- 38.1			
^{73}As	80.30 d	^{73}Ge(p,n)^{73}As	-1.1	EC (100)	53.4	10
		^{74}Ge(p,2n)^{73}As	- 11.3			
		^{76}Ge(p,4n)^{73}As	- 27.3			
^{74}As	17.8 d	^{74}Ge(p,n)^{74}As	- 3.3	β^- (32.1), β^+ (30.9), EC (37.0)	596	59
		^{76}Ge(p,3n)^{74}As	- 19.3		635	15.4

*Taken from Firestone and Ekström, 2004.

The radionuclide ^{73}As has a half-life of 80.3 d and decays exclusively via electron capture, emitting only a γ-ray of 53.4 keV. Because of the long half-life and soft emitted radiation, it is mainly applied as a tracer for environmental sciences (Guin et al., 1997; Spahn et al., 2007a).

The radionuclide ^{74}As is also a positron emitter, but has a much longer half-life ($T_{1/2}$ = 17.8 d) than ^{72}As. It has a positron emission rate of 30.9 % with a low positron energy of $E_{\beta+}$ = 440 keV and an electron emission rate of 32.1 % and E_{β^-} = 137 keV. ^{74}As was one of the first isotopes used in the very preliminary stages of PET in the 1950s and 1960s (Jennewein et al., 2005) called positrocephalography at that time. Due to its long half-life, it is more appropriate for animal use than human use, but could also provide a useful tool for the study of long-lasting metabolic processes, like antibody-antigen interactions or, in general, long

term pharmacokinetics of developmental drugs. Recent advances in using ^{74}As labelled antibodies directed against the apoptotic marker phophatidylserine (PS) in a Dunning R2337 AT1 prostate cancer model (Jennewein et al., 2004a) clearly demonstrate the potential of this nuclide of arsenic.

1.6.2 Production Routes

The radionuclides $^{71-74}$As can be produced via a variety of nuclear reaction pathways. The most relevant proton induced nuclear reactions contributing to their formation and the respective Q-values are listed in Table 1.2. The various routes of nuclear reactions can be followed while observing the chart of nuclides (Fig. 1.3).

Fig. 1.3: Relevant part of the "Karlsruher Nuklidkarte" (Magill et al., 2007).

The radionuclide ^{72}As is generally obtained via the generator ^{70}Ge(α,2n)^{72}Se → ^{72}As (Rösch and Knapp, 2003). All arsenic isotopes mentioned above can be produced in clinically sufficient amounts by (p,n)- or (d,n)- reactions on enriched germanium targets using a low energy cyclotron. Thus ^{72}As can also be produced directly in high yields via the ^{72}Ge(p,n)^{72}As reaction at small-sized cyclotrons (Basile et al., 1981). More recently (Spahn et al., 2007a; Spahn et al., 2007b) studied excitation functions of the reactions ^{nat}Ge(p,xn)$^{71-74}$As up to 100 MeV. Fig. 1.4 gives the excitation functions and integral yields for the formation of

^{71}As, ^{72}As, ^{73}As and ^{74}As in proton-induced reactions on ^{nat}Ge. Based on those data the theoretical yields of radioarsenic production were calculated and compared with the experimental yields determined in this work.

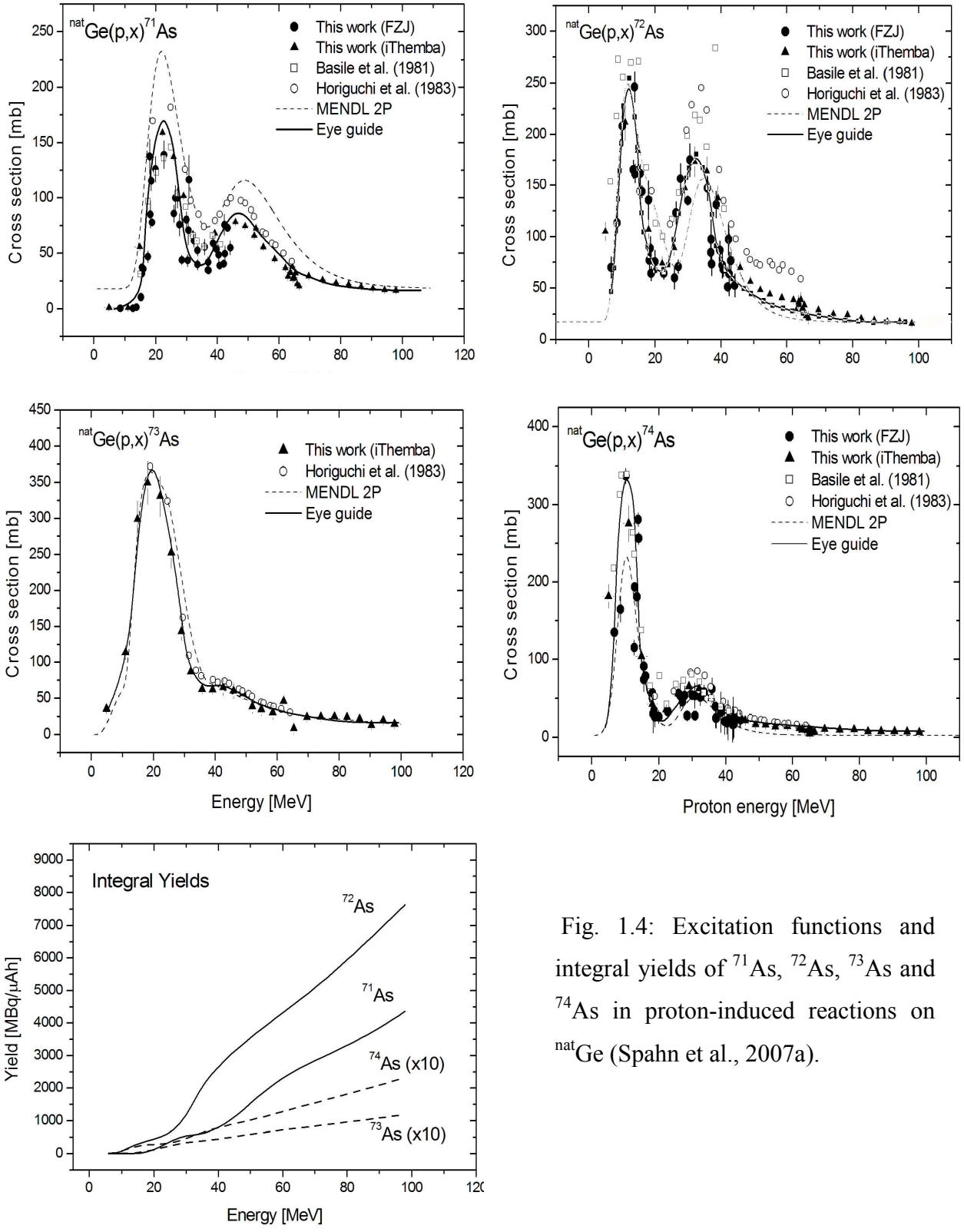

Fig. 1.4: Excitation functions and integral yields of ^{71}As, ^{72}As, ^{73}As and ^{74}As in proton-induced reactions on ^{nat}Ge (Spahn et al., 2007a).

1.6.3 Chemical Separation

Various methods for the separation of germanium and arsenic have been reported. They include dry distillation (Tolmachev and Lundqvist, 2001), solvent extraction (Beard and Cuninghame, 1965; Ward et al., 1970; Billinghurst et al., 1990; Chattopadhyay et al., 2007), ion exchange (Pacey and Ford, 1981; Guin et al., 1998; Jahn, 2009) and thin layer chromatography (Maki and Murakami, 1974; Pacey and Ford, 1981). The review article by (Mirzadeh and Lambrecht, 1996) gives an account of the different radiochemical separation methods of germanium. In particular the solvent extraction technique has proven to be very useful and several effective systems have been worked out. An important consideration in all the separations is the speciation of arsenic since it could exist as As(III) or As(V), or as a mixture of both, upon dissolution of the irradiated target, which may be of crucial significance for any solvent extraction system.

As(III) can be extracted from > 8 M HCl into benzene or into carbon tetrachloride (Beard and Lyerly, 1961; Korkisch and Feik, 1967; Forehand et al., 1976; Hubert, 1983; Azarez et al., 1985; Chappell et al., 1995). Methylisobutylketone extracts 91% of As(III) and 28% of As(V) from a mixture of 8 N HCl +2 N H_2SO_4. As(III) is also extracted from HF solutions by ether and from HI solutions by chloroform (Ward et al., 1970) while arsenic (V) is not extracted. Prior to extraction, however, arsenic (V) can be reduced with potassium iodide to As(III) and then extracted from the iodide solution (Tanaka and Takagi, 1969; Byrne and Gorenc, 1972; Byrne, 1972; Maher, 1981; Suzuki et al., 1986; Donaldson and Wang, 1986; Palanivelu et al., 1992; Rashid et al., 1992). The solvent extraction of arsenic (V) was investigated using heptane containing ultrafine magnetite particles and hydrophobic ammonium salt (Wakui et al., 2002) with best results from aqueous solutions with a pH ranging between 2 and 7. More recently, (Jennewein et al., 2005) described a method to separate no-carrier-added arsenic triiodide, [^{77}As]AsI_3, from irradiated GeO_2 dissolved in a hydrofluoric acid medium using a polystyrene-based solid-phase extraction system.

It has been shown (Chappell et al. 1995) that in the presence of an excess of hydrochloric acid chlorination of arsenic occurs, yielding arsenic trichloride and arsenic pentachloride. Arsenic trichloride is a covalent molecule while arsenic pentachloride forms complex ions in solution. Thus the trivalent arsenic can be extracted into an organic phase such as chloroform, cyclohexane or benzene, while arsenic pentachloride is excluded owing to its ionic properties. The extraction of As(III) and Ge(IV) depends on the concentration of hydrochloric acid as well as of potassium iodide (Tanaka and Takagi, 1969). The method was used for the extraction of micro amounts of As and Ge from different environmental matrices. The aim of

the present work was to adapt that method to the separation of no-carrier-added (n.c.a) radioarsenic from a GeO_2 bulk target. In this respect optimization experiments on the extraction of radioarsenic were essential under various conditions involving different acids and organic solvents.

1.7 The Radionuclide ^{68}Ge

1.7.1. Importance of ^{68}Ge

The radionuclide ^{68}Ge ($T_{1/2}$ = 270.8 d) decays to ^{68}Ga ($T_{1/2}$ = 67.63 min) by electron capture. The latter is a positron emitter and gets quickly in equilibrium with the parent nuclide. The first application of ^{68}Ge in equilibrium with the daughter ^{68}Ga was as a long-lived positron source for the attenuation correction and calibration of PET scanners. ^{68}Ge(^{68}Ga) has been used as a positron source in positron annihilation studies in nuclear physics and in industrial metal radiography (Naidoo et al., 2002). Currently, interest is growing in the use of ^{68}Ge as the parent radionuclide for the preparation of ^{68}Ge/^{68}Ga generators (cf. Rösch and Filosofov, 2010). Recently the use of ^{68}Ge/^{68}Ga radionuclide generator system in nuclear medicine has attracted interest because of the significant potential for PET imaging using ^{68}Ga labelled radiopharmaceuticals (see section 1.8).

1.7.2 Production Routes and Target Processing

The radionuclide ^{68}Ge can be produced via a variety of nuclear reactions, all using charged particle irradiation. The most relevant processes are listed in Table 1.3, categorized according to the type of the particle utilized. The excitation functions for ^{69,71}Ga(p,xn)^{68}Ge reactions have been reported in the literature (Porile et al., 1963). Horiguchi et al. (1983) provided excitation functions and thick target yields for the Ge(p,pxn)^{68}Ge reactions and compared them with those of the Ga(p,xn)^{68}Ge and ^{66}Zn(α,2n)^{68}Ge reactions. For the Ga(p,xn) production routes, potentially useful target compounds include Ga_2O_3 (melting point 1900 ^{o}C) and Ga_4Ni alloy (melting point 900 ^{o}C) (Loc'h et al., 1982). Mixtures of Ga metal and Ga_2O_3 have been used, as has been also Ga_2O (Naidoo et al., 2002). However, the Ga metal (melting point 39 ^{o}C) itself is also used as a target, usually encapsulated in Nb containers. Corrosion resistant Nb allows effective water cooling of the target.

Table 1.3: Overview* of the most relevant nuclear reactions yielding ^{68}Ge.

Radionuclide ($T_{1/2}$)	Decay mode (%)	Production route	Q- Value [MeV]
^{68}Ge (270.8 d)	EC (100)	^{69}Ga(p,2n)^{68}Ge	-11.201
		^{nat}Ga(p,xn)^{68}Ge	-11.201 to -28.5
		^{nat}Ge(p,pxn)^{68}Ge	-19.7 to -70.8
		^{66}Zn(α,2n)^{68}Ge	-15.637
		^{nat}Zn(^{3}He,xn) ^{68}Ge	-2.112 to -12.310.

*Taken from Firestone and Ekström, 2004.

The most effective route of ^{68}Ge production appears to be the proton irradiation of Ga targets. The high cross-section values of the (p,2n) reaction allow irradiation of natural Ga without isotopic enrichment of ^{69}Ga at medium proton energies of between 20 and 30 MeV. In addition, if protons of higher energies are available, the (p,4n) process on ^{71}Ga contributes to the production yield. High beam intensities in the range of 100 μA or more are required to produce batch activities of 37 GBq of ^{68}Ge. As the number of accelerators with the above features is limited worldwide, the number of ^{68}Ge production sites is also limited. The recommended cross-section curve and the corresponding yield are illustrated in Fig.1.5.

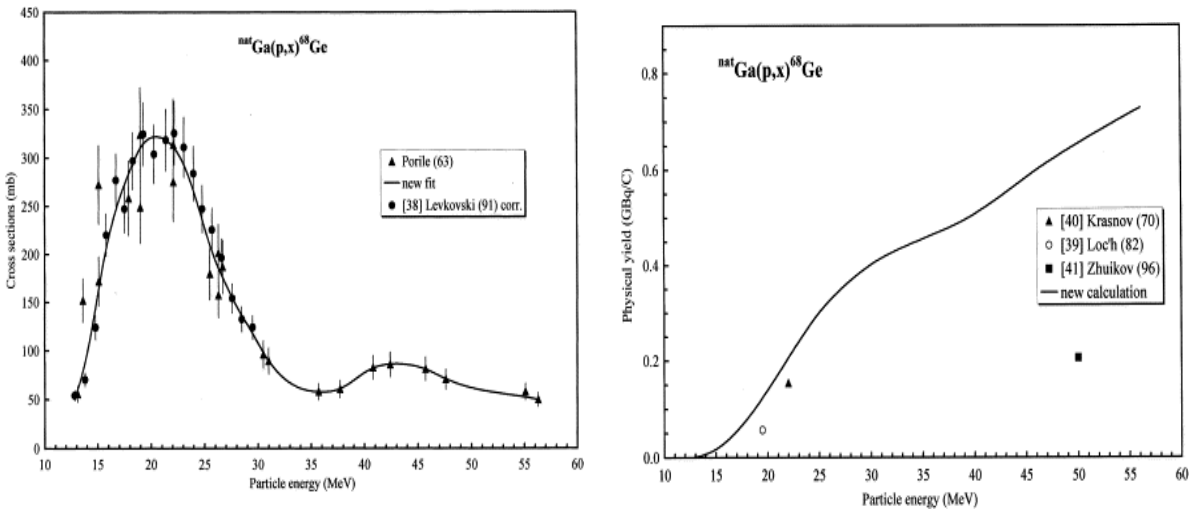

Fig. 1.5: left: Evaluated cross section of the ^{nat}Ga(p,x)^{68}Ge reaction, right: Integral yield of the ^{nat}Ga(p,x)^{68}Ge reaction, calculated from the evaluated cross sections (Qaim et al., 2001).

1.7.3 Chemical Separation

Several articles describe in detail a variety of chemical methods for the separation of ^{68}Ge. The principal methods include distillation of ^{68}Ge (Mirzadeh et al., 1981; Gleason, 1960), ion exchange chromatography (Loc'h et al., 1982; Naidoo et al., 2002), and liquid-liquid extraction (Kopecky et al., 1973; Pao et al., 1981; Fassbender et al., 2005). The solvent extraction technique using carbon tetrachloride is known to be one of the most widely used methods for the isolation of carrier-free ^{68}Ge (Kopecky et al., 1973). One of the most selective methods for separating germanium, however, is the extraction of $GeCl_4$ by nonpolar organic solvents from strong acidic chloride solutions (Meinken et al., 2005). For Ga/Nb systems, ^{68}Ge is extracted into CCl_4 after dissolution of the target in 12 M H_2SO_4 (with the aid of HCl and H_2O_2). ^{68}Ge is back-extracted into 0.05 N HCl and evaporated to the appropriate volume. For Ga_4Ni targets, a semi-automated processing, consisting of electrochemical target dissolution, is used. Following extraction of ^{68}Ge from 9.0-9.5 M HCl into CCl_4, the ^{68}Ge is back-extracted into water (Loc'h et al., 1982). Barong and Yinsong (1992) reported on the dissolution of Ga_2O_3 in concentrated H_2SO_4 solution, followed by liquid-liquid extraction of ^{68}Ge in H_2SO_4-HCl and H_2SO_4-KI systems. Aardaneh et al. (2006) used benzene and carbontetrachloride for the separation of ^{68}Ge from 9 M H_2SO_4-0.3 M HCl system. In our work, the extraction of ^{68}Ge from H_2SO_4-HCl system was studied using toluene and chloroform as organic solvents. The effect of various H_2SO_4 and HCl concentrations was investigated with both organic solvents.

1.8 The Radionuclides ^{66,67,68}Ga

1.8.1 Properties and Importance of Radionuclides of Gallium

The chemistry of Ga is like that of its Group III homologues aluminum and indium. The Ga^{3+} ion is classified as a hard acid, bonding most strongly to highly ionic, non-polarizable Lewis bases. As a result, its chelate chemistry is dominated by ligands containing oxygen and nitrogen donor atoms. Gallium behaves in the human body in a similar way as the ferric iron. The three radionuclides ^{66}Ga, ^{67}Ga and ^{68}Ga are widely used in the field of nuclear medicine, commonly as a trivalent citrate compound imaging, but are also valuable agents in the detection and localization of certain neoplasms and inflammatory lesions.

The decay data of these gallium radioisotopes are given in Table 1.4. ^{66}Ga ($T_{1/2}$= 9.4 h) has been proposed for application in PET. It has been used in the radiolabelling of blood cells and albumin colloids for various diagnostic purposes (Ellis and Sharma, 1999). ^{67}Ga ($T_{1/2}$=

3.2 d), which decays by electron capture and emission of γ-rays, is widely used as a single photon marker for detecting the presence of malignancy and diagnosis of inflammatory diseases (Kakavand et al., 2010).

Table 1. 4: Decay data* and some of the production routes of ^{66,67,68}Ga using Zn target.

Nuclide	$T_{1/2}$	Production route	Q- Value [MeV]	Mode of decay (%)	γ-ray [keV]	γ-ray (%)
^{66}Ga	9.4 h	^{66}Zn(p,n)^{66}Ga ^{67}Zn(p,2n)^{66}Ga ^{68}Zn(p,3n)^{66}Ga	-5.957 -13.009 -23.207	EC (44) β^+ (56)	833.5 1039	5.9 37
^{67}Ga	3.26 d	^{67}Zn(p,n)^{67}Ga ^{68}Zn(p,2n)^{67}Ga	-1.782 -11.98	EC (100)	93.3 184.6	39.2 21.2
^{68}Ga	67.63 min	^{68}Zn(p,n)^{68}Ga ^{70}Zn(p,3n)^{68}Ga	-3.703 -19.401	EC (12) β^+ (88)	1077	3

*Taken from Firestone and Ekström, 2004.

The radionuclide ^{67}Ga has found numerous applications in nuclear medicine. It is used to investigate tumoural proliferation in peripheral nerve sheaths (Shanthly and Thakur, 2006), in the management of Hodgkins disease (Anderson et al., 1983) and elsewhere. No-carrier-added (n.c.a) ^{67}Ga can be accumulated in certain viable primary and metastatic tumours, as well as in focal sites of infection.

The radionuclide ^{68}Ga is gaining considerable interest in nuclear medicine, especially for use in positron emission tomography (PET). It is best obtained via a ^{68}Ge-^{68}Ga generator system. The parent radionuclide ^{68}Ge has a long half-life of 270.82 days and decays 100 % by electron capture to the short-lived daughter ^{68}Ga ($t_{1/2}$ = 67.63 min) which decays mainly by positron mission (β^+ = 88 %, EC = 12 %) and therefore is suitable for PET imaging. The ^{68}Ge/^{68}Ga generator system has an advantage in diagnosis, because milking of ^{68}Ga from ^{68}Ge allows preparing various kinds of chemical compounds at a hospital without a medical cyclotron. ^{68}Ga-based imaging agents have been investigated in connection with the study of pulmonary, myocardial and cerebral perfusion, renal and hepatobiliary function, in the detection of blood-brain barrier defect, as well as to image tumour, brain and bone (Green and Welch, 1989). Furthermore, ^{68}Ga is employed for transmission measurements for encoding calibration and normalization of detector efficiencies of PET scanners.

1.8.2 Production Routes and Target

The radionuclides ^{66,67}Ga are produced by irradiating thick copper or zinc targets with lighter projectiles like protons, deuterons or α-particles in a cyclotron. Many authors (Bonardi and Birattari, 1983; Kopecky, 1990; Szelecsényi et al., 1998; Hermanne et al., 1999; Gul, 2001; Szelecsényi et al., 2003; Tárkányi et al., 2005; Uddin et al., 2007; Al-Saleh et al., 2007; Wachter et al., 2008) studied experimentally or theoretically the production of ^{66,67}Ga in irradiation of zinc target with protons. Table 1.4 shows the production of ^{66}Ga, ^{67}Ga and ^{68}Ga via various nuclear reactions with a proton beam, which can also be followed using the nuclide chart of radionuclides shown in Fig.1.3.

Nagame et al. (1978) produced ^{67}Ga by bombardment of natural zinc with alpha particles. The n.c.a. ^{65}Zn and ^{66,67,68}Ga were simultaneously produced by activation of thick copper target with a 50 MeV α-particle beam (Lahiri et al., 1997). Nayak and Lahiri (2001) developed an alternative method for the production of ^{66,67}Ga radionuclides by irradiating naturally occurring monoisotopic cobalt metal with heavy ions like ^{11}B or ^{12}C. The yields were, however, very low.

The most important route for the production of ^{68}Ga is the decay from the parent ^{68}Ge.

1.8.3 Separation Methods

1.8.3.1 Separation methods of ^{66,67}Ga

Numerous methods have been attempted to separate ^{66,67}Ga from zinc targets such as anion exchange chromatography (Papardells et al., 1984; Környel et al., 1986; Tárkányi et al., 1990; Das et al., 1997; El-Azony et al., 2003; Sabet et al., 2006), solvent extraction (Nachtrieb and Fryxell, 1949), and precipitation (Sadeghi and Mokhtari, 2010).

According to the literature, both anion and cation exchange resins have been used for the separation of ^{67}Ga from zinc targets. Környel et al. (1986), for example, used a long column (20 cm) containing a modified Dowex 1 anion exchanger resin in 6 M HCl medium for the separation of ^{67}Ga from the Zn target. A Dowex 50W-X2 cation exchange resin was employed (Tárkányi et al., 1990) for the separation of ^{67}Ga from Zn and Cu with a good yield and in a short time (1 hour). The ^{67}Ga was eluted by 4 M HCl that needs to be evaporated for further processing of ^{67}Ga citrate preparation. ^{67}Ga was separated from zinc and copper target materials using anion-exchanger (Dowex 21k) and 0.1 M citrate buffer at pH 6 (El-Azony et al., 2003) in citrate solution in a high yield (80.65 %) and can be directly used for medical application.

A number of organic adsorbents of Amberlite XAD series have been extensively studied by Brits and Strelow (1990) for separation of ^{67}Ga from a Zn target. It was concluded that the use of XAD-7 and 7 M HCl was most efficient for the separation (Aardaneh and Shirazi, 2005). A solvent extraction system using diisopropyl ether / 7 M HCl has also been used successfully for the separation (Nachtrieb and Fryxell, 1949; Brown, 1971). Sadeghi and Mokhtari (2010) studied the separation of ^{67}Ga from Zn and Cu by a precipitation method. A characteristic feature of Ga(III) hydroxide is that it is amphoteric, meaning it is soluble in both acidic and basic solution. Above pH = 9.6 the gallate ion $Ga(OH)_4^-$ forms and redissolves. This allows an efficient and rapid separation of Ga from Zn and Cu by precipitating Zn as $Zn(OH)_2$ and Cu as $Cu(OH)_2$.

In this work a longer-lived tracer of gallium was needed for optimization studies on the separation of n.c.a. ^{68}Ga from the ^{68}Ge/^{68}Ga generator system. The separation of n.c.a. ^{67}Ga from a proton irradiated zinc target using anion exchange (Amberlite CG-400-II Cl^- form and Dowex 50WX8 H^+ form) and solvent extraction processes was aimed at. Furthermore, the solvent extraction process using diisopropyl ether was also considered worth investigating.

1.8.3.2 Separation methods of ^{68}Ga from parent ^{68}Ge

Several ^{68}Ge/^{68}Ga generator systems have been developed over the past several years. They included a large number of methods for the separation of ^{68}Ga, e. g. ion-exchange chromatography with inorganic and organic adsorbents or synthetic resins in diluted acid or alkaline media (Greene and Tucker, 1961; Carlton and Hayes, 1971; Dmitriev et al., 1972; Ehrhardt and Welch, 1978; Neirinckx and Davis, 1980; Schumacher et al., 1981; Neirinckx et al., 1982; Lambrecht et al., 1983; McElvany et al., 1984; Ambe, 1988; Egamediv et al., 2000; Cheng et al., 2000; Nakayama et al., 2002; Nakayama et al., 2003; Velikyan et al., 2004; Rösch et al., 2006; Konstantin et al., 2007; Sadeghi et al., 2009) and solvent extraction (Egamediev et al., 2001; Fassbender et al., 2007; Bokhari et al., 2009). Gleason (1960) described the first generator which utilized extraction by acetylacetone buffered solution with cyclohexane. The first series of new or improved generators have been regularly described since 1961 by Greene and Tucker, who proposed the first chromatographic generator which consisted of the parent ^{68}Ge adsorbed onto an alumina column. The inorganic supporting materials used for the adsorption of ^{68}Ge were Al_2O_3, Sb_2O_5, ZrO_2, TiO_2, $Fe(OH)_3$ and SnO_2. The eluents used for the elution of ^{68}Ga were so far diluted EDTA, HCl and HNO_3 or NaOH. Among these studies, Loc'h et al. (1982) have defined a very promising commercially available generator of ionic ^{68}Ga based on elution from tin dioxide with 1 N HCl, with special

regard to the simplicity of the operation. A $^{68}Ge/^{86}Ga$ generator consisting of an alumina column eluted with diluted sodium hydroxide to yield ^{68}Ga as the gallate ion has also been described (Lewis and Camin, 1981). Sadeghi et al. (1992) studied the separation of ^{68}Ga from proton irradiated ^{68}Zn using cation exchange resin (BIO-Rad AG 50W) and used a solvent extraction method to achieve high purity ^{68}Ga.

The $^{68}Ge/^{68}Ga$ radionuclide generator systems available today are not necessarily optimally designed for direct application in making diagnostic products for human use. The eluate from the commercial generator still contains measurable levels of long-lived ^{68}Ge. In addition, the rather large volume and the relatively high concentration of hydrochloric acid in many cases prevent direct use for labelling reactions. Furthermore, labelling yields and specific activities might not reach the maximum values due to the presence of metallic impurities. For example, significant amounts of Zn(II) are generated from the decay of ^{68}Ga. In the case of fresh generators, the amount of stable ^{71}Ga generated from the ^{71}Ge decay may be up to one order of magnitude higher than the amount of stable ^{68}Zn generated. In addition, Ti(IV) or other residuals from the generator column material and Fe(III) are present in the eluate. All these metallic impurities will adversely affect the ^{68}Ga labelling yields as well as the specific activity of the labelled product. Thus, dedicated procedures for processing the eluate from the radionuclide generator, including the labelling and purification of the ^{68}Ga radiopharmaceutical need to be developed. Several approaches to further processing of the generator derived $^{68}Ga(III)$ are described in the literature.

Using tracer studies, two methods of separation of radiogallium from radiogermanium were aimed to be developed in the present work. The first method is based on an anion-exchange solvent extraction using the strong anion exchanger Aliquat 336 (trioctylmethylammonium chloride) in o-xylene and hydrochloric acid, while the second involves cation-exchange column chromatography using the strong cation exchanger Amberlite IR-120.

1.9 The Radionuclides ^{75,76,77,80m}Br

1.9.1 Properties and Importance of Bromine Radioisotopes

The chemistry of bromine is very similar to that of iodine and the physical properties such as electro-negativity or van der Waals radius are between those of fluorine and iodine. There is a growing interest in the use of radionuclides of bromine in nuclear medicine because of their suitable nuclear and chemical characteristics. Table 1.5 gives the decay data of some medically interesting radioisotopes of bromine (cf. Firestone and Ekström, 2004).

Table 1.5: Nuclear data* of some radiobromines.

Nuclide	$T_{1/2}$	Nuclear reaction	Q- Value [MeV]	Mode of decay (%)	γ-ray [keV]	γ-ray (%)
^{75}Br	1.5 h	^{76}Se(p,2n)^{75}Br	-14.966	EC (24) β^+ (76)	141 286.6	6.6 88
		^{77}Se(p, 3n)^{75}Br	-22.386			
		^{74}Se(d,n)^{75}Br	1.99			
		^{75}As(^{3}He,3n)^{75}Br	-13.18			
		^{78}Kr(p,^{4}He)^{75}Br	-0.176			
^{76}Br	16.2 h	^{76}Se(p,n)^{76}Br	-5.74	EC (42) β^+ (58)	559 657 1853.7	74 15.9 14.7
		^{77}Se(p,2n)^{76}Br	-13.16			
		^{75}As(^{3}He,2n)^{76}Br	-3.95			
		^{nat}Br(p,xn)^{76}Kr→ ^{76}Br	-32.05 to -50.01			
		^{76}Se(^{3}He,3n)^{76}Kr→^{76}Br	-15.52			
^{77}Br	57.4 h	^{77}Se(p,n)^{77}Br	-2.17	EC (99)	238.9 520	23 22.4
		^{78}Se(p,2n)^{77}Br	-12.64			
		^{75}As(^{4}He,2n)^{77}Br	-13.51			
		^{79}Br(d,4n)^{77}Kr→ ^{77}Br	-25.05			
^{80m}Br	4.42 h	^{80}Se(p,n)^{80m}Br	-2.65	IT(100)	37	40
		^{nat}Se(p,xn)^{80m}Br	-2.65 to -18.63			

*Taken from Firestone and Ekström, 2004.

The C-Br bond has a binding energy which is 40-60 kJ/mol (10-15 kJ/mol higher than that of the corresponding C-I bond) and is therefore more stable (Coenen et al, 1983; Maziere and Loc'h, 1986). For this reason bromine is sometimes preferable to iodine for labelling. An additional advantage is that bromide ions, when they are released from the labelled compound by some cause, will not be localized in the thyroid. Bromine radioisotopes may also be used in nuclear medicine as inorganic anions, e.g. for estimation of extracellular fluid volumes

(Janssen et al 1980). The high nucleophilicity of bromide bears advantages in synthesis of radiolabelled compounds, and n.c.a. products via interhalogen-exchange can be obtained easily (Maziere and Loc'h, 1986; Coenen et al., 1983). Further, it can rather easily be oxidized in situ, thus facilitating n.c.a. electrophilic substitution reactions in vinyl and aryl positions (Coenen et al., 1986).

Bromine-75 decays with 76 % positron emission and 24% electron capture. The positron end point energy is 1.7 MeV, and there are several gamma rays, with the most prominent being at 286.5 keV. Bromine-75 decays to ^{75}Se, which has a 120 day half-life and several gamma rays in the 100–300 keV range. This contributes to the overall dosimetry of the ^{75}Br-containing radiotracers. Among the neutron deficient bromine isotopes ^{75}Br is of special interest and has found application in labelling of some biomolecules for use in positron emission tomography (Qaim and Stöcklin, 1993).

Bromine-76 decays with both positron emission (58%) and electron capture. The half-life (16.2 h) allows radiotracers to be used that have accumulation times of one or two days. The high end point energy of the positron emitted may affect the positron emission image to some extent. Over the last decade the available γ-cameras were mostly suitable for the low energy γ-rays of ^{123}I rather than for the higher energy γ-rays of the bromine isotopes (Tárkányi et al., 1993). Therefore, more efforts have been devoted to the production of ^{123}I. Recently, through the development of PET and high-energy γ-ray cameras, bromine isotopes have received some more attention.

Bromine-77 has a half-life of 57 h and decays nearly exclusively (99.3%) by electron capture, with prominent gamma rays at 239.0 and 520.7 keV, and several low intensity gamma rays, varying in energy from 238 to 820 keV. Its half-life is suitable for long term physiological investigations using Single Photon Emission Computed Tomography (SPECT). Furthermore, the Auger electrons emitted in the decay of ^{77}Br are of some therapeutic interest. In addition to its direct uses as a labeling agent, ^{77}Br is also of promising utility as the generator of its very short-lived daughter ^{77m}Se (Grant et al., 1981). This isomeric state decays to stable ^{77}Se with 17.45 s half-life and a γ-ray ideal for imaging with the Anger camera (162 KeV), but without the emission of any primary particulate radiation. Its intensity is, however, very low.

The radioisotope ^{80m}Br (4.4 h) appears to be suitable for therapeutic purposes due to its decay by converted internal transition which involves the release of about seven Auger electrons per decay. ^{80m}Br is attractive in the treatment of steroid hormone positive cancers since its half-life is very well matched to the biology of estrogen receptor (ER) (Mease et al., 1991).

1.9.2 Production Routes and Target

The various techniques of preparation of the neutron deficient radioisotopes of bromine have been extensively reviewed (Waters et al., 1973; Nunn and Waters, 1975; Nozaki et al., 1979; Blessing et al., 1982; Qaim and Stöcklin, 1983; Blessing and Qaim, 1984; Kovács et al., 1985; Qaim, 1986; Gallano and Tilbury, 1998; Tolmachev et al., 1998; Hassan et al., 2004; Spahn et al., 2009). The bromine isotopes are obtained by irradiating stable arsenic, selenium, krypton or bromine targets with charged particles. As these four elements possess 1 to 6 stable isotopes the choice of the transmutation reaction that can be used is large. The variety of possible production routes can be followed in the chart of nuclides (Fig. 1.4).

An arsenic target has to be irradiated with ^{3}He or ^{4}He ions to allow the production of ^{75,76,77}Br. As natural arsenic has only one stable isotope, the number of interfering nuclear reactions is limited. Proton irradiation of a selenium target gives easy access to bromine isotopes (Waters et al., 1973; Nozaki et al., 1979; Nunn and Waters, 1975); however, natural selenium has six stable isotopes, and consequently a high yield of a radionuclidically pure product necessitates the use of an enriched target (Kovács et al., 1985; Hassan et al., 2004; Spahn et al., 2009). In particular the route ^{80}Se(p,n)^{80m}Br needs to be investigated since so far it was not studied for the production of ^{80m}Br.

A bromine target irradiated with deuterons or protons can be used to prepare radioactive isotopes of krypton which decay to ^{75}Br, ^{76}Br or ^{77}Br (Qaim, 1977; Nozaki et al., 1979; Qaim and Weinreich, 1981; Maziere and Loc'h, 1986; Tarkányi et al., 1993) (see Fig. 1.3). Also, a krypton target bombarded by protons or deutrons can be theoretically used to produce ^{75}Br or ^{76}Br .

The highest yield of ^{75}Br is obtained using the ^{76}Se(p,2n)^{75}Br reaction on enriched ^{76}Se (Kovács et al., 1985; Vaalburg et al., 1985). Although proton induced reactions give higher yields for ^{77}Br production, the ^{75}As(α, 2n)^{77}Br reaction has been used most commonly (cf. Blessing and Qaim, 1984), due to the more advantageous properties of an arsenic target (Gallano and Tilbury, 1998). An overview of the nuclear reactions useful for the production of radiobromines is given in Table 1.5.

1.9.3 Chemical Separation

For the radiochemical separation of radiobromine from an arsenic or selenium target, possible contamination by nonradioactive bromine from reagents and laboratory atmosphere should always be considered. The following three methods have been reported:

(1) Dry distillation and thermochromatography (Janssen et al., 1980; Blessing et al., 1982; Blessing and Qaim, 1984; Kovács et al., 1985; Vaalburg et al., 1985; Tolmachev et al., 1998; Wachsmuth et al., 2000)

(2) Distillation from a solution (Helus, 1970; Nunn and Waters, 1975; Iofa et al., 1975; Alfassi and Helus, 1983) and

(3) Co-precipitation and subsequent removal of cations by ion exchange (Nozaki et al., 1979; Ballaux et al., 1967; Norton et al., 1978; Madhusudhan et al., 1979; Grant et al., 1981; Broden and Skarnemark, 1981).

Several methods for dry distillation of bromine isotopes are described in the literature. Janssen et al. (1980) used an enriched target with the composition of $Na_2SeO_{3.88}$ $0.38Na_2O$ for the production of ^{77}Br. The possibility of a dry distillation technique for both a carrier-free separation of ^{77}Br from irradiated enriched selenium targets and a quantitative recovery of the selenium is discussed. Dry distillation methods were applied for the production of ^{75}Br (Vaalburg et al., 1985). Radiochemical yields of about 40-52 % were obtained. The dry distillation at 300 ^{o}C is convenient since the same target can be reused without involving any reprocessing. Radiobromine was separated from Cu_2Se by dry distillation at 1473 K and collected 80-95 % on platinum wool pretreated with $CaCl_2$ (Vaalburg et al., 1985). Radiochemical analysis showed the radiobromine to be Br^- for 95% and BrO^- for 5 %. The total loss of selenide after irradiation and distillation was found to be less than 0.1 %. The isolation of radiokrypton from KBr pellets irradiated with protons and Na_2Se pellets irradiated with ^3He particles was done (Jong et al., 1979). The $^{79}Br(p,xn)^{76,77}Kr$ reaction leads to high yields of ^{76}Br and ^{77}Br compared to other direct and indirect methods, with high specific activities. Radiobromine was separated from a Cu_3As target (Blessing et al., 1982) without adding any carrier via dry distillation at 950 ^{o}C. Arsenic and selenium distill only negligibly and condense at the end of the quartz tube near the oven. The radiochemical yield of this distillation process was reported to be >90 %.

Thermochromatography was used for separation of radiobromine from irradiated Cu_3As alloy (Blessing and Qaim, 1984). The application of thermal chromatography in conjunction with dry distillation allowed the separation of selenium-free ^{76}Br from a Cu_2Se target enriched in ^{76}Se (Tolmachev et al., 1998). The target remains intact with only minor loss of material (1% per run) and is directly ready for the next irradiation. Bromine-76 is separated with an efficiency of 65-75 % within 60-75 min.

The distillation of radiobromine from selenium after dissolution of the target in concentrated nitric acid (Iofa and Sevast'yanov, 1975) gives low yields (40% in 2 hours) of

bromine and a distillate which contains a high concentration of dissolved oxides of nitrogen. The H_2SO_4-$K_2Cr_20_7$ distillation method used by (Helus, 1970; Nunn and Waters, 1975) for the separation of ^{77}Br from arsenic targets was unsuccessful when applied to selenium targets. Nozaki et al. (1979) tried various methods to obtain carrier- free ^{77}Br in neutral salt free water from arsenic and selenium targets. Ballaux et al. (1967) reported the separation of ^{82}Br formed in the neutron activation analysis of high purity selenium. The irradiated Se was dissolved in nitric acid, carrier bromide was added, and silver bromide precipitated. A procedure for the synthesis and isolation of ^{77}Br for nuclear medicine research has been developed at LASL (for review cf. Qaim, 1986). Metallic Mo targets are irradiated at LAMPF with medium energy protons at high beam current. Following dissolution, volatilization, volatile radiobromine was quantitatively precipitated as AgX (96% average yield). The ensuring cation exchange column gave an average yield of 95% for that step, for an overall, cumulative radiobromine recovery of 91.7 % which is completely free of all other radioactive species with the exception of small levels of ^{76}Br and ^{82}Br.

A silver chloride co-precipitation and ion exchange separation method was described for the carrier-free isolation of ^{77}Br bromide from isotopically enriched ^{77}Se targets following dissolution of the irradiated ^{77}Se in nitric acid (Norton et al., 1978). A cation exchange (AG 50W-X8) procedure was devised to remove the silver and yield a dilute hydrochloric acid solution containing 90 % of the ^{77}Br precipitated as bromide. Broden et al. (1981) developed fast on-line chemical separation procedures delivering pure fractions of short-lived Zr^-, Nb^-, Tc^-, Br^-, and I^- isotopes from complex reaction product mixtures using the multistage solvent extraction system 'SISAK 2' in combination with a gas-jet recoil transport system. An improved method for production of >100 mCi of ^{77}Br with the ^{78}Se(p,2n)^{77}Br nuclear reaction using a water-cooled target containing encapsulated metallic ^{78}Se or a Pb^{78}Se alloy was developed (Madhusudhan et al., 1979). The ^{77}Br was separated with ~98% radiochemical yield and a radionuclidic purity of 98.9%.

In the present work the separation of no-carrier-added radiobromine and no-carrier-added radiogallium from an irradiated ZnSe target was aimed at.

2. Aims and Objectives of the Present Work

The radionuclides $^{71\text{-}74}$As, ^{68}Ge/^{68}Ga and ^{76,77,80m}Br are important for application, especially in nuclear medicine. The radionuclides ^{71,72,74}As are suitable for positron emission tomography, while the radionuclide ^{73}As is mainly applied as a tracer for environmental studies. The radionuclide ^{68}Ga finds considerable interest in nuclear medicine, especially for use in positron emission tomography (PET). Its availability via the ^{68}Ge/^{68}Ga generator system is of great advantage, because periodic milking of ^{68}Ga from ^{68}Ge allows preparation of various kinds of chemical compounds at a hospital on routine basis. Recently, through further development of PET and high-energy γ-ray cameras, the bromine isotopes have received some more attention. This thesis deals with these radionuclides and their production methods. In particular, it covers some nuclear data measurements and novel radiochemical separation methods.

The present work had four major objectives:

(1) Development of a radiochemical separation method for no-carrier-added arsenic radionuclides from bulk amount of GeO_2 target irradiated with protons. The speciation of radioarsenic produced, viz. the ratio of As(III) to As(V), needs to be determined. The extraction of radioarsenic by different organic solvents from acid solutions of various concentrations containing alkali iodide should be studied and optimized. The practical application of the optimized procedure in the production of ^{71}As and ^{72}As, including quantitative assay of the yield and purity, should be demonstrated.

(2) Development of a novel separation route for ^{68}Ge/^{68}Ga generator system. At first the radiotracers ^{69}Ge and ^{67}Ga should be prepared in pure forms for tracer studies. The radiotracer ^{68}Ge should be separated from proton irradiated Ga_2O_3 via liquid-liquid extraction, using H_2SO_4-HCl/ toluene system. The various parameters affecting the extraction process via toluene should be optimized.

For the separation of n.c.a. ^{67}Ga from a proton-irradiated zinc target anion exchange and solvent extraction processes should be investigated and optimized.

Using the no-carrier-added longer lived tracers, viz. ^{69}Ge and ^{67}Ga, the radiochemical separation of radiogallium from radiogermanium should be studied using ion exchange chromatography (Amberlite IR-120) and solvent extraction (Aliquat 336 in o-xylene). Both Amberlite IR-120 and Aliquat 336 in o-xylene have not been used before for separations involving radiogallium and radiogermanium. The novel optimized method should then be applied to the separation of ^{68}Ga from its parent ^{68}Ge and the quality of the final product should be ascertained.

(3) Development of a separation scheme for n.c.a. radiobromine and n.c.a. radiogallium from a proton-irradiated ZnSe target. The adsorption behaviour of n.c.a. radiobromine, n.c.a. radiogallium, zinc and selenium towards the cation-exchange resin Amberlyst 15, in H^+ form, and towards the anion-exchange resin Dowex 1x10 in Cl^- and OH^- forms should be studied. The separation of radiobromine should also be tested via solvent extraction using TOA in o-xylene. The optimium separation scheme should be applied to the production of ^{77}Br and ^{67}Ga from the same target.

(4) The formation of the Auger electron emitter ^{80m}Br ($T_{1/2}$= 4.4 h) through the ^{80}Se(p,n)^{80m}Br reaction should be investigated up to 18 MeV using enriched ^{80}Se targets, allowing a determination of the excitation function of the reaction. The expected thick target yield should be calculated.

3. Experimental

3.1 Chemicals and Reagents

All chemicals purchased were of high purity. Aluminium and copper foils (99.99 % pure) of natural isotopic composition and thickness between 10 and 100 μm, which were employed as beam monitor and/or absorber foils in cyclotron irradiations, were supplied by Goodfellow, UK. Germanium (IV) oxide (99.999%) was purchased from Strem Chemicals Inc., Germany. Gallium(III)-oxide (99.99%) and zinc selenide powder (corn size 5 μm, 99.99 %) were purchased from Sigma-Aldrich Co., Germany. GeO_2, Ga_2O_3 and ZnSe were used as target materials in proton irradiations at the cyclotron.

Concentrated nitric acid (65 %), hydrochloric acid (37%), sulphuric acid (98 %), acetic acid (98 %) and other reagents like potassium iodide, sodium hydroxide, hydrogen peroxide, zinc sulphate and ammonium chloride were supplied by Fluka AG, and Sigma-Aldrich Co, Germany. They were of analytical grade.

Organic solvents like toluene, o-xylene, benzene, carbontetrachloride, n-hexane, cyclohexanone, liquid anion exchangers like Aliquat 336 (trioctylmethyl ammonium chloride) and tri-octyl amine, and strongly acidic cation exchange resins Amberlite IR-120 (H^+ form, 20-50 mesh) resin, Amberlyst 15 (H^+ form, 20-50 mesh) and Dowex 1x10 (Cl^- form, 200-400 mesh) were purchased from Merck, Germany. Diisopropylether was obtained from Fluka AG, Germany.

3.2 Irradiation Experiments

3.2.1 Irradiation Facilities

The irradiations were performed at the Baby Cyclotron BC1710 (Fig 3.1) and at the injector cyclotron of the Cooler Synchrotron COSY (Fig 3.2), both at the Forschungszentrum Jülich GmbH. The incident proton energy used in irradiations at the BC1710 was 17 MeV. Its target system includes an external irradiation facility, as shown in Fig. 3.1. For irradiations with proton energies up to 45 MeV the injector of COSY was used. The target system at the injector consists of an internal irradiation facility, a sketch of which is shown in Fig. 3.2. The irradiation beam is extracted with a tungsten septum. The energy adjustment in the target was done by introducing degrader foils into the stack. The beam current used was about 250 to

500 nA and the usual irradiation time was about 1 hour. During the bombardment the targets were cooled at the back by circulating water. Fig. 3.3 shows the target holder, in which the stack and/or Al capsule containing the pressed target material is placed. This holder consists of an Al body and an adjustable stack holder.

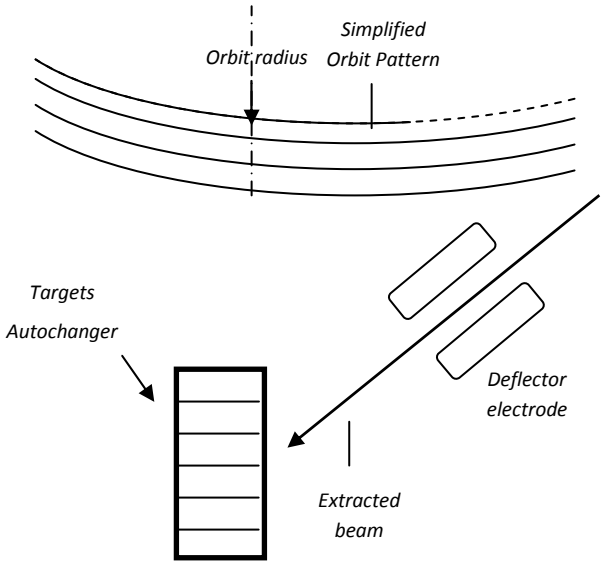

Fig. 3.1: The Baby cyclotron BC1710 and its remotely controlled target, Autochanger (Japan-Steel Works, Ltd), installed at the INM-5.

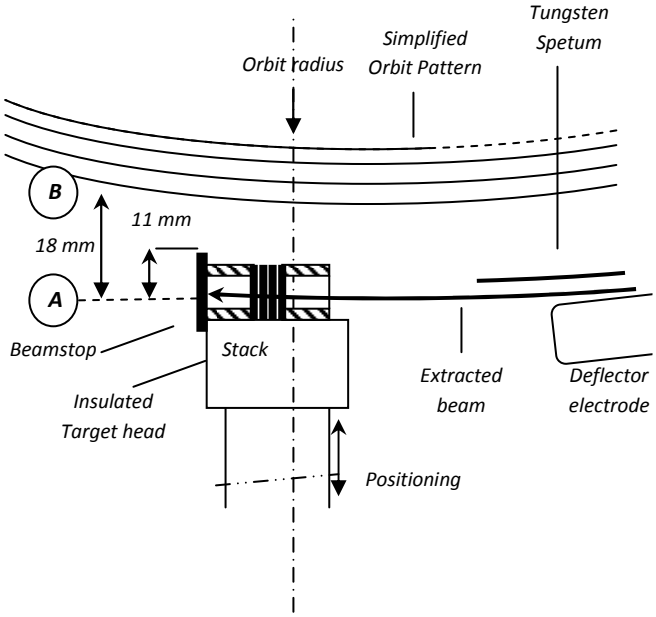

Fig. 3.2: Photograph of the Jülich Isochronous Cyclotron (JULIC) used as injector for COSY, and sketch of the target set-up inside the cyclotron chamber for irradiations.

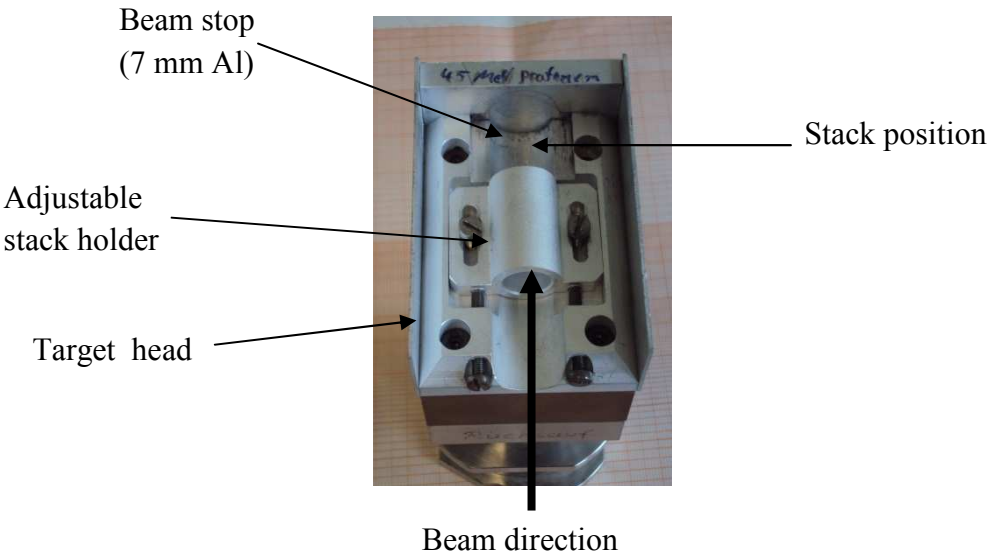

Fig. 3.3: Target holder for irradiation of samples at the injector of COSY

3.2.2 Stacked-foil Irradiation Technique

The stacked-foil technique was used for irradiations of samples for production and cross section measurements. A combination of target samples with monitor and absorber foils enables the adjustment of different projectile energies in the individual samples (see section 1.2.4).

3.2.3 Determination of Charged Particle Flux

The individual charged particle flux during different irradiation experiments was measured via beam integrators at Farady cups, which are available at the cyclotrons used. In addition, in all experiments monitor foils were inserted to estimate the beam current.

The proton beam currents were generally determined using Cu foils, utilizing the nuclear reactions $^{nat}Cu(p,xn)^{62,63}Zn$. For high energies the cross sections of the $^{nat}Cu(p,xn)$ processes are rather low; so the use of Ni monitor foils was more advantageous using $^{nat}Ni(p,x)^{57}Ni$ reaction. Figs. 3.4, 3.5 and 3.6 show the monitor excitation functions, from which the reaction cross section at a particular projectile energy was taken. The fluxes were calculated using the absolute activity induced in the monitor foils.

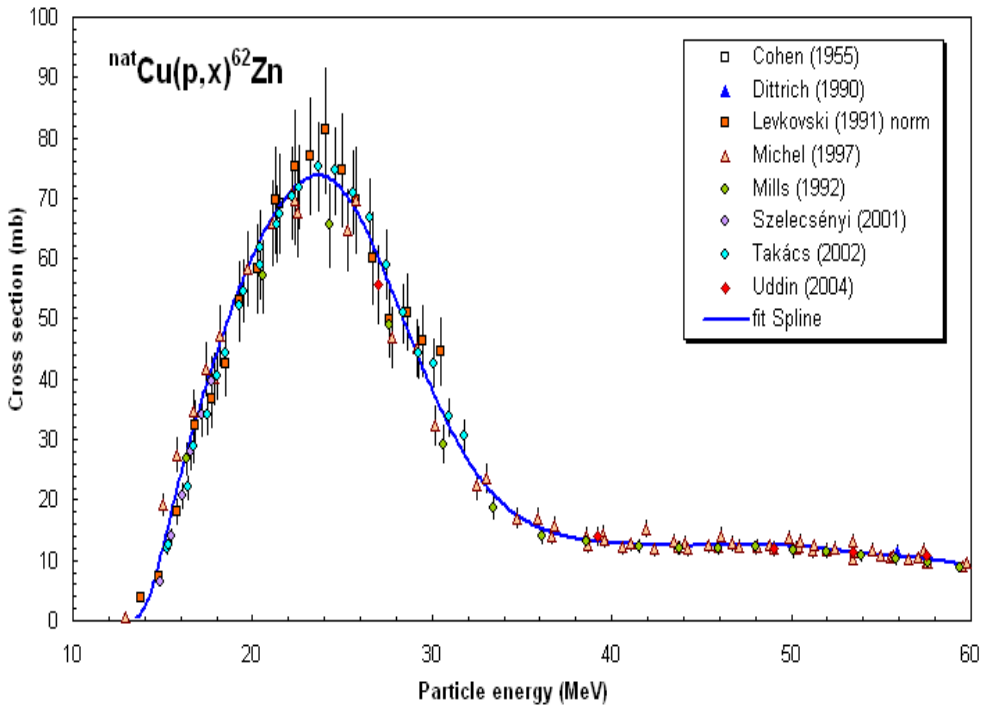

Fig. 3.4: Excitation function of the $^{nat}Cu(p,x)^{62}Zn$ reaction, taken from IAEA-TECDOC-1211, for the determination of the proton flux.

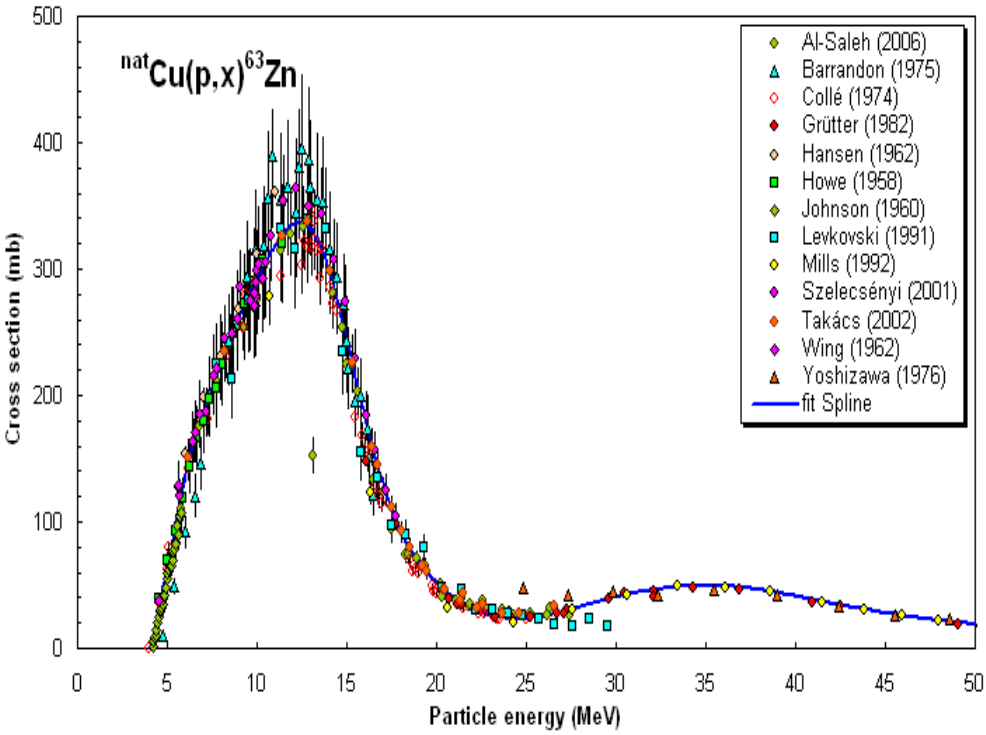

Fig. 3.5: Excitation function of the $^{nat}Cu(p,x)^{63}Zn$ reaction, taken from IAEA-TECDOC-1211, for the determination of the proton flux.

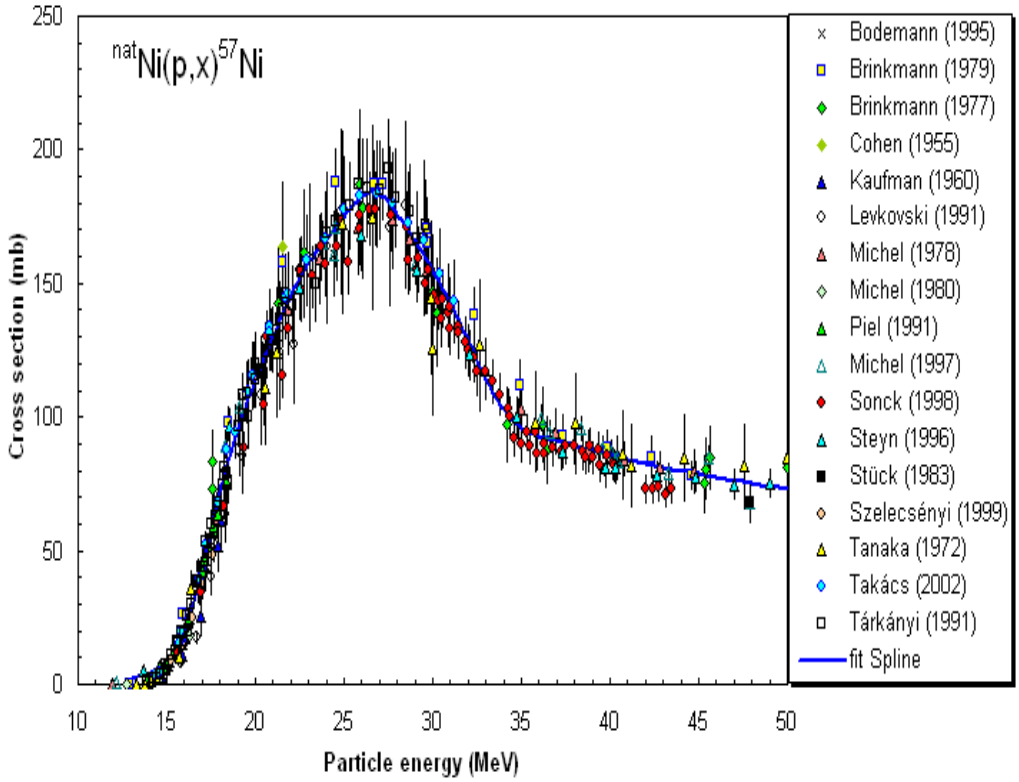

Fig. 3.6: Excitation function of the $^{nat}Ni(p,x)^{57}Ni$ reaction, taken from IAEA-TECDOC-1211, for the determination of the proton flux.

3.3 Target Preparation

Materials like Al, Ti, Cu, Mo, Ag and Au are commercially available as high purity foils of various thicknesses. In other cases, several techniques can be used to prepare thin samples. These are; mechanical pressing, sedimentation of a suspension, electro-deposition, evaporation, or sputtering. Some of these techniques like sedimentation and mechanical pressing are used only for materials in a powder form. The others can be used for any form of materials, depending on their chemical and physical behaviors. The preparation of enriched isotope samples needs considerable precautions due to their high cost, and their availability only in small quantities. Uniformity of the prepared sample is a crucial parameter in cross-section work. In general, the calculation of energy degradation is more accurate in case of homogenous thin foils.

3.3.1 Preparation of Targets via Mechanical Pressing

For the preparation of GeO_2, Ga_2O_3, ZnSe samples, pellets of different thicknesses were pressed using high-purity materials at 10 tons/cm^2. Fig 3.7 shows the real photo and construction of the tool used for this purpose. It was made of stainless-steel. It consists of two cylinders; one of them is used as a base, with a big central hole, in which the second cylinder can be inserted. The second cylinder also involves a central hole with 10 mm diameter through which the rod of 10 mm diameter passes. The pressed pellet was placed into an Al capsule for production of radionuclide.

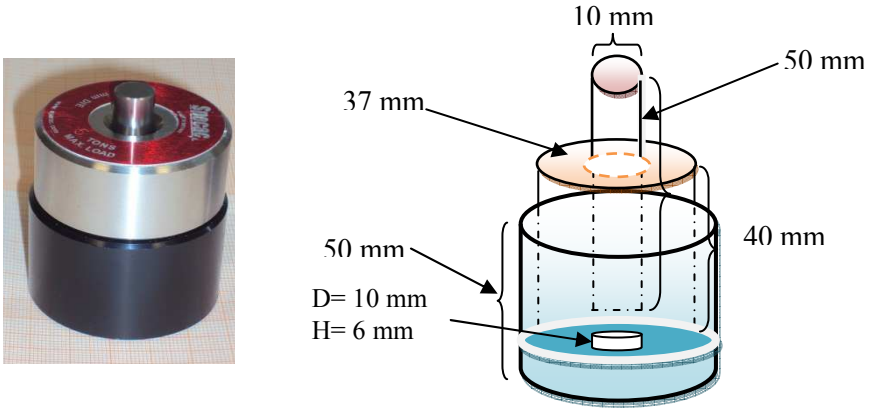

Fig. 3.7: Pressing device used for sample preparation

3.3.2 Preparation of Zn Targets via Electrodeposition

The radionuclide ^{67}Ga was produced using the ^{nat}Zn(p,xn)^{67}Ga nuclear reaction. Zinc targets used for this purpose were prepared by electrodeposition using a stirring anode. The electrolytic solution used for zinc deposition was prepared by dissolving 3-5 g of $ZnSO_4$ in distilled water (50 mL). A copper cathode and a platinum anode were used. The electrolytic cell takes 10 ml of solution. The voltage was adjusted to 5.5 V and the current to 150 mA. The applied current decreased during electrodeposition process due to the decrease in the conductivity of the solution as the zinc layer grew. A layer of 200-300 mg of zinc was obtained, depending on the time of electrodeposition, anode stirring and solution temperature. Fig. 3.8 represents the cell used for electrodeposition (cf. Mushtaq and Qaim, 1990).

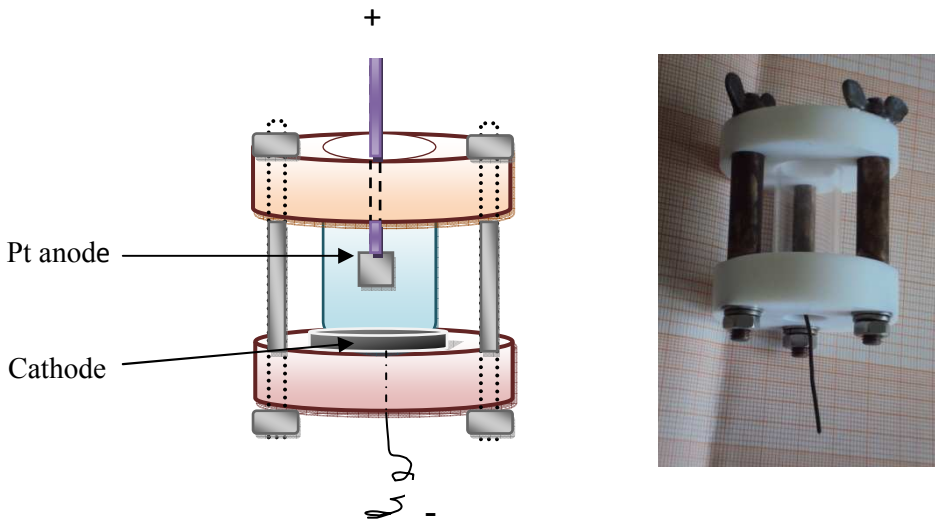

Fig. 3.8: Electrodeposition cell with stirring Pt anode (Mushtaq and Qaim, 1990)

3.3.3 Preparation of Thin Targets via Sedimentation using Enriched ^{80}Se

For the preparation of thin targets needed in the investigation of the ^{80}Se(p,n)^{80m}Br reaction, the sedimentation technique was applied (Rösch et al. 1993), using a sedimentation cell made of Teflon, as it is shown in Figure 3.9. Aluminium foils of 100 µm thickness (99.5% pure) were used as backings. The foil was fixed and the enriched ^{80}Se (99.9 %) material to be sedimented was transferred on top in the form of a suspension. The solvent was slowly evaporated, leading to the formation of thin layers attached to the backing foil. The homogeneity of the sample was verified using either a microscope or a strong magnifying lens (LUXO Deutschland GmbH). The deposited layer was carefully covered with an aluminium foil of 10 µm thickness for protection.

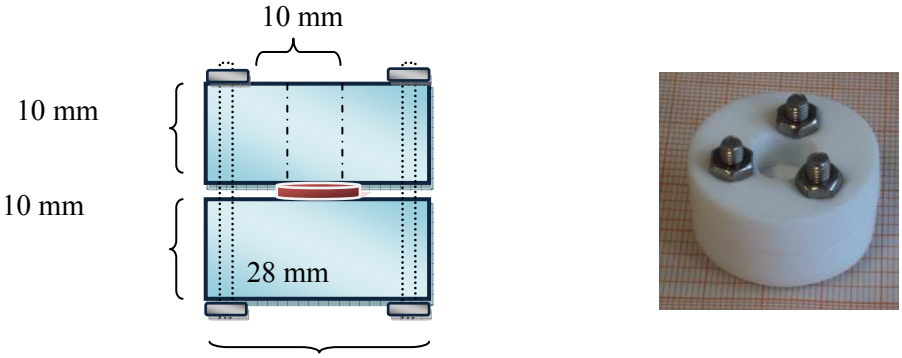

Fig. 3.9: Scheme and picture of a sedimentation cell

3.4 Determination of Radioactivity

3.4.1 γ-ray Spectrometery

To determine the radioactivity of each radionuclide, γ-ray spectrometery with a high purity germanium (HPGe) detector was used. The detector was shielded from the background radiation by a lead cylinder with an inner layer of copper to reduce gamma-ray scattering. The software Gamma Vision (Version 6.06, EG&G Ortec) was used for peak area analysis. The program applies Gaussian fittings to the peaks of interest, whose search was done manually.

There are several factors that affect the detection accuracy of the radiation. Among them the detector efficiency, is most important. It represents the probability with which an emitted particle or photon is detected in the counter. The efficiency includes the geometrical aspect, indicating the probability that the emitted radiation reaches the detector, as well as the physical aspects within the counting volume of the detector. Measurement of the absolute photo-peak detection efficiency at different distance as a function of energy was carried out with certified γ-ray standard sources of ^{133}Ba, ^{137}Cs, ^{154}Eu, ^{60}Co. In Fig. 3.10 an example of the correlation of counting efficiency and γ-ray energy can be observed.

In addition, the use of standard sources allows the determination of the dead time (TD), which refers to the time interval in which the associated electronics are busy and cannot record any incoming pulses. As the activity increases the count rate increases and more fractional loss occurs. Therefore the source to detector distance should be optimized according to minimum dead time and suitable count rate.

The other two important factors are the pile-up and random coincidence. In this case the probability of summing up coincidence pulses is higher than the result from randomly emitted photons. The summing loss depends mainly on the source to detector distance and the detector size. In random coincidence, it is possible at high count rate that two pulses are detected simultaneously and recorded as one pulse. The distance of each sample to the detector was between 10 and 50 cm, so that the dead time was always lower than 5 % and the loss in count rate due to coincidence effects could be neglected.

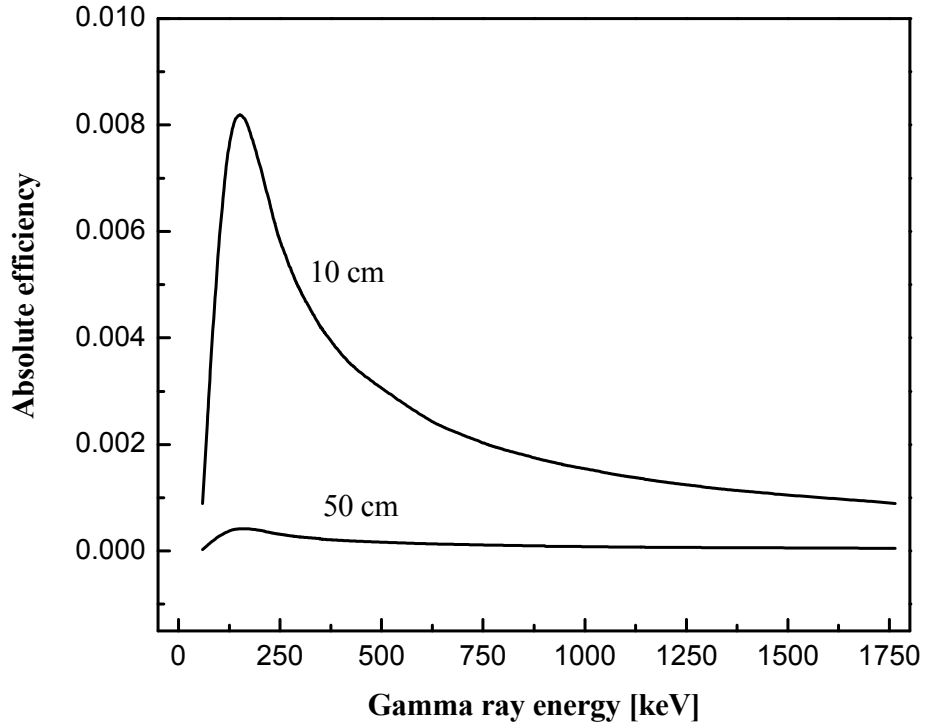

Fig. 3.10: Absolute efficiency fitted curves of a HPGe γ-ray detector for two different source to-detector-distances.

While counting ^{72}As ($T_{1/2}$= 26.01 h), the formation of ^{72}Ga($T_{1/2}$=14.1 h) via (p,αn) and (p,2p3n) processes on ^{76}Ge had to be taken into consideration, because of its interference with both the significant γ-lines of ^{72}As.

For measurement on ^{80m}Br, emitting only a low energy γ-ray of 37.1 keV, a well calibrated thin HPGe SLP-detector (EG&G Ortec) was used, which consisted of an active layer of diameter of 3.2 cm, a depth of 1.3 cm and a thick 0.03 mm Be window. Concerning the detection of ^{77}Br, the possibility of interference caused by coproduced ^{77}As had to be considered. This was taken into account by analysing the rather weak 297.2 keV γ-ray of ^{77}Br, which is not shared by its isobar, in addition to the two main γ-rays of energies 239.0 keV and 520.6 keV. Within the limits of uncertainty, no ^{77}As activity was detected.

The radioactivity of the monitor reaction products ^{62}Zn ($T_{1/2}$= 9.26 h; E_γ= 596.7 keV; I_γ = 25.7 %), ^{63}Zn ($T_{1/2}$= 38.1 min; E_γ= 669.76 keV; I_γ= 8.4 %; E_γ=962.17 keV, I_γ = 6.6 %) and and ^{57}Ni ($T_{1/2}$= 35.6 h; E_γ= 127.16 keV; I_γ= 16.7 %; E_γ= 1377.63 keV, I_γ = 81.7 %) was determined via standard gamma ray spectrometry.

3.5 Radiochemical Separation of Radioarsenic from GeO_2

The GeO_2 pellet was irradiated at the injector of COSY (see above). The radionuclides of arsenic formed were ^{71}As, ^{72}As, ^{73}As and ^{74}As. In addition, the radionuclides ^{69}Ge ($T_{1/2}$ =1.63 d) and ^{67}Ga ($T_{1/2}$ = 3.26 d) useful for tracer studies were also formed.

3.5.1 Target Dissolution

Dissolution of the irradiated GeO_2 pellet in concentrated or dilute HCl was avoided because of the potential formation of volatile $GeCl_4$. At first a stock solution of the activated sample was prepared by dissolving the pellet (1 g) with gentle heating in 250 mL H_2O to avoid possible interferences from K^+ ions or KCl. This solution was used for studying the effects of KI-concentration, as well as those of various acids and organic solvents. Later the target (1 g) was dissolved in 20 mL of 2 M KOH solution at room temperature to make the dissolution faster and to achieve the solution in a small volume. The alkaline solution was thereafter acidified with HCl and used for further studies.

3.5.2 Determination of the As(III)/ As(V) Ratio

The As(III)/ As(V) ratio after dissolution of the target in H_2O was determined by thin layer chromatography (TLC) (Jahn, 2009). A 20 µL aliquot of the respective solution was spotted about 1 cm from the end of a Si-60 thin layer on Al plate. The plate was developed for 10 min in a mixture of 0.01 M aqueous $NaHC_4H_4O_6$ /CH_3OH solution in a ratio of 3/1 as mobile phase. After drying in open air, the locations of the origin, As(III), As(V) and the front on the developed plate were identified by electronic autoradiography (Instant-Imager, Packard Instruments Company). The retention factor was determined using the equation:

$$R_f = \frac{\text{distance travelled by substance}}{\text{distance travelled by solvent front}} \qquad 3.1$$

The retention factors (R_f) of 0.6 and 0.9 were used to specify As(III) and As(V), respectively (Jahn, 2009). In order to examine the radionuclidic purity of these species, the radioactivity of the corresponding zone was assayed using gamma ray spectrometry.

3.5.3 Development of Radioarsenic Separation

3.5.3.1 Solvent extraction of radioarsenic in presence of bulk germanium

The radiochemical separation of n.c.a. radioarsenic from n.c.a. radiogallium and bulk Ge was carried out via solvent extraction from acid media using organic solvents. The

predominant radionuclides generated in the target, i.e. ^{71,72,74}As, ^{69}Ge and ^{67}Ga (see above) were used to achieve complete balance of the separation process. Several optimization experiments were performed to determine the optimum conditions for separation and recovery of arsenic radionuclides which are described in detail below. In general, for extraction 10 mL each of organic and aqueous phases were shaked for 1 min in a 25 mL separatory funnel. After separation 5 mL of each phase were taken and the activity of the radionuclides in both phases was determined by γ-ray spectrometry; therefrom the radiochemical yield was calculated. All experiments were carried out at room temperature.

After the optimization process to find the optimum separation conditions, using several fractions of the whole target, the extraction of radioarsenic was also studied after removal of the bulk amount of germanium.

3.5.3.1.1 Effect of acidity and iodide concentration

At first the extraction of radioarsenic by cyclohexane from an aqueous solution of the target acidified with hydrochloric acid (containing bulk germanium) was investigated to study the effect of pH. The HCl concentration was varied stepwise from 4 to 9 M without adding KI, and then from 2 to 7 M with varying KI concentrations (0.1, 0.5 and 1.0 M). Thereafter the effect of KI concentration up to 1.0 M in steps of 0.1 M was studied at 5 M HCl in detail. The use of KBr instead of KI was also tested, but there was no extraction of radioarsenic from 5 M HCl and 1 M KBr.

3.5.3.1.2 Effect of various acids

Besides HCl, the extraction of As with cyclohexane was investigated using the acids $HClO_4$, HNO_3, HBr, and H_2SO_4, each of them 5 M at 1 M KI concentration.

3.5.3.1.3 Effect of organic solvents

With the optimized conditions, i.e, 1 M KI and 5 M HCl, the effect of the organic solvents cyclohexane, chloroform, toluene, heptane and diethyl ether on the extraction capability was studied.

3.5.3.1.4 Back extraction of arsenic

The back extraction of radioarsenic from the cyclohexane into the aqueous phase was investigated using different media, namely 7 M ammonia, 0.1 - 2 M HCl, 0.1 -2 M NaOH, water and 0.1% H_2O_2.

3.5.3.2 Extraction of radioarsenic after removal of bulk germanium

For precipitation of the bulk GeO_2 matrix the irradiated target (1 g) was dissolved in 20 mL of 2 M aqueous KOH and the pH of the solution was carefully adjusted to 7 - 8 with a minimum volume of concentrated HCl. At this pH, Ge was precipitated as hydrated GeO_2, which was removed from the solution by filtration using a 0.2 μm filter paper. The filtrate and the precipitate were then subjected to gamma ray spectrometry. After acidification of the filtrate up to a concentration of 5 M HCl, and adjusting to 1 M KI, the radioarsenic was extracted with cyclohexane as described above. Depending on the results obtained, a series of experiments was done on the solution obtained after precipitation to decrease the content of germanium. The extraction of radioarsenic and germanium was studied by decreasing the amount of KI to 0.5 M and at various HCl concentrations.

3.5.3.3 Optimized procedure for separation of radioarsenic

The GeO_2 target was dissolved in 20 mL of 2 M KOH and the radioarsenic was extracted after acidification of the solution with HCl. A selective extraction, consisting of extraction of radioarsenic by cyclohexane followed by a re-extraction in the aqueous medium, was developed and optimized.

3.5.4 Production and Quality Control of ^{71}As and ^{72}As

The optimized separation method was used in the production of ^{71}As and ^{72}As via proton irradiation of GeO_2. Two GeO_2 targets, each of them weighing about 1 g, were irradiated, in a row for one hour at a beam current of 1 μA. The proton energy range in the first target was E_p= 44 → 28.5 MeV, and in the second E_p= 25.8 → 0 MeV. The proton energy degradation within the stack was calculated using the program STACK, which is based on the range-energy relationship described by Williamson et al. (1966). Table 3.1 gives a stack calculation for GeO_2. The exact proton flux was determined as described earlier. The separation of radioarsenic from the irradiated germanium dioxide via solvent extraction was done as follows.

The irradiated target was dissolved in 10 mL of 2 M KOH and the radioarsenic was extracted with cyclohexane from that solution after acidification to 4.75 M HCl and adjusting the KI concentration to 0.5 M. The radioarsenic was back-extracted into 10 mL of an aqueous 0.1 % H_2O_2 solution. Traces of co-extracted germanium were extracted with cyclohexane after adding 10 μL (30 %) H_2O_2 solutions and making HCl concentration as 9.2 M.

Table 3.1: Results of the calculation of energy degradation within the GeO_2 sample using the computer code *STACK*.

Projectile data			
Type	Atomic no. of projectile	Molar weight	**Primary energy [MeV]**
H	1	1.0079	**45**

Target	**Atomic no. of target**	**Molar weight [g/mol]**	**Thickness [g/cm^2]**	**Average energy [MeV]**	**Energy in [MeV]**	**Energy out [MeV]**	**Energy absorption [MeV]**	
Cu	29	63.546	7.926E-03	44.97	45.00	44.93	0.07	
Al	13	26.98154	5.402E-02	**44.64**	44.93	44.36	0.57	
Ge	**32**	**72.59**	**1.015E-01**	**43.93**	**44.36**	**43.49**	**0.86**	Degradation of energy in front target
O	8	15.9994	4.474E-02	**43.22**	43.49	42.95	0.54	
Ge	32	72.59	1.015E-01	**42.51**	42.95	42.07	0.88	
O	8	15.9994	4.474E-02	**41.79**	42.07	41.51	0.56	
Ge	32	72.59	1.015E-01	**41.06**	41.51	40.60	0.91	
O	8	15.9994	4.474E-02	**40.32**	40.60	40.03	0.57	
Ge	32	72.59	1.015E-01	**39.57**	40.03	39.10	0.93	
O	8	15.9994	4.474E-02	**38.81**	39.10	38.51	0.59	
Ge	32	72.59	1.015E-01	**38.03**	38.51	37.55	0.96	
O	8	15.9994	4.474E-02	**37.25**	37.55	36.94	0.61	
Ge	32	72.59	1.015E-01	**36.45**	36.94	35.95	0.99	
O	8	15.9994	4.474E-02	**35.64**	35.95	35.32	0.63	
Ge	32	72.59	1.015E-01	**34.81**	35.32	34.30	1.03	
O	8	15.9994	4.474E-02	**33.97**	34.30	33.64	0.65	
Ge	32	72.59	1.015E-01	**33.11**	33.64	32.58	1.06	
O	8	15.9994	4.474E-02	**32.24**	32.58	31.90	0.68	
Ge	32	72.59	1.015E-01	**31.34**	31.90	30.79	1.11	
O	8	15.9994	4.474E-02	**30.43**	30.79	30.08	0.71	
Ge	32	72.59	1.015E-01	**29.50**	30.08	28.92	1.16	
O	8	15.9994	4.474E-02	**28.54**	28.92	28.17	0.75	
Al	13	26.98154	5.402E-02	**27.75**	28.17	27.34	0.83	
Cu	29	63.546	7.963E-03	**27.29**	27.34	27.24	0.10	
Al	13	26.98154	5.402E-02	**26.81**	27.24	26.39	0.85	
Ge	**32**	**72.59**	**9.588E-02**	**25.78**	**26.39**	**25.18**	**1.21**	Degradation of energy in back target
O	8	15.9994	4.227E-02	**24.78**	25.18	24.38	0.79	
Ge	32	72.59	9.588E-02	**23.74**	24.38	23.09	1.29	
O	8	15.9994	4.227E-02	**22.67**	23.09	22.24	0.85	
Ge	32	72.59	9.588E-02	**21.55**	22.24	20.86	1.39	
O	8	15.9994	4.227E-02	**20.39**	20.86	19.93	0.93	
Ge	32	72.59	9.588E-02	**19.17**	19.93	18.42	1.51	
O	8	15.9994	4.227E-02	**17.90**	18.42	17.39	1.03	
Ge	32	72.59	9.588E-02	**16.54**	17.39	15.70	1.69	
O	8	15.9994	4.227E-02	**15.11**	15.70	14.52	1.18	
Ge	32	72.59	9.588E-02	**13.54**	14.52	12.56	1.96	
O	8	15.9994	4.227E-02	**11.85**	12.56	11.13	1.43	
Ge	32	72.59	9.588E-02	**9.89**	11.13	8.66	2.47	
O	8	15.9994	4.227E-02	**7.65**	8.66	6.64	2.02	
Ge	32	72.59	9.588E-02	**4.47**	6.64	2.29	4.35	
O	8	15.9994	4.227E-02	**1.15**	2.29	0.00	2.29	
Al	13	26.98154	5.402E-02	**0.00**	0.00	0.00	0.00	

Experimental and theoretical radionuclidic yields were compared and the radionuclidic impurities with the separated radioarsenic were determined using γ-ray spectrometry. The chemical impurities in the separated radioarsenic solution were detected by ICP-MS after the decay of the radionuclides (Elan 6100 at the Central Department for Chemical Analysis of the Forschungszentrum Jülich).

3.6 Radiochemical Separation of Radiogermanium from Irradiated Ga_2O_3

The radionuclides ^{68}Ge ($T_{1/2}$ =270.8 d), ^{69}Ge ($T_{1/2}$ = 1.63 d), ^{67}Ga ($T_{1/2}$ = 3.26 d) and ^{68}Ga ($T_{1/2}$ = 67.63 min) were produced by the proton irradiation of Ga_2O_3. Several optimization studies were carried out using ^{69}Ge and ^{67}Ga as tracers, both of them were formed in 45 MeV proton-irradiation of ^{nat}Ga via the nuclear reactions ^{69}Ga(p,n)^{69}Ge and ^{69}Ga(p,p2n)^{67}Ga, respectively. The n.c.a. ^{68}Ge and ^{69}Ge mixture was separated from the Ga_2O_3 target via solvent extraction. For the determination of the distribution coefficients and the optimization studies a stock solution of the activated sample was prepared by dissolving the irradiated matrix in 20 mL of 8 M H_2SO_4 with heating for 30 min.

3.6.1 Effect of H_2SO_4 and HCl Concentration on the Extraction of Radiogermanium

The effect of H_2SO_4 concentration in the range of 6 to 14 M on the separation of radiogermanium from proton irradiated Ga_2O_3 with and without the presence of different concentrations of HCl was studied using toluene. The K_d value were determined. After extraction, ^{68}Ge/^{69}Ge was back extracted into H_2O. Separation of ^{68}Ge/^{69}Ge mixture from the irradiated Ga_2O_3 using chloroform at different sulphuric acid concentration was also investigated at 0.4 M HCl. A 5 mL aliquot was taken from each phase and measured using γ-ray spectrometry to calculate the distribution of radigermanium and gallium between the aqueous and organic phases.

3.6.2 Optimized Procedure for Radiogermanium Separation

The optimized procedure for the separation of radiogermanium consisted of the following: Proton irradiated Ga_2O_3 was dissolved in 8 M H_2SO_4 and HCl was added to reach a concentration of 0.4 M. It was then shacken with 10 mL of toluene for 2 min. Radiogermanium was extracted in toluene while gallium remained in the aqueous phase. Thereafter radiogermanium was back-extracted from toluene into 10 mL H_2O.

3.6.3 Production and Quality Control of ^{68}Ge

To test the radiochemical separation yield of radiogermanium, production experiments were performed following the optimized separation scheme, and the resulting yield was compared with the theoretical one. A Ga_2O_3 pellet was irradiated with protons, in the energy range E_p= 31→ 15.6 MeV. Table 3.2 gives an example of the calculation performed for the required target thickness for degradation of proton beam from 31 to 15.6 MeV. The incident proton energy of 45 MeV was degraded to the desired energy by Al absorber foils. After dissolution of the irradiated target in 8 M H_2SO_4, and addition of 0.4 M HCl, ^{68}Ge (n.c.a.) was separated with toluene and back extracted into water.

The theoretical yield for the certain energy range was taken from the calculated literature values (see section 1.7.2),. The separation yield of radiogermanium from the proton irradiated Ga_2O_3 was determined by a comparison of the practical yield of the separated radiogermanium with the calculated theoretical yield. The radionuclidic purity of the separated radiogermanium was determined by γ-ray spectrometry. The chemical impurities in the separated radiogermanium solution were detected after the decay of the radionuclides by ICP-MS (Elan 6100).

Table 3.2: Calculation of the required thickness of Ga_2O_3 to degrade the proton energy from 31 to 15.6 MeV and loss in yield at a given beam current compared with a pure Ga target.

Composition	R (mg/cm^2)	$R_{Ga_2O_3}$	Loss of yield
Ga (74 %)	935.1	$\frac{1}{R_{Ga_2O_3}} = \frac{0.74}{935.1} + \frac{0.26}{666.8}$	$\frac{846.5}{935.1}(0.74) = 0.67$
O (26%)	666.8	$R_{Ga_2O_3} = 846.5$	33 % loss in yield at a given beam current

3.7 Radiochemical Separation of Radiogallium from Radiogermanium

For optimization studies on the separation of n.c.a. ^{68}Ga from a mixture of ^{68}Ge and ^{69}Ge, a longer-lived tracer of gallium, e.g. ^{67}Ga ($T_{1/2}$= 3.26 d), was also needed. It was produced by the ^{nat}Zn(p.x)^{67}Ga nuclear reaction on natural zinc.

3.7.1 Separation of n.c.a. ^{67}Ga from Irradiated Zinc Target for Tracer Use

The electroplated ^{nat}Zn target was irradiated with 17 MeV prtons at the Baby Cyclotron (BC1710). A stock solution was preparead by dissolving the irradiated target in HCl, the Cu

backing is not dissolved under this conditions and taken out of the solution, evaporation to almost dryness and dissolution in water. The radiochemical separation of n.c.a. ^{67}Ga from zinc was done via solvent extraction and anion exchange chromatography. Distribution coefficients of ^{67}Ga and zinc on anion exchange resin Amberlite CG-400-II (Cl^- form, 200-400 mesh) at various HCl concentrations were studied (see below). For solvent extraction, diisopropylether was used. The organic and aqueous phases were transferred to a separatory funnel and shaken for 2 min. The effect of various HCl concentrations (3-10 M) on the extraction of radiogallium from zinc target was studied. After optimizing the extraction condition, ^{67}Ga was back-extracted by shaking with 10 mL of H_2O for 2 min. The solution was evaporated to almost dryness and the residue dissolved in 5 mL H_2O. The purity of ^{67}Ga was ascertained by the absence of ^{65}Zn via γ-ray spectroscopy.

3.7.2 Cation Exchange Separation of Radiogallium from Radiogermanium

Batch experiments: The separation of radiogallium from the ^{68}Ge/^{69}Ge in admixture was carried out using the strong cation-exchanger Amberlite IR-120, which is a gel type strongly acidic cation exchange resin of the sulfonated polystyrene type. As aqueous phase, HCl was used. The distribution coefficient (K_d) was calculated using the equation, given below:

$$K_d = \frac{\text{Activity / g of adsorbent}}{\text{Activity / mL of eluent}} \qquad 3.2$$

In each experiment, 100 mg anion-exchanger was placed in a vial (15 mL) with 10 mL of HCl of different concentrations containing n.c.a. radiogallium and n.c.a. ^{68}Ge/^{69}Ge. After shaking for 60 minutes (this time was found to be sufficient to reach the equilibrium), the phases were left to settle down; 5 mL of the aqueous phase was pipetted out, and measured by γ-ray spectrometry.

Column experiments: A glass column (1 cm in diameter, 24 cm high) was packed with Amberlite IR-120 (H^+ form) and washed with 0.5 M HCl immediately prior to use. A 500 µL portion of the solution containing n.c.a ^{68}Ge/^{69}Ge was taken and 200 µL of a solution of n.c.a ^{67}Ga was added. The two solutions were mixed and hydrochloric acid was added to achieve a concentration of 0.5 M in a total volume of 10 mL. Then this mixture was loaded on to the column. According to the results of the K_d measurements, the column was then rinsed with 150 mL of 0.5 M HCl at a flow rate of 3 mL/min. Under these conditions all the activity of radiogallium was adsorbed on the resin and n.c.a. ^{68}Ge/^{69}Ge are eluted. The elution process was continued till no ^{67}Ga was detected in the eluate. The elution profiles of radiogallium and

radiogermanium as a function of eluted volumes were measured. 3 M HCl were used to elute radiogallium, the eluted fractions were then counted using a HPGe detector.

3.7.3 Solvent Extraction Separation of Radiogallium from Radiogermanium

The separation of radiogallium from radiogermanium via solvent extraction was also investigated. The solution was prepared as described above, transferred to a separatory funnel and shaken for 2 min with 10 mL of 0.1 M Aliquat 336 in an organic solvent. After disengagement, both aqueous and organic phases were investigated by γ-ray spectrometry, for ^{67}Ga and ^{69}Ge, in order to calculate their distribution coefficients. Various solvents, like o-xylene, carbon tetrachloride, benzene, n-hexane, and cyclohexanone were tested as diluents. The phase to volume ratio was kept at 1:1 to eliminate the problem of emulsification. Back extraction of radiogallium and radiogermanium from 0.1 M Aliquat 336 in o-xylene was studied with different concentrations of HCl (0, 0.5, 3, 4 M), 0.5 M H_2SO_4 and 0.5 M KOH.

3.7.4 Optimized Procedure for Separation and Quality Control of ^{68}Ga

The separation of the daughter n.c.a.^{68}Ga from the parent ^{68}Ge was done using the optimized procedure. The parent ^{68}Ge was acidified to 3 M HCl and n.c.a.^{68}Ga was separated via 0.1 M aliquat 336 in o-xylene. Traces of ^{68}Ge were back extracted from the organic phase by 3 M HCl (two times) while n.c.a.^{68}Ga was back extracted by 0.5 M KOH.

The separation yield of the daughter n.c.a.^{68}Ga from the parent ^{68}Ge was determined by a comparison of the activity of the separated n.c.a.^{68}Ga to the total activity before separation. The latter was determined non-destructivitly via γ-ray spectrometry prior to separation. The chemical impurities in the separated ^{68}Ga solution were detected after the decay of the radionuclides by ICP-MS.

3.8 Separation of Radiobromine and Radiogallium from Irradiated ZnSe Target

The target material ZnSe in the form of powder was pressed under a pressure of 10 tons /cm^2 to a 13-mm diameter pellet (see above). After putting this pellet in an Al capsule, it was irradiated at the injector of COSY with 45 MeV protons. The radionuclides ^{75}Br ($T_{1/2}$ = 1.5h), ^{76}Br ($T_{1/2}$ = 16.2 h), ^{77}Br ($T_{1/2}$ =57 h), ^{67}Ga ($T_{1/2}$ = 3.26 d), ^{65}Zn ($T_{1/2}$ = 244.26 d) and ^{75}Se ($T_{1/2}$ = 119.64 d) were formed.

3.8.1 Dissolution of ZnSe Target

The dissolution of ZnSe (250 mg) was investigated using HCl, HNO_3, and different concentrations of KOH. In the case of HCl, the sample was not completely dissolved even after addition of H_2O_2. ZnSe was dissolved very easily in conc. HNO_3 (4 mL). For KOH at least 10 mL of 10 M KOH and heating was needed to complete dissolution within 1 hour. So the sample was dissolved in conc. HNO_3 and 10 M KOH in the beginning to optimize the separation process. The dissolution of the sample in 10 M KOH proved to be the best.

3.8.2 Anion and Cation Exchange Studies

A series of experiments was done to study the effect of different concentrations of HCl, HNO_3, and KOH as the aqueous phase on the distribution coefficients (K_d) of no-carrier-added radiobromine, n.c.a. radiogallium, zinc and selenium on both Amberlyst 15 and Dowex 1x10 resin as solid phase. Amberlyst 15 resin is a strong acid cation exchanger, H^+-form, 20-50 mesh, while Dowex 1x10 resin is a strong base anion exchanger, Cl^- form, 200-400 mesh. In case of Amberlyst 15, we used it in the H^+ form, while Dowex 1x10 was washed with water and KOH to transfer it to OH^- form. 100 mg of pre-treated resin and 10 ml of aqueous phase were shaken for 60 min. The phases were left to settle and then 5 mL of an aqueous phase was pipetted out for counting by γ-ray spectrometry. The distribution coefficients (K_d) were determined using Eq. 3.2.

Resin preparation; The resin (20 g of Dowex 1x10) was washed with 100 mL of 1 mol L^{-1} hydrochloric acid followed by extensive rinsing with de-ionized water to neutral pH. Conversion to the hydroxide form was achieved by washing with 100 mL of 1 mol L^{-1} potassium hydroxide solution. After washing with de-ionized water the resin was dried overnight at 40 ^oC.

The effect of chloride ion concentration in the solution on the adsorption of radiobromine, radiogallium, zinc and selenium was studied. NH_4Cl was added to the aqueous phase to increase the chloride concentration, while the solid phase consisted of Dowex 1x10. The effect of sulfate ion concentration in the solution on the adsorption of radionuclides under investigation was studied, as well. For this propose Na_2SO_4 was added to the aqueous phase in order to increase the sulfate concentration, while the solid phase was Dowex 1x10.

Column chromatography experiments; A glass column (1cm in diameter, 6 cm high) was packed with Dowex 1x10 (3 g) and conditioned first with KOH in case of radiobromine

adsorption. In this work, 0.2 M H_2SO_4, tetra octyl methyl ammonium chloride in o-xylene have been used to find the optimum elution conditions. The column was then rinsed with 1 M KOH at a flow rate 1±0.2 mL/min. The solution containing the active sample 10 M KOH was diluted first to 1 M KOH and loaded onto the column. At this molarity all the radiobromine was adsorbed on the resin while radiogallium, zinc and selenium were not. 100 mL of 1 M KOH and 50 mL H_2O were passed through the column. Radiobromine was then eluted with 100 mL of 0.2 M H_2SO_4, and the eluted fractions were then counted. The elution profiles of radiobromine, radiogallium, zinc and selenium as a function of eluted volumes were measured. Comparison was made at the elution of bromine with 50 mM trioctyl methyl ammonium chloride in o-xylene.

The residue solution after adsorption of bromine contains radiogallium, zinc and selenium. Two experimental conditions were studied to separate radiogallium from Zn and Se; the first by dissolving 4 M NH_4Cl in a residue solution. For this, the sample was put into a Dowex 1x10 column (3 g, 6 cm height, Cl^- form) preconditioned with NH_4Cl. Under these conditions radiogallium was adsorbed while zinc and selenium were not. Then radiogallium was eluted with 0.1 M HCl. In case of the second experimental set up the residue solution was acidified up to 9 M HCl concentration. The column was first preconditioned by passing through 9 M HCl. The residue solution at 9 M HCl was passed through the column. For elution of zinc and selenium 9 M HCl was then passed through the column followed by 0.1 M HCl to elute radiogallium. Comparison of the two eluted conditions was done.

3.8.3 Separation of Radiobromine via Solvent Extraction

The solvent extraction of n.c.a. radiobromine and n.c.a. radiogallium using Trioctylamine (TOA) dissolved in o-xylene was done. The extraction solutions of desired concentrations were prepared by adding calculated amounts of TOA to xylene. In order to study the separation and extraction of radiobromine, about 10 mL of HNO_3 solution of a particular concentration containing measured activities were shaken with equal volume of TOA solution of a desired concentration for about 2 min. The effect of HNO_3 (0.1 -15 M) concentration on the extraction process of radiobromine was investigated using 0.7 M TOA in xylene. Different concentrations of TOA in o-xylene at 1 M HNO_3 were used to study the effect of TOA on the extraction process. Back extraction of radiobromine from the organic phase was studied with 0.5 and 1 M KOH.

3.8.4 Optimized Procedure for Separation of Radiobromine and Radiogallium

The procedure for the separation of radiobromine and radiogallium via anion exchange was optimized. After the dissolution of the ZnSe target in 10 M KOH, the solution was diluted to 1 M KOH, and passed through the anion exchange resin (Dowex 1x10 column preconditioned with 1 M KOH). Elution was done with 1 M KOH to remove radiogallium, zinc and selenium whereas radiobromine was adsorbed on the column. Then, the radiobromine was eluted using 0.2 M H_2SO_4. For separation of radiogallium, NH_4Cl was dissolved in the residue solution and its concentration made 4 M. The solution was then passed through the Dowex 1x10 column in chloride form, preconditioned with 4 M NH_4Cl. Radiogallium was adsorbed while zinc and selenium were eluted. Radiogallium was then eluted with 0.1 M HCl.

3.8.5 Quality Control of ^{76,77}Br and ^{66,67}Ga

The radionuclides ^{75}Se and ^{65}Zn formed in the irradiated target were used to measure the contamination of the solution with Se and zinc. The optimized separation method was used in the production of ^{76,77}Br and ^{66,67}Ga via proton irradiation of ZnSe target. A 260 mg ZnSe pellet was irradiated with E_p= 17→10 MeV protons for 1 hour at a beam current of 2 μA.

The separation yield of radiobromine and radiogallium was determined by a comparison of the practical yields of the separated radiobromine and radiogallium with the theoretical yields. The radionuclidic purity of the separated radiobromine and radiogallium was determined by γ-ray spectrometry. The chemical impurities in the separated solutions were detected after the decay of the radionuclides by ICP-MS (Elan 6100).

3.9 Study of the ^{80}Se(p,n)^{80m}Br Reaction

For production of the Auger electron emitting radionuclide ^{80m}Br, cross sections were determined for the nuclear process ^{80}Se(p,n)^{80m}Br from threshold up to 18 MeV. Thin targets of enriched ^{80}Se powder, used in irradiations, were prepared by utilizing the sedimentation technique, as described earlier (section 3.3.3). The samples were irradiated in a stacked-foil arrangement together with different monitor Cu foils at the Compact Cyclotron CV 28 of the Forschungszentrum Jülich. The proton energy degradation within the stack was calculated using the computer code STACK as described above.

3.9.1 Determination of the Absolute Activity

The measured radioactivity of all samples and monitor foils was converted to the radioactivity at the end of bombardment (EOB). The basis for the determination of the radioactivity from the measured γ-ray spectra is the counted number of decay incidents, represented by the peak area ***P*** of the specific γ-ray energy. This peak area is summed over the period of the measuring time T_{live}, thus the radioactive decay of the analysed sample during this time has to be considered and a corresponding decay correction has to be made. Therefore, for the calculation of the absolute radioactivity ***A*** at the beginning of the measurement, equation 3.2 is supplemented with the appropriate decay term.

$$A = \frac{\lambda P}{\varepsilon \ \ I_\gamma (1 - e^{-\lambda T_{live}})} \qquad 3.2$$

The dead time correction was included automatically in the registration of the measurement time. Due to the relatively large distance between the sample and the detector, the correction for coincidence effects could be neglected. The radioactivity A_{EOB} at the end of bombardment can then be calculated according to the equation of the radioactive decay.

$$A_{EOB} \ = \ A.e^{\lambda t} \qquad 3.3$$

t = time until beginning of measurement

3.9.2 Calculation of Nuclear Reaction Cross Section

From the experimentally determined absolute activity of the product at the end of bombardment (EOB), and the proton flux deduced via monitor reactions, the reaction cross section was calculated at each effective proton energy using the well known activation equation. Based on the known half-life ($T_{1/2}$), the bombardment time (t_B), the number of nuclei of the target element (N_X) in the sample and the abundance of the target isotope in the target element (H), the reaction cross section was calculated by reformulating the activation equation as follows.

$$\sigma = A_{EOB} \left(\Phi N_x H \left(1 - e^{-\frac{\ln(2)}{T_{1/2}} t_B} \right) \right)^{-1} \qquad 3.4$$

The projectile flux Φ was deduced from the measured radioactivity at EOB produced in the monitor foils.

3.9.3 Yield of the Produced Radionuclide

The produced quantity of the radionuclide is characterized by the yield value, which is calculated using the cross section data of the reaction. As the incident beam propagates through several thin foils in a row, its energy decreases due to the stopping powers of the materials involved. The reaction cross section in this case within the target includes an interval of values varying with the energy degradation. For the calculation of the yield, firstly the whole target thickness is divided into intervals of 1 MeV absorbed energy, which are considered as separate targets of the same material in cascade positions. The computer code *STACK* was used to calculate the thickness of selenium target in g/cm^2 corresponding to each energy step through all the energy range. Table 3.3 gives the calculations to degrade the energy from 18 to 1 MeV, in 1 MeV steps. The cross section values were taken from the experimental excitation function of the reaction, which was determined in this work.

The yield (in Bq) was then calculated using the following equation:

$$Y = \Phi \frac{N_A H}{M}(1 - e^{-\lambda t}) \int_{E_1}^{E_2} \left(\frac{dE}{dpx} \right)^{-1} \sigma(E) dE \qquad 3.5$$

where N_A = Avogadro number, H = abundance of the target isotope in the target element, M = atomic weight of the target element, Φ = beam current, (dE/d(px) = stopping power, σ(E) = cross section at the mean energy E of each interval, λ = decay constant of the product radionuclide, t = irradiation time

The value obtained by calculating the produced activity at each energy interval using the activation formula is called partial yield (differential yield). A summation over the whole energy range absorbed within the target results in a value known as the integral yield or thick target yield. From the resulting yields, it was possible to calculate the expected yield of a radioisotope over a certain range of energy by subtracting the integral yield at the end point from that at the starting point.

Table 3.3: Calculation of ^{80}Se thickness that degrades the proton energy in 1 MeV steps over the energy range 18 → 1 MeV using the computer code *STACK*.

Projectile data							
Type	Atomic no. of projectile	Molar weight	**Primary energy [MeV]**				
H	1	1.0079	18				
Target	**Atomic no. of target**	**Molar weight [g/mol]**	**Calculated thickness [g/cm^2]**	**Average energy [MeV]**	**Energy in [MeV]**	**Energy out [MeV]**	**Energy absorption [MeV]**
Se	34	80	6.236E-02	**17.50**	18.00	17.00	1.00
Se	34	80	5.919E-02	**16.50**	17.00	16.00	1.00
Se	34	80	5.665E-02	**15.50**	16.00	15.00	1.00
Se	34	80	5.405E-02	**14.50**	15.00	14.00	1.00
Se	34	80	5.106E-02	**13.50**	14.00	13.00	1.00
Se	34	80	4.859E-02	**12.50**	13.00	12.00	1.00
Se	34	80	4.534E-02	**11.50**	12.00	11.00	1.00
Se	34	80	4.261E-02	**10.50**	11.00	10.00	1.00
Se	34	80	3.976E-02	**9.50**	10.00	9.00	1.00
Se	34	80	3.638E-02	**8.50**	9.00	8.01	1.00
Se	34	80	3.352E-02	**7.50**	8.01	7.00	1.00
Se	34	80	3.014E-02	**6.50**	7.00	6.01	1.00
Se	34	80	2.702E-02	**5.50**	6.01	5.00	1.00
Se	34	80	2.344E-02	**4.50**	5.00	4.00	1.00
Se	34	80	1.982E-02	**3.51**	4.00	3.01	1.00
Se	34	80	1.614E-02	**2.51**	3.01	2.01	1.00
Se	34	80	1.221E-02	**1.51**	2.01	1.01	1.00

3.9.4 Determination of Uncertainties

The total uncertainty of the measured cross section was obtained by combining all the individual uncertainties in quadrature. In general the major uncertainties were associated with proton flux, γ-ray detector efficiency and peak area analysis. The sources of uncertainty can affect the calculated cross section values directly, or indirectly. For example, homogeneity of the prepared sample is not expressed by a certain parameter in the formula of the cross section but is considered as a source of error in calculated mass per cm^2. It also affects the degradation of energy within the stack and consequently contributes to the uncertainty of the estimated energy at every sample. The uncertainty can be classified also as random and systematic uncertainty. The random uncertainty expresses the random errors in experimental work, which are caused by unknown and unpredictable changes in the experiment. These

changes may occur in the measuring instruments or in the environmental conditions. The systematic uncertainty expresses the error which is found in all the experiments. It may occur because there may be something wrong with the instrument or its data handling system, or because the experimenter wrongly uses the instrument. The systematic uncertainty is for example, in beam current, γ-ray detector efficiency, isotopic enrichment etc. The most significant uncertainties and their estimated magnitudes are summarized in Table 3.4.

Table 3.4: The estimated uncertainties in cross-section calculation.

Individual uncertainties	**Magnitude [%]**
Target mass	0.1
Target homogeneity	3 – 7
Isotopic enrichment	0.5- 1
Target area	0.5 – 1
γ-ray detector efficiency	2 – 5
Peak area and counting statistics	3 – 8
γ-ray abundance	1- 3
Irradiation time	<1
Beam current (Monitor reaction)	8 - 10
	Total = 11 – 16 %

4. Results and Discussion

4.1 Separation of Radioarsenic from Irradiated Germanium Oxide Targets

Although a few methods for separation of arsenic radionuclides from germanium oxide target have been reported [see section 1.6.3], there is still need for new methods that provide high yields of radioarsenic with low radionuclidic and chemical impurities. In the present work the production and radiochemical separation of arsenic isotopes was carried out using $^{nat}GeO_2$ as target material; however, for production of an individual arsenic radionuclide in high radionuclidic purity, isotopically enriched germanium targets would be needed.

In this section radiochemical separation of radioarsenic (^{71}As, ^{72}As, ^{73}As and ^{74}As) from irradiated germanium oxide, as well as from radiogallium was studied and optimized using solvent extraction from acid solutions containing alkali iodide. A γ-ray spectrum of the germanium dioxide target irradiated with 45 MeV protons is illustrated in Fig. 4.1. Besides the radionuclides of arsenic, the radionuclides ^{69}Ge and ^{67}Ga were also produced; they were used as tracers for determination of Ge and Ga in the experiments.

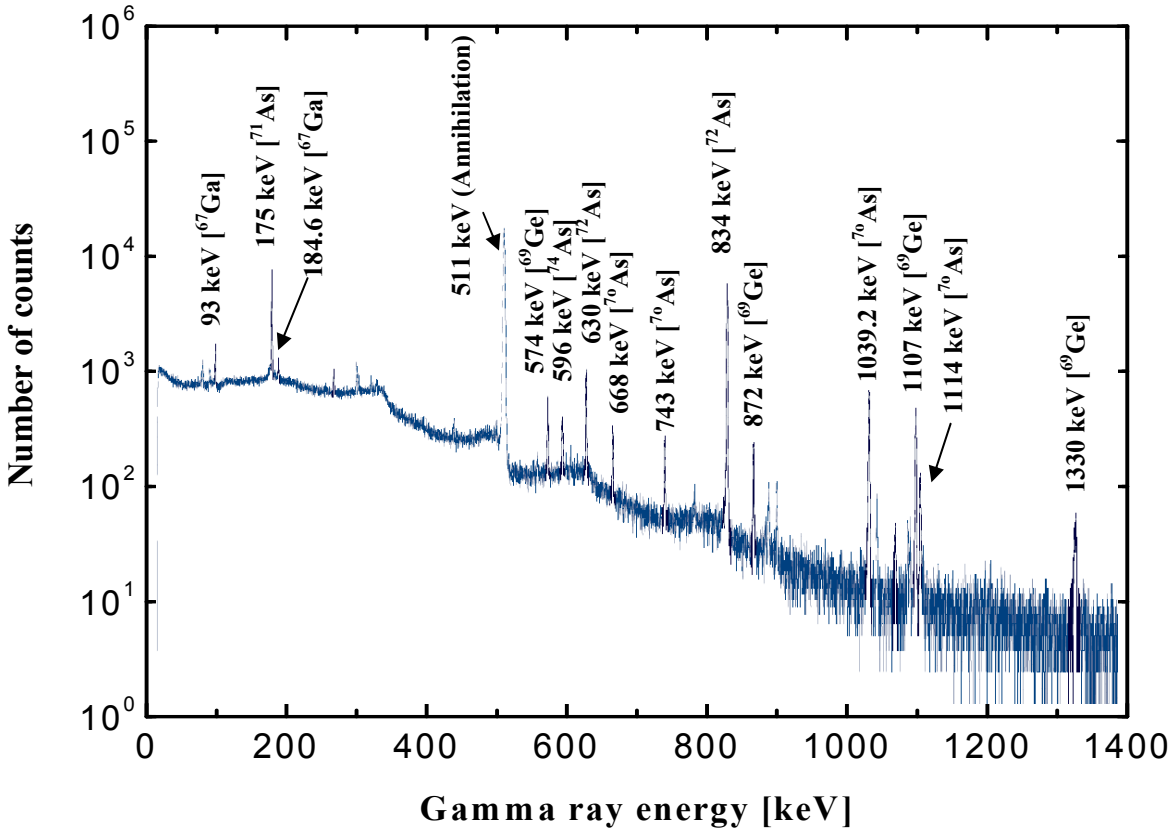

Fig. 4.1: Gamma-ray spectrum of a GeO_2 target irradiated with 45 MeV protons.

4.1.1 Determination of the As(III)/ As(V) Ratio

After dissolution of the proton irradiated GeO_2 in pure water, the produced radioarsenic will be present in the form of As(III) and As(V). The ratio As(III)/As(V) was determined by thin layer chromatography (TLC), identifying the species by their retention factors and γ-ray spectra as described in section 3.5.2. Fig. 4.2 shows the radiochromatogram obtained using an Instant-Imager.

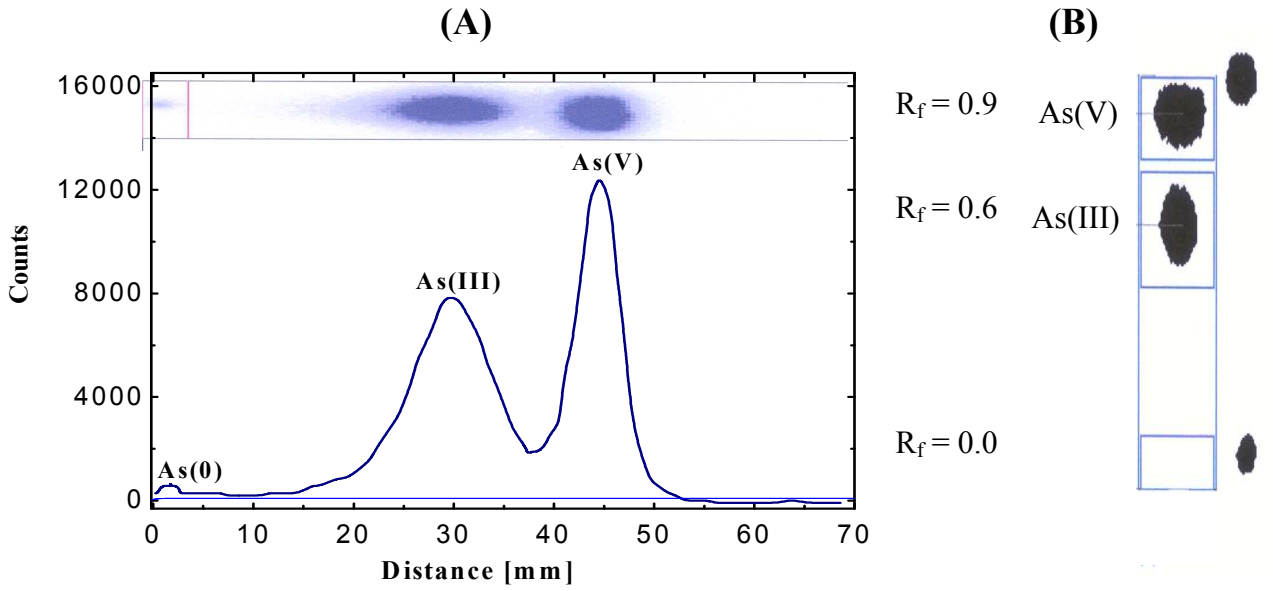

Fig. 4.2: Radiochromatogram of no-carrier added As(III) and As(V) developed with a mixture of 0.01 M $NaHC_4H_4O_6$ / CH_3OH in the ratio of 3 : 1 and using Si-60 phase thin layer plate. (A) Activity profile of a typical sample, (B) Image of TLC plate showing distribution of the activity at three spots; the starting point and the front end are marked on the right side.

Fig. 4.2 (A) shows the image of a TLC plate and the presence of radioactivity at three spots: the first spot was the origin point, the second was As(III) (containing some radioactivity of Ge and Ga) and the third was As(V) (also containing some radioactivity of Ge and Ga). Fig. 4.2(B) displays the activity profile of radioarsenic. The exact amount of radioactivity of As, Ge and Ga at each spot was determined using a HPGe detector. Table 4.1 shows the percentage of radioarsenic, radiogallium and germanium in each zone. The retention factors $R_f = 0.6$ and $R_f = 0.9$ were used to identify As(III) and As(V), respectively (Jahn, 2009). It was found that the ratio of As(III) /As(V) was 35/60, while Ge was found to be nearly evenly distributed in the two spots at $R_f = 0.6$ and 0.9. In contrast, Ga was found to

remain mostly at the origin; its amount decreased with the distance. Thus, for the extraction of radioarsenic it is better to use an oxidizing or reducing agent to transfer radioarsenic to one significant oxidation state, as is explained below.

Table 4.1: Relative ratios of radioactivities of As, Ge and Ga in various zones after TLC separation.

	As [%]	Ge [%]	Ga [%]
Origin point	4.6	6.2	83.2
As(III) zone	35.4	47.1	13.0
As(V) zone	60.0	47.0	3.8
	100	100	100

4.1.2 Solvent Extraction of Radioarsenic in Presence of Bulk Germanium

The solvent extraction behaviour of radioarsenic from proton irradiated GeO_2 via cyclohexane in the presence of bulk germanium was investigated. The effects of various parameters were studied.

4.1.2.1 Effect of acidity and iodide concentration

Since the extraction of As(III) and Ge(IV) depends on the concentration of hydrochloric acid as well as of potassium iodide (Tanaka and Takagi, 1969), extraction studies were performed with cyclohexane by varying the concentrations of HCl and KI.

The results on the extraction of radioarsenic(III) with increasing HCl concentration are shown in Fig. 4.3. Without KI, radioarsenic was not extracted at low HCl concentration but the extraction rate of radioarsenic and Ge increased with the acid concentration, reaching values of 14 % and 95.8 %, respectively, at 9 M HCl. In this case radioarsenic and germanium were extracted as $AsCl_3$ and $GeCl_4$. Radioarsenic cannot be extracted with cyclohexane from a solution of irradiated target at high HCl concentration without co-extracting big amounts of germanium, while it was not extracted at low concentration of acid. Both the oxidation states of arsenic are found in that case, leading to very low extraction of radioarsenic because about 60 % of the radioarsenic is present in the oxidation state As(V) [section 4.1.1], which is not equally transferred into the organic phase. It is known that arsenic trichloride is a covalent

molecule while arsenic pentachloride probably exists as a complex ion. If this is the case, then it is quite obvious that the trivalent arsenic can be extracted into an organic phase, while arsenic pentachloride is excluded owing to its ionic properties (Chappell et al., 1995).

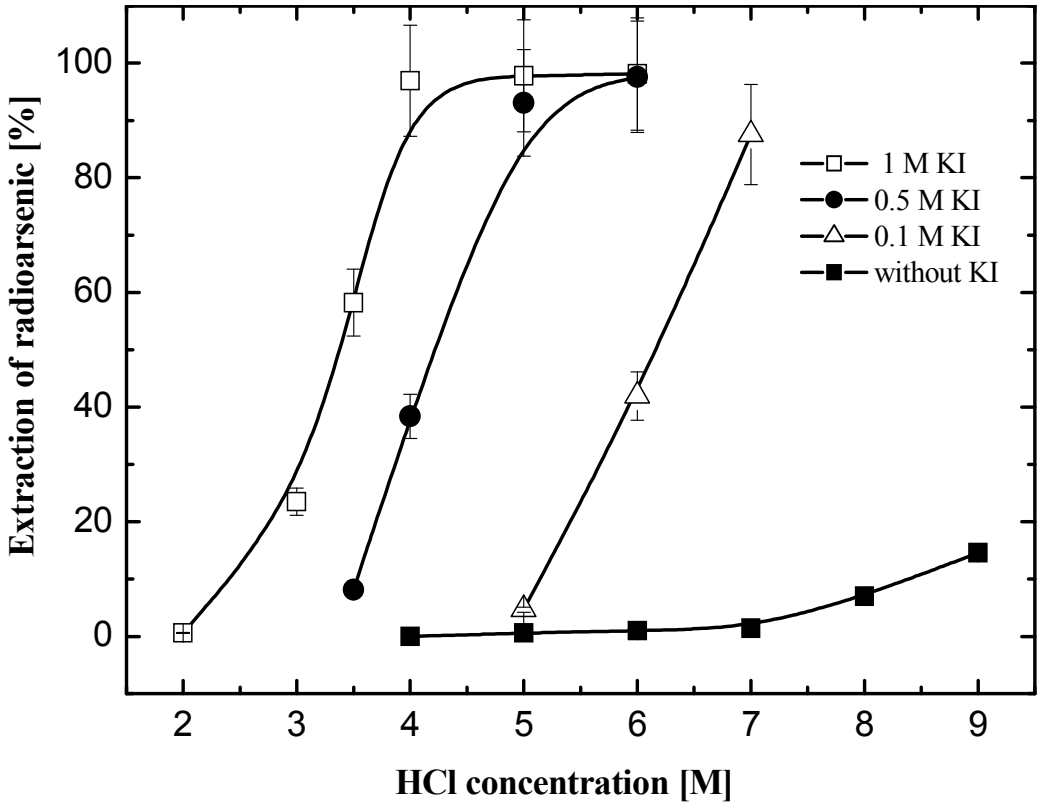

Fig. 4.3: Effect of hydrochloric acid concentration on the extraction of radioarsenic by cyclohexane using 0.0, 0.1, 0.5 and 1 M KI as salting out agent.

The extraction of radioarsenic by the aromatic hydrocarbon (cyclohexane) probably takes place through hydration, solvation or hydration-ionic association type mechanisms. It can be assumed that hydrochloric acid forms adducts with the aromatic hydrocarbon (Rashid et al., 1992). They assumed that $AsCl_3$ is extracted through replacement of HCl in the organic phase to give a complex of the type $AsCl_{3-n}H_2O$ in benzene, where n=0, 1, or 2, depending on the acidity of the aqueous phase. On the other hand, Ge, which occurs in the form of various hydrated germinates after dissolution, is extractable with cyclohexane as $GeCl_4$ from aqueous media containing excess molecular HCl.

$$GeO_2(H_2O)x + 4\ HCl \leftrightarrow GeCl_4 + (x+2)H_2O \qquad 4.1$$

$GeCl_4$ is practically insoluble in concentrated HCl and due to its own low polarity moves readily into non-polar phases (Fassbender et al., 2005).

By adding KI to the acid solution the extraction of radioarsenic into cyclohexane improved with the increasing KI concentration. Radioarsenic (III) was extracted as the iodide while germanium may be extracted into cyclohexane to a considerable extent as its chloride with a small amount of the iodide (Tanaka and Takagi, 1969). KI has three functions: to reduce As(V) to As(III) , to form AsI_3, and to act as salting out agent. The concentration of hydrochloric acid also has a significant effect on the reduction of arsenate to arsenite. Literature suggests that reduction by potassium iodide as reducing agent requires the concentration of hydrochloric acid to be at least 1 M. Enhancement of extraction with potassium iodide could be due to the increased formation of extractable arsenic iodide complexes, since iodide complex formation is thermodynamically more favoured than chloride. This is partly because of the basic nature of the iodide ion and its relatively low charge density and resulting smaller enthalpy changes in aqueous hydration (Rashid et al., 1992).

The extractability of radioarsenic by cyclohexane increased with increasing acid strength in the presence of KI. The maximum extraction of up to 98 % is already achieved with 5 M HCl in presence of 1 M KI. At higher hydrochloric acid concentrations the extraction of radioarsenic is still high but two problems arise; firstly, germanium is co-extracted with radioarsenic, and secondly, a precipitate of potassium halide is formed which affects the separation process. The results shown in Fig. 4.3 are comparable to those reported by Tanaka and Takagi (1969) using sulphuric acid.

In Fig. 4.4 the dependence of extraction of radioarsenic and germanium on KI concentration is shown. Maximum extraction was achieved at KI concentrations of > 0.7 M. Germanium was also extracted in some traces. It can be seen that the extraction of Ge can be avoided by using low concentrations of HCl and KI. For example, the extraction of radiogermanium with 1 M KI and 4 M HCl was only 1 % but with 6 M HCl it increased to 42.4 %. Thus the optimum condition for the separation of radioarsenic emerged as 5 M HCl and 1 M KI at that conditions 2.3 % of Ge was co-extracted. Gallium was not co-extracted with radioarsenic under all conditions studied, even with high concentrations of acid and iodide. Using KBr instead of KI, no extraction of radioarsenic from 5 M HCl and 1 M KBr could be observed.

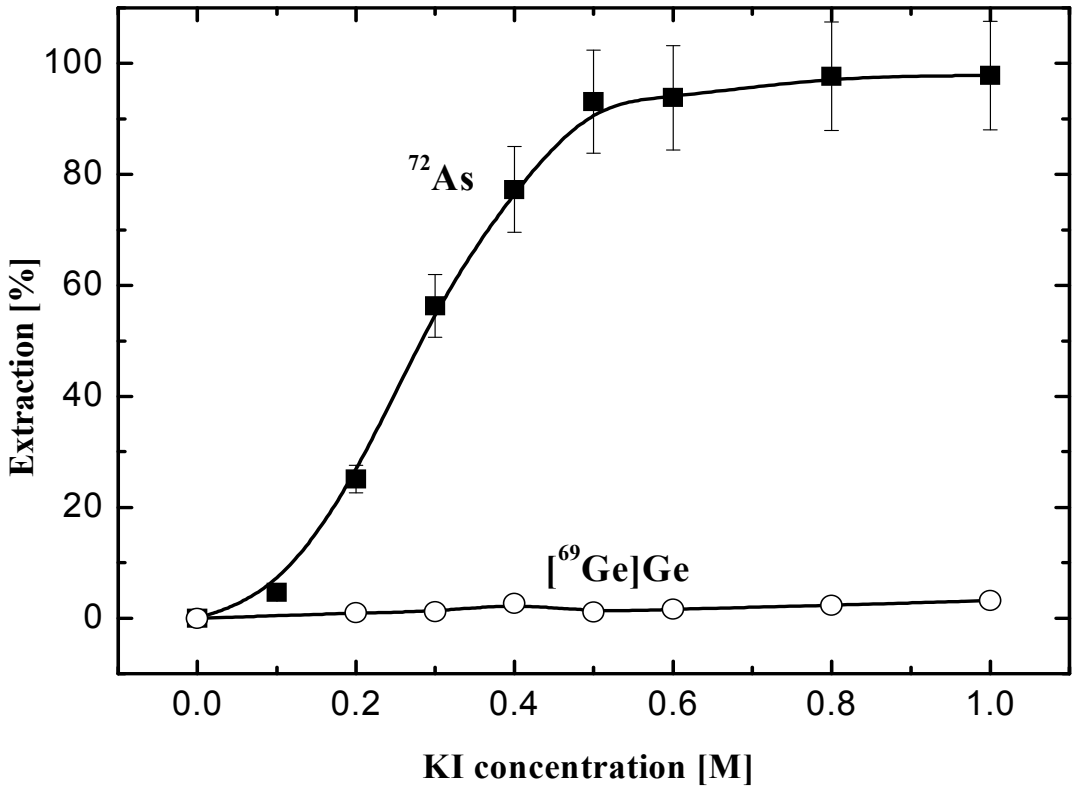

Fig. 4.4: Effect of KI concentration on the extraction of radioarsenic and germanium with cyclohexane from solutions of irradiated GeO_2 target at 5 M HCl.

4.1.2.2 Effect of different acids

Various acids were tried in the separation of radioarsenic with cyclohexane. The results are summarized in Table 4.2. When using $HClO_4$ and HBr, the extraction of radioarsenic was high, but germanium was also extracted in high amounts, while the extraction of radiogallium was negligible. The extraction of radioarsenic from nitric acid solutions under identical conditions was found to be very low (< 3 %). In HNO_3, KI can not reduce As(V) to As(III) but HNO_3 oxidize As(III) to As(V), which was not extracted under these conditions. A dark pink colour in both organic and aqueous phases was noted, probably due to the oxidation of iodide to iodine (Rashid et al., 1992). In the case of H_2SO_4 also a high extraction yield was found but the results were not reproducible. The latter two acids are therefore not listed in Table 4.2; nor were they considered in further experiments.

Table 4.2: Effect of acids on the extraction of radioarsenic and bulk germanium using cyclohexane from solutions of 5 M acid and 1 M KI.

Acid [5M]	Radioarsenic [%]	Germanium [%]
HCl	97.8±0.5	2.3±0.8
$HClO_4$	93.2±3.5	32.3±0.5
HBr	96±1	94±2

No Ga activity was detected in the organic phase.

4.1.2.3 Effect of different organic solvents

Extractions were performed under optimum conditions (1 M KI and 5 M HCl), but using different organic solvents, namely; cyclohexane, chloroform, toluene, heptane, and diethyl ether. The results are compared in Table 4.3. The extraction of radioarsenic was high in all investigated solvents. However, the extraction of germanium was also appreciable, except for cyclohexane and heptane. Radiogallium was extracted by about 1% while using chloroform, and by 85.4 % in the case of diethylether. No ^{67}Ga was detected in case of cyclohexane, toluene and heptane. Thus, the best organic solvent for radioarsenic extraction was found to be cyclohexane.

Table 4.3: Extraction of radioarsenic and bulk germanium by different organic solvents from solutions with concentrations of 5 M HCl and 1 M KI.

Solvent	Radioarsenic [%]	Germanium [%]	Radiogallium [%]
Cyclohexane	97.8±0.5	2.3±0.8	--
Chloroform	99.1±0.5	25.6±3	1±0.5
Toluene	99.3±0.3	21.8±2	--
Heptane	95.6±0.2	5.6±1	--
Diethylether	98.2±0.5	72.6±2	85.4±2

Figure 4.5 shows the extraction of radioarsenic by cyclohexane, toluene, and chloroform at different HCl concentrations and 1 M KI. The three organic solvents show the same behaviour regarding the extraction of radioarsenic. The problem with toluene and chloroform was that the germanium was co-extracted with radioarsenic.

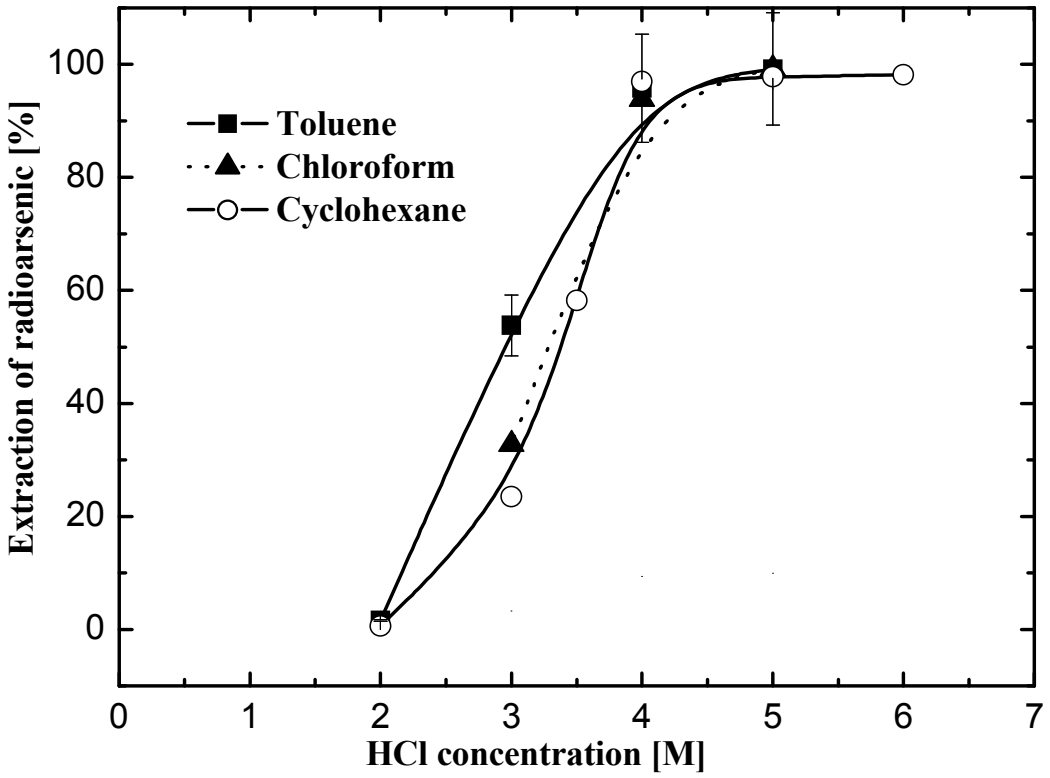

Fig. 4.5: The extraction of radioarsenic by various organic solvents at 1 M KI and different HCl concentrations.

4.1.2.4 Back extraction of radioarsenic

The back-extraction of radioarsenic from cyclohexane using various concentrations of HCl and NaOH was studied. It was found that the back-extraction was nearly constant while increasing HCl or NaOH concentration. In each case the back-extraction of radioarsenic from cyclohexane was about 90 % and that of germanium about 80 %. The back-extraction was better in water, resulting in values of about 95 %, and increasing up to 98 % by addition of about 100 µl of H_2O_2 (30 %) to the water (1 % v/v H_2O_2 solution). The results obtained are summarized in Table 4.4. In the case of pure water all the extracted germanium was unfortunately also back extracted with radioarsenic. In the presence of H_2O_2, however, the back extraction of germanium was considerably reduced.

Table 4.4: Back-extraction of n.c.a. radioarsenic from cyclohexane using different concentrations of H_2O_2.

H_2O_2 [%]	Radioarsenic [%]
0.0	95.0 ± 2
0.1	97.6 ± 2
0.5	98.1 ± 1
1.0	98.2 ± 1

4.1.3 Study of Extraction of Radioarsenic after Removal of Bulk Germanium

A precipitation method was used to remove bulk of germanium before extraction of n.c.a. radioarsenic. Germanium was precipitated as hydrated GeO_2 (Chattopadhyay et al., 2007) after dissociation of the sparingly soluble tetrahydroxide species, which has limited solubility, with $K_{sp}=2.39x10^{-45}$.

$$Ge(OH)_4 \rightarrow GeO_2 + 2H_2O \qquad 4.2$$

More than 85 % of the germanium activity was precipitated after neutralization of the basic solution with concentrated hydrochloric acid containing nearly 5 % of the radioactive arsenic. Thus about 95 % of the radioarsenic and less than 15 % of germanium were found in the filtrate.

The extraction of radioarsenic at a concentration of 5 M HCl and 1 M KI was nearly 99 % and that of germanium 6.5 % of the amount in the filtrate. This result showed that the overall extraction procedure leads to quantitative separation of radioarsenic containing only about 1 % of total germanium. After precipitation of bulk germanium the percentage of the remaining germanium extracted with radioarsenic from the solution increased. This may be due to the presence of KCl which was formed during the neutralisation process. Palanivelu et al. (1992) postulated that the presence of sodium chloride as a salting-out agent affected the extraction process. Depending on the results obtained on extraction of radioarsenic after precipitation, a series of experiments was done to decrease the amount of germanium in the extracted radioarsenic fraction upon Ge precipitation. Tables 4.5 and 4.6 show the results obtained using 0.5 M KI and different HCl concentrations. By decreasing the HCl concentration the extraction of radioarsenic and germanium decreased. The optimum extraction of radioarsenic occurred from a solution of 4.75 M HCl and 0.5 M KI.

Table 4.5: Extraction of radioarsenic and germanium from 0.5 M KI and various HCl concentrations using cyclohexane.

HCl [M]	Radioarsenic [%]	Germanium [%]
4	40.4 ± 3	0.95 ± 0.4
4.75	85.3 ± 3	1.3 ± 0.5
5.3	97.5 ± 2	3.4 ± 1

Table 4.6: Extraction of radioarsenic and germanium from 4.75 HCl and 0.5 M KI with cyclohexane.

	Radioarsenic [%]	Germanium [%]
First extraction	85.3 ± 3	1.3 ± 0.5
Second extraction	12.9 ± 3	0.8 ± 0.3
Overall both extraction processes	98.2 ± 1	2.1 ± 0.5
Over all precipitation-extraction	92 ± 2	0.29 ± 0.1

Two extraction steps were found to be sufficient to extract about 98 % of radioarsenic and 2 % of the germanium. From this result the overall extraction yield of radioarsenic was calculated as 89 % and the product contained less than 0.3 % of the germanium.

Fig. 4.6 represents the flow sheet of the complete process for the separation of radioarsenic from proton irradiated GeO_2 by solvent extraction using cyclohexane. The disadvantages of this process are (a) the first use of the precipitation process leads to about 5-10 % loss of radioarsenic depending on the conditions, and (b) after the precipitation the amount of germanium found in the end product is still too high.

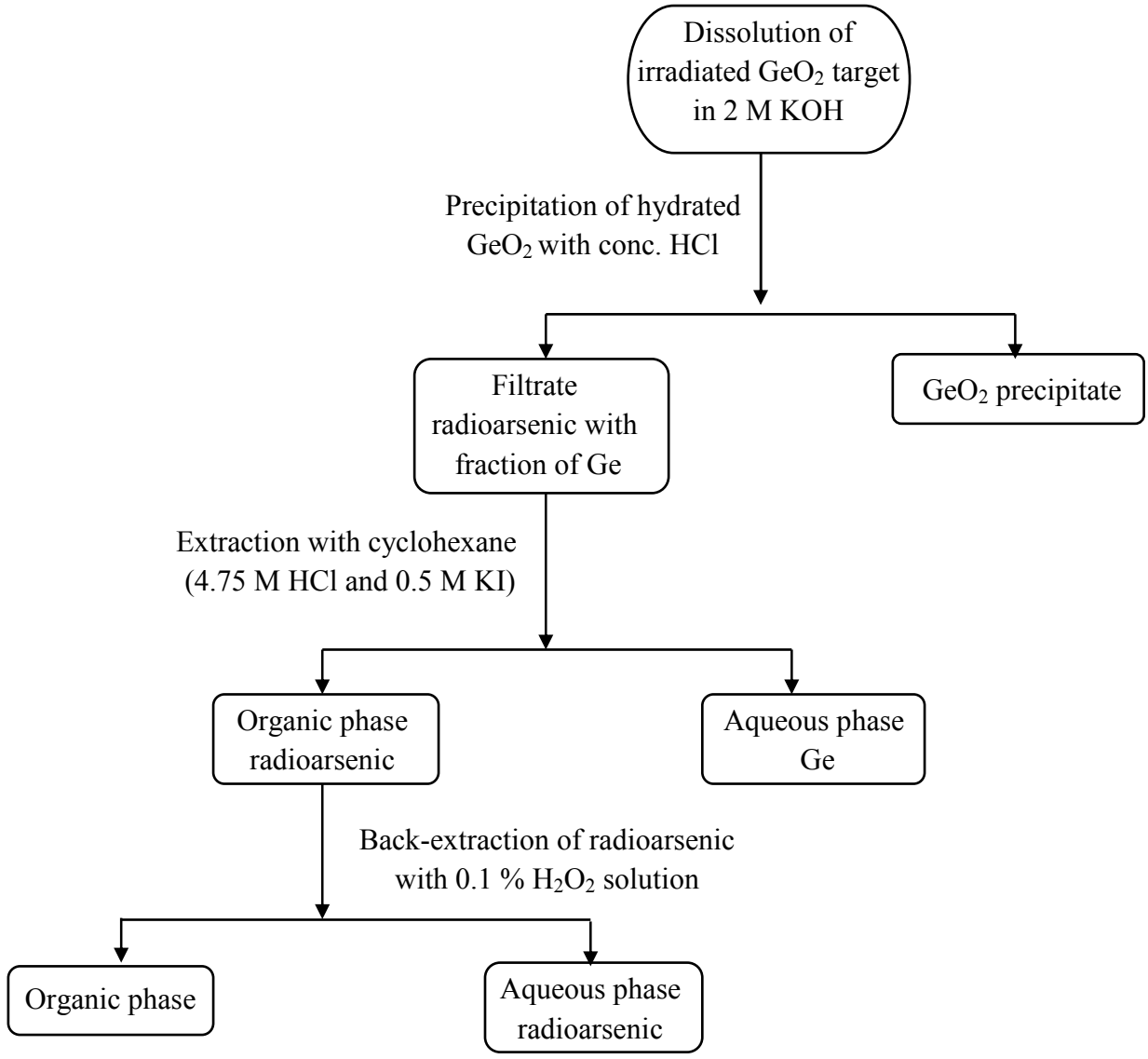

Fig. 4.6: Flow sheet of the separation process of radioarsenic from a GeO_2 target by solvent extraction using cyclohexane (after precipitation of the bulk target material).

4.1.4 Extraction of Radioarsenic from Alkaline Solution

The separation process consisted of the following: the radioarsenic was extracted from a solution composed of 0.5 M KI and 4.74 M HCl using cyclohexane. In this case more than 99 % of radioarsenic and 1.4 % of Ge was extracted. The presence of potassium chloride as a salting-out agent increased the extraction of radioarsenic. The radioarsenic was back-extracted using 0.1 % H_2O_2 solution, 10 µL of 30 % H_2O_2 was added to ensure that all radioarsenic(III) was oxidized to the oxidation state (V). Finally, the remaining germanium was removed from the solution at 9.2 M HCl using cyclohexane. After the completion of this process more than

95% of radioarsenic and nearly 0.001% of germanium were extracted. Thus, by using this separation scheme radioarsenic could be obtained in high yield and purity.

4.1.5 Comparison of Investigated Separation Methods

From the results obtained on the two methods used for the separation of no-carrier-added radioarsenic from irradiated ^{nat}Ge targets, it was apparent that the separation of As/Ge system using cyclohexane without precipitation of Ge is favourable than using cyclohexane after precipitation of Ge for getting the activity in a shorter time with high efficiency without a lot of *loss* of radioarsenic.

4.1.6 Optimized Conditions for Separation of Radioarsenic

Based on the information gained through the experiments described above, the following optimized method of separation of radioarsenic was adopted. A flow sheet of the optimized separation method is given in Fig.4.7. The target was dissolved in 2 M KOH and the radioarsenic was extracted directly from that solution after acidification to 4.75 M HCl and 0.5 M KI without precipitation of germanium. A second selective-extraction led to high purity radioarsenic.

The extraction of radioarsenic was done at first from 4.75 M HCl and 0.5 M KI with cyclohexane whereby > 99 % of radioarsenic and 1.4 % of Ge were extracted. After back-extraction of radioarsenic into 10 mL of 0.1 % H_2O_2 solution, another 10 μL of 30 % H_2O_2 solution were added to ensure that all As(III) was oxidized to As(V). Then in a second step, HCl was added to a concentration of 9.2 M and the accompanying trace germanium was extracted into cyclohexane while the radioarsenic remained in the acid solution (95 % of radioarsenic and only about 0.001% of germanium remained in the aqueous HCl solution).

4.1.7 Radiochemical Yield and Quality Control of ^{71}As and ^{72}As

The above described optimized method of separation of n.c.a. radioarsenic was used in the production of ^{71}As and ^{72}As via proton irradiation of GeO_2. A comparison of the practical yield with the theoretical yield was done. The thick target yields of ^{71}As and ^{72}As from a GeO_2 target for the energy ranges effective in the experiments were calculated using the data of Spahn et al. (2007) (see section 1.6.2) on the excitation functions of the ^{nat}Ge(p,x)^{71,72}As reactions.

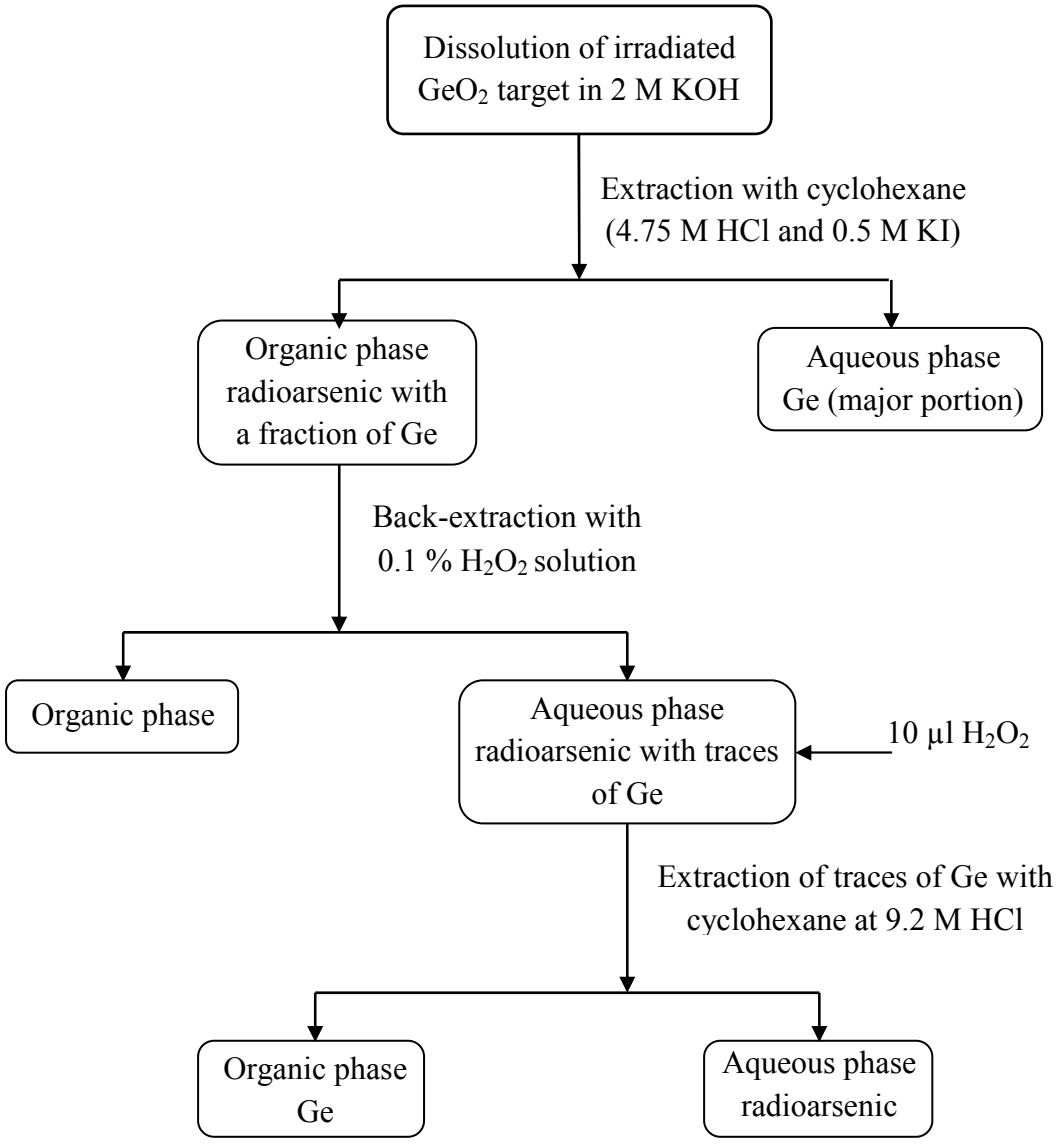

Fig. 4.7: Flow sheet of the optimized method of separation of n.c.a. radioarsenic from the irradiated GeO_2 target.

It was found that the experimental yields of ^{72}As over the two energy ranges amounted to 76.0 and 83.8 % of the theoretical values, respectively, while the experimental yields of ^{71}As amounted to 74.6 and 78.0 % of the theoretical values, respectively. The inactive impurities were Ge and K at a level of <10 µg and < 6 µg, respectively.

The results are summarized in Table 4.7. As Spahn et al. (2007) concluded, neither ^{71}As nor ^{72}As, i.e., the two radionuclides of interest for PET studies, can be produced in large yield and high isotopic purity via the (p,xn) reactions on ^{nat}Ge. The radionuclide ^{72}As is more dominant. For better production, a highly enriched ^{72}Ge target would be advantageous; the

yield of ^{72}As would considerably increase, and the isotopic impurities would decrease accordingly. Considering the various factors affecting the experimental yields (uncertainty in the beam current measurement, radiation damage effect, loss in radiochemical separation, etc.), an experimental yield of 74.6 - 83.8 % of the theoretical value, as found in this work, suggests that the production process followed is satisfactory.

Table 4.7: Thick target yields of ^{71}As, ^{72}As and associated radionuclidic impurities, after separation from a proton irradiated GeO_2 target.

Energy range [MeV]	**Radionuclide**	**Theoretical yield of radionuclide at EOB [MBq/µAh]**	**Experimental yield of radionuclide at EOB [MBq/µAh]**	**Experimental/ Theoretical [%]**	**Composition of radioarsenic [%]**	**Non-isotopic radionuclidic impurities [%]**	**Chemical impurity**
44 → 28.5*	^{71}As	21	15.7	74.8	^{71}As 14.6 ^{72}As 84	^{69}Ge < 0.001	Ge < 10 µg
	^{72}As	118.9	90.3	76.0	^{73}As 0.2 ^{74}As 1.3	^{67}Ga **	K< 6 µg
25.5 → 0*	^{71}As	29.5	23.0	78.0	^{71}As 21.9 ^{72}As 75.3	^{69}Ge < 0.001	Ge<10 µg
	^{72}As	94.5	79.2	83.8	^{73}As 0.8 ^{74}As 2	^{67}Ga **	K< 6 µg

* At both energy ranges the dominating product is ^{72}As. This is due to the use of ^{nat}Ge as target material.

** No Ga activity was detected.

4.2 Separation of n.c.a. $^{68}Ge/^{69}Ge$ from irradiated Ga_2O_3 Targets

Radiochemical separation of n.c.a. $^{68}Ge/^{69}Ge$ from proton irradiated Ga_2O_3 was studied via liquid-liquid extraction using H_2SO_4-HCl/CCl_4 system [see section 1.7.3], but further detailed investigations using another less dangerous organic solvents are necessary. Fig. 4.8 shows the γ-ray spectrum of the radionuclides produced in the irradiation of a Ga_2O_3 target with 45 MeV protons at the injector of COSY. The radionuclides ^{67}Ga and ^{69}Ge, produced during the irradiation, were used as tracers in extraction studies. The radionuclide ^{65}Zn was also present. The nuclear reactions responsible for the production of ^{65}Zn are $^{69}Ga(p,\alpha n)^{65}Zn$ and $^{69}Ga(p,2p3n)^{65}Zn$.

The irradiated material was dissolved in H_2SO_4 and various parameters affecting the extraction with toluene were optimized.

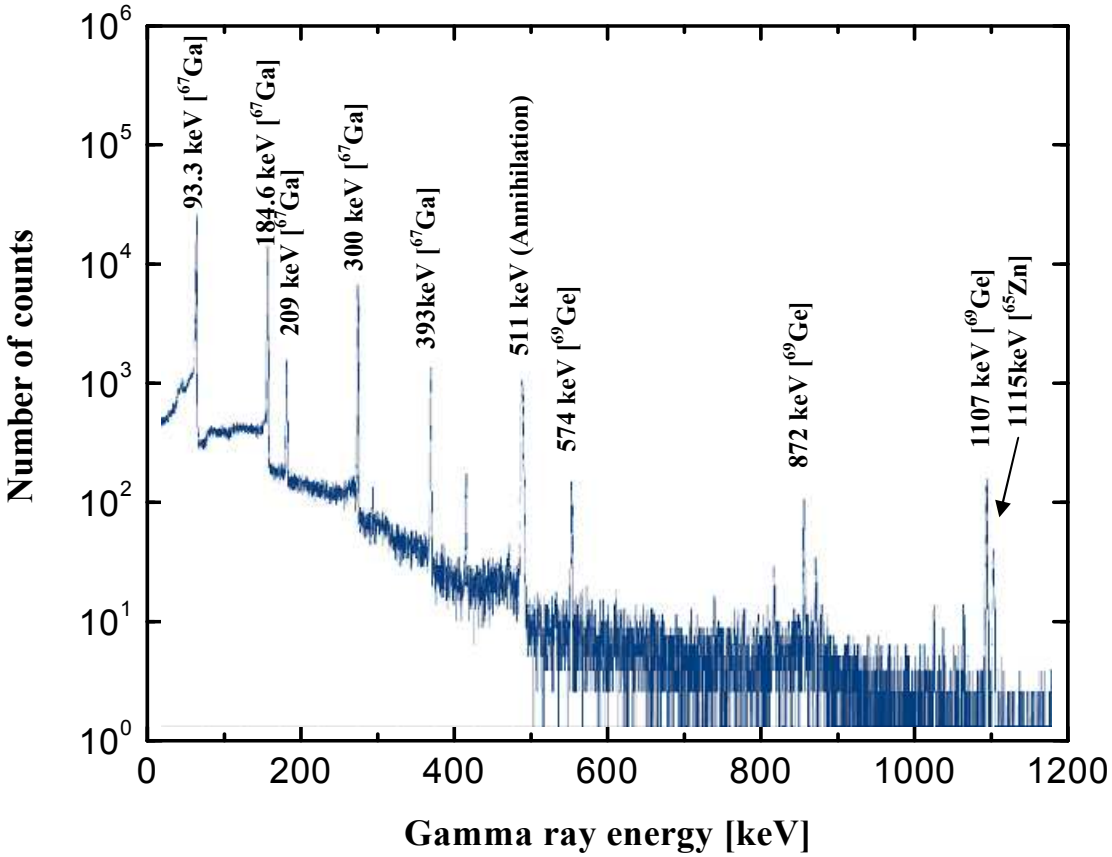

Fig. 4.8: Gamma-ray spectrum of a Ga_2O_3 target irradiated with 45 MeV protons.

4.2.1 Effect of HCl Concentration

The effect of varying HCl concentration on the extraction of n.c.a. $^{68}Ge/^{69}Ge$ using toluene was investigated at 10 M H_2SO_4. Fig. 4.9 represents the results obtained. Without

addition of HCl, the extraction of n.c.a. radiogermanium was negligible; at HCl concentrations above 0.2 M, however, the extraction of radiogermanium increased tremendously, reaching values of about 100%. The HCl the germanium is probably transformed to $GeCl_4$ which is extracted in toluene due to its own low polarity. No ^{65}Zn activity was found in the separated radiogermanium solution.

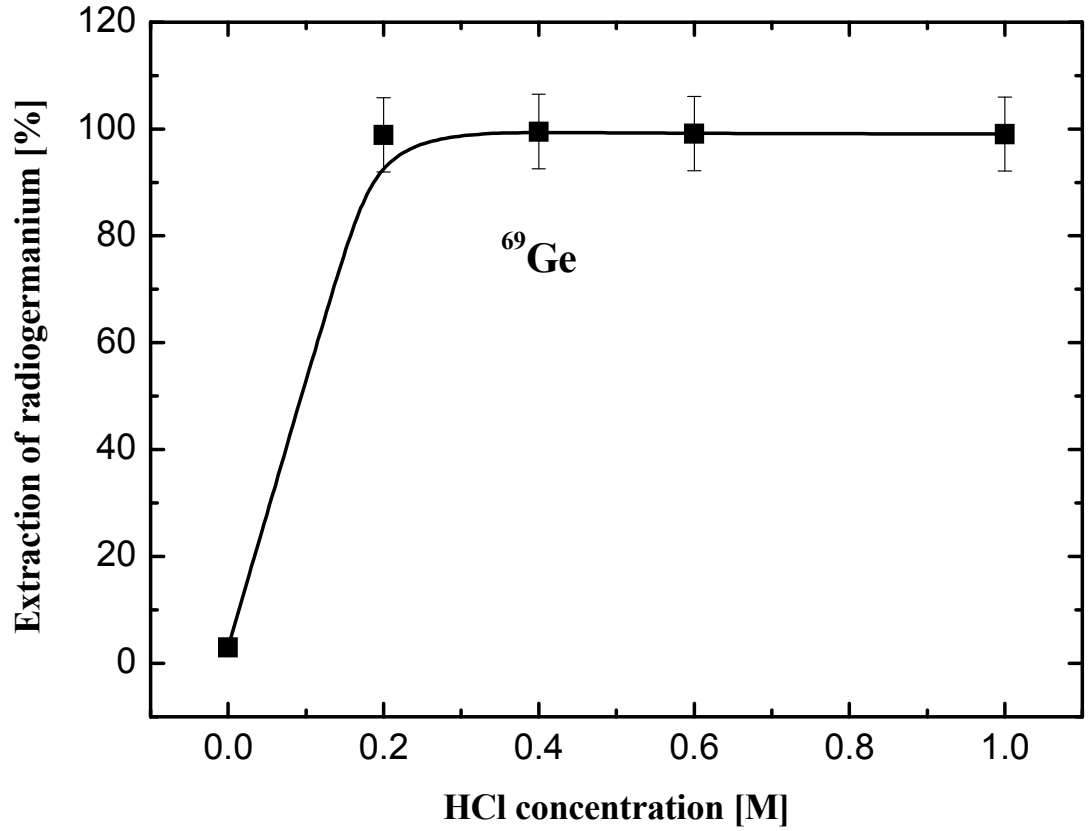

Fig. 4.9: Extraction of n.c.a. radiogermanium with toluene in the presence of various HCl concentrations at 10 M H_2SO_4.

4.2.2 Effect of H_2SO_4 Concentration

To an aliquot of the solution with varying H_2SO_4 concentration, HCl was added and its concentration adjusted to 0.4 M. The extraction of radiogermanium was then studied using toluene. The distribution coefficients of both ^{67}Ga and ^{69}Ge were measured and the results are shown in Fig. 4.10. Obviously, the extraction of radiogermanium increases with increasing H_2SO_4 concentration, the maximum reaching between 8 and 10 M H_2SO_4. With further increase of H_2SO_4 concentration, the extraction of radiogermanium decreased. Gallium was co-extracted with radiogermanium at high concentration of H_2SO_4 and decreased with

decreasing acid concentration. From a solution of 8.0 M H_2SO_4 and 0.4 M HCl the maximum extraction occurred and n.c.a. ^{69}Ge was separated very well from gallium with high yield. $GeCl_4$ is readily hydrolyzed, and Ge is thus conveniently back-extracted into water. About 98±2 % of radiogermanium was back-extracted from toluene into water. No ^{65}Zn activity was found in the separated radiogermanium solution.

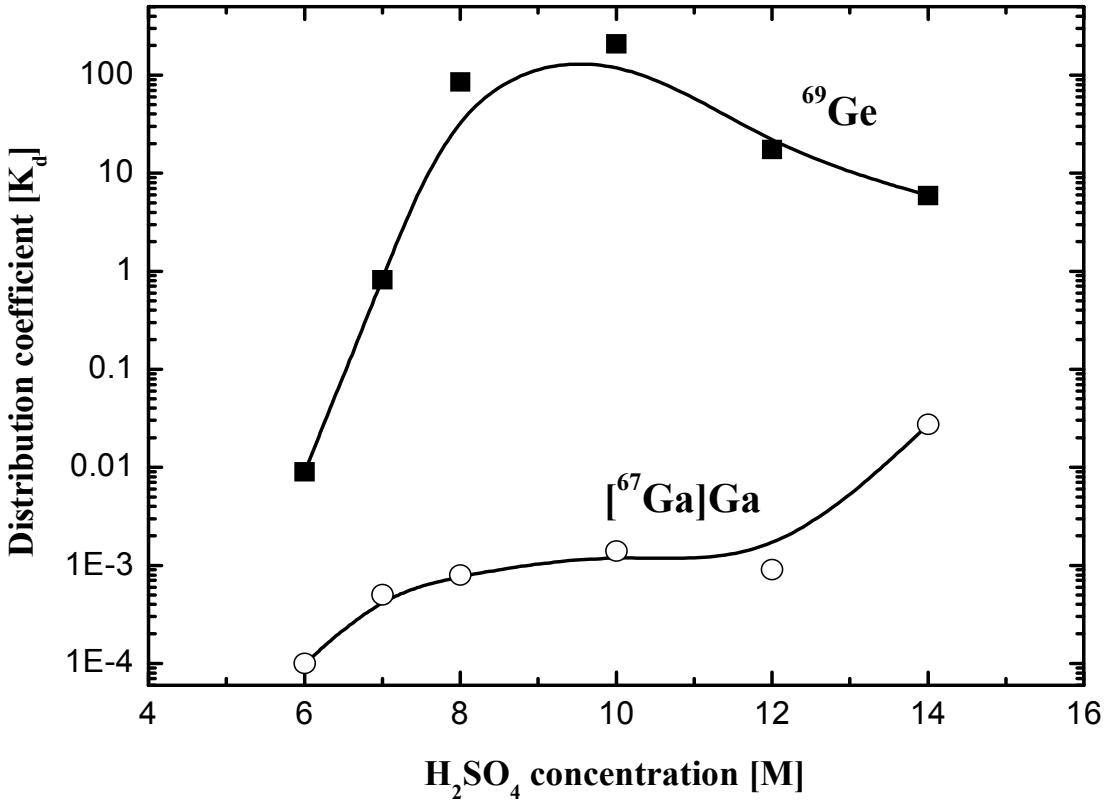

Fig. 4.10: The effect of H_2SO_4 concentration on distribution coefficients of no- carrier-added ^{69}Ge and carrier-added ^{67}Ga in the presence of 0.4 M HCl using toluene.

4.2.3 Extraction of Radiogermanium in Chloroform

Fig. 4.11 gives the distribution coefficients of n.c.a. radiogermanium and gallium at various H_2SO_4 concentrations in the presence of 0.4 M HCl and chloroform. The extraction of radiogermanium increased with increasing H_2SO_4 concentration, and became constant after 8 M H_2SO_4, reaching a value of about 99 ± 1 %. The extraction of gallium, however, remained small, though with chloroform more gallium was co-extracted than with toluene.

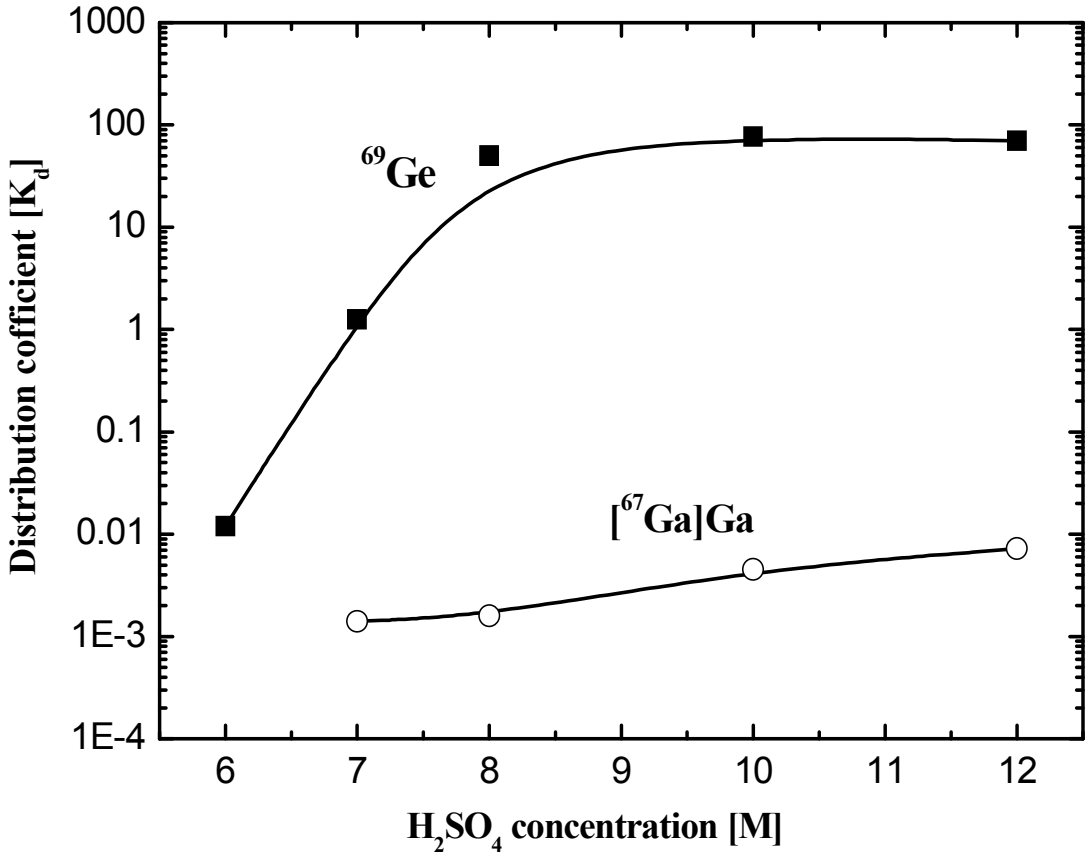

Fig. 4.11: Effect of H_2SO_4 concentration on distribution coefficients of no- carrier-added ^{69}Ge and carrier-added ^{67}Ga in the presence of 0.4 M HCl using chloroform.

4.2.4 Optimized Conditions for Separation of Radiogermanium

A flow sheet of the optimized method of separation of no-carrier-added radiogermanium from proton irradiated Ga_2O_3 target is given in Fig. 4.12. The optimum method of n.c.a. ^{68}Ge/ ^{69}Ge tracer production thus consisted of the irradiation of Ga_2O_3 with 31 MeV protons for 1 h, dissolution of the irradiated material in 8 M H_2SO_4, addition of 0.4 M HCl and extraction in toluene. Thereby 96.3±2 % of the radiogermanium was extracted into the organic phase. The radioactivity was back extracted in the aqueous phase by simply treating the organic phase with water (yield ≈ 99.4 %). Neither ^{67}Ga nor ^{65}Zn activity was found in the separated radiogermanium solution.

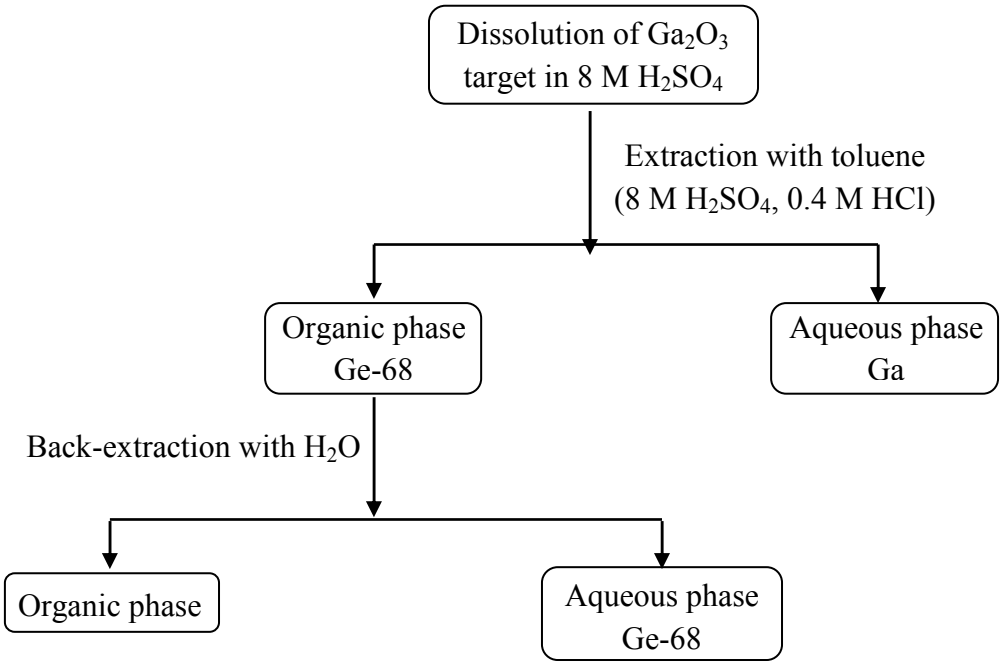

Fig. 4.12: Flow sheet of the separation method of ^{68}Ge from Ga_2O_3.

4.2.5 Production and Quality Control of ^{68}Ge

The optimized separation method elaborated above was used practically in the production of n.c.a. ^{68}Ge via the ^{nat}Ga(p,x) ^{68}Ge reaction. The results are summarized in Table 4.8. The separated n.c.a. ^{68}Ge was of high radionuclidic purity. It was advantageous to carry out the separation of ^{68}Ge after one month so that ^{69}Ge and ^{67}Ga had decayed out. ^{65}Zn which is produced during irradiation of Ga_2O_3 was not detected by γ-ray spectrometry. The only inactive impurity was Ga at a level of < 6 μg. Fig. 4.13 reproduces the gamma-ray spectrum after separation of ^{68}Ge/^{69}Ge from proton irradiated Ga_2O_3 under optimal conditions as described in section 3.6.3. No radiogallium and ^{65}Zn were detected in the separated solution.

A comparison of the practical yield with the theoretical yield was done. We calculated the thick target yields of ^{68}Ge from a Ga_2O_3 target for the respective energy ranges used in the experiments utilizing the data of Qaim et al. (2001) on the excitation function of the ^{nat}Ga(p,x)^{68}Ge process. The experimental yield of ^{68}Ge amounted to 83 ± 4 % of the theoretical value. Considering the various factors affecting the experimental yields (uncertainty in the beam current measurement, radiation damage effect, loss in radiochemical separation, etc.), an experimental yield of 83±4 % of the theoretical value, as found in this work, suggests that the production process followed is satisfactory.

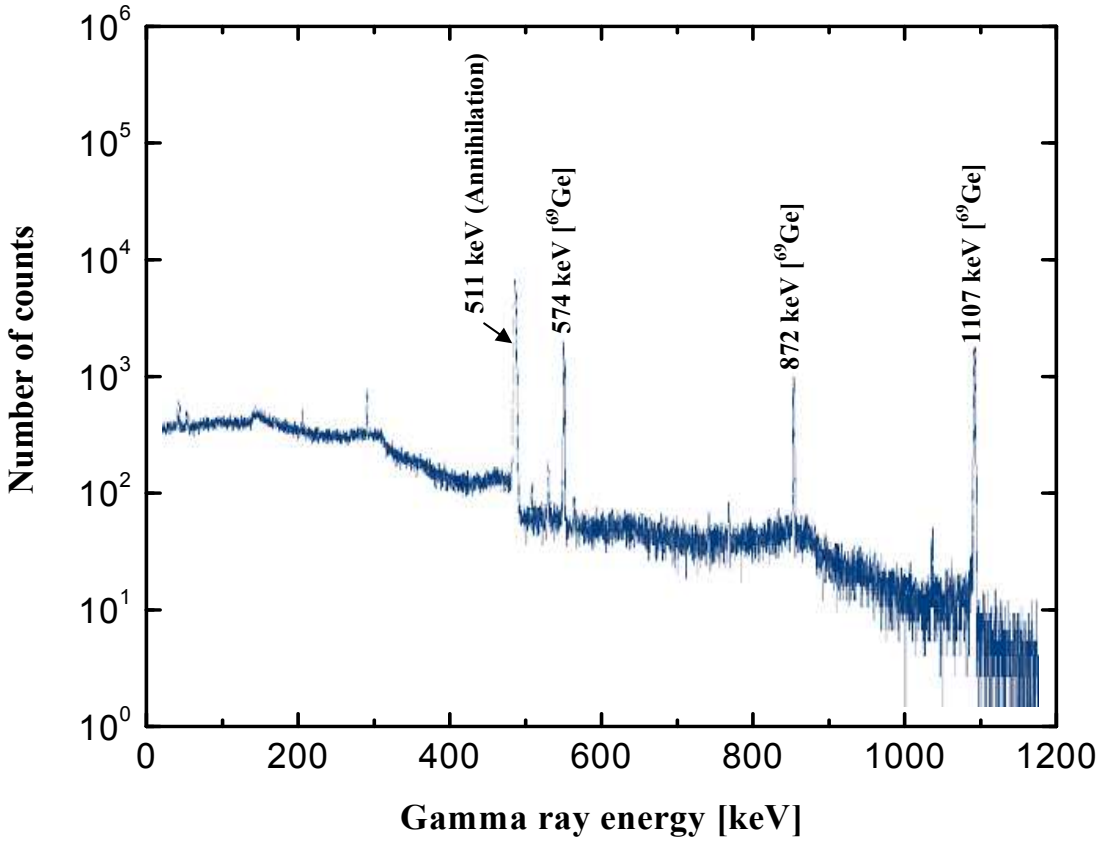

Fig. 4.13: Gamma-ray spectrum of the separated radiogermanium from proton irradiated Ga_2O_3 under optimized conditions.

Table 4.8: Thick target yield of ^{68}Ge and associated radionuclidic impurities after separation from proton irradiated Ga_2O_3 target.

Nuclear process	Energy range [MeV]	Theoretical yield of radionuclide at EOB [MBq/µAh]	Batch yield of radionuclide at EOB [MBq/µAh]	Experimental /Theoretical [%]	Chemical impurity
$^{nat}Ga(p,xn)^{68}Ge$	31→15.6	0.94	0.78 ± 0.04	83±4	Ga< 6 µg

4.3 Isolation of ^{67}Ga Tracer from Irradiated Zinc Targets

For optimization studies on the separation of n.c.a. ^{68}Ga from the ^{68}Ge/^{68}Ga generator system, a longer lived tracer of gallium was needed. The radionuclide ^{67}Ga ($T_{1/2}$ =3.2 d) was produced by the ^{nat}Zn(p.x)^{67}Ga nuclear reaction on natural zinc. In this section the separation of n.c.a. ^{67}Ga from a proton irradiated zinc target using anion exchange and solvent extraction processes is described. The distribution coefficients of radiogallium and zinc on the anion exchange resin Amberlite CG-400-II (Cl^- form), and the cation exchange resin Dowex 50Wx8 (H^+ form) were determined. A solvent extraction process using diisopropylether was also investigated. Figs. 4.14 and 4.15 show the gamma-ray spectra of Zn targets irradiated with 17 MeV protons at the Baby Cyclotron BC1710, exhibting the distinctive γ-ray peaks of ^{66,67}Ga and ^{65}Zn. The 1115 keV γ-ray peak of ^{65}Zn is rather masked in Fig. 4.14. However, it becomes very distinct after some decay of the 9 h ^{66}Ga (see Fig. 4.15).

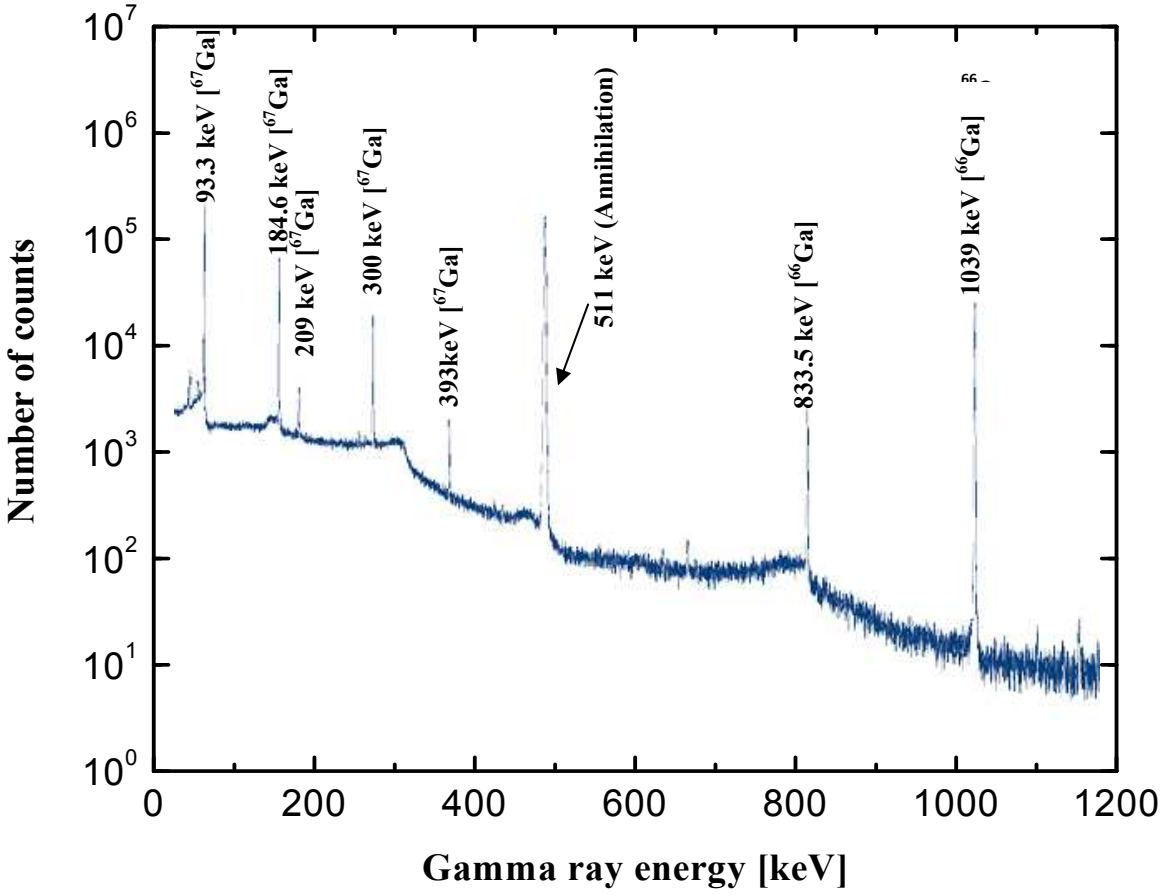

Fig. 4.14: Gamma-ray spectrum of electroplated zinc target irradiated with 17 MeV protons at the BC1710 Baby Cyclotron of the Forschungszentrum Jülich GmbH.

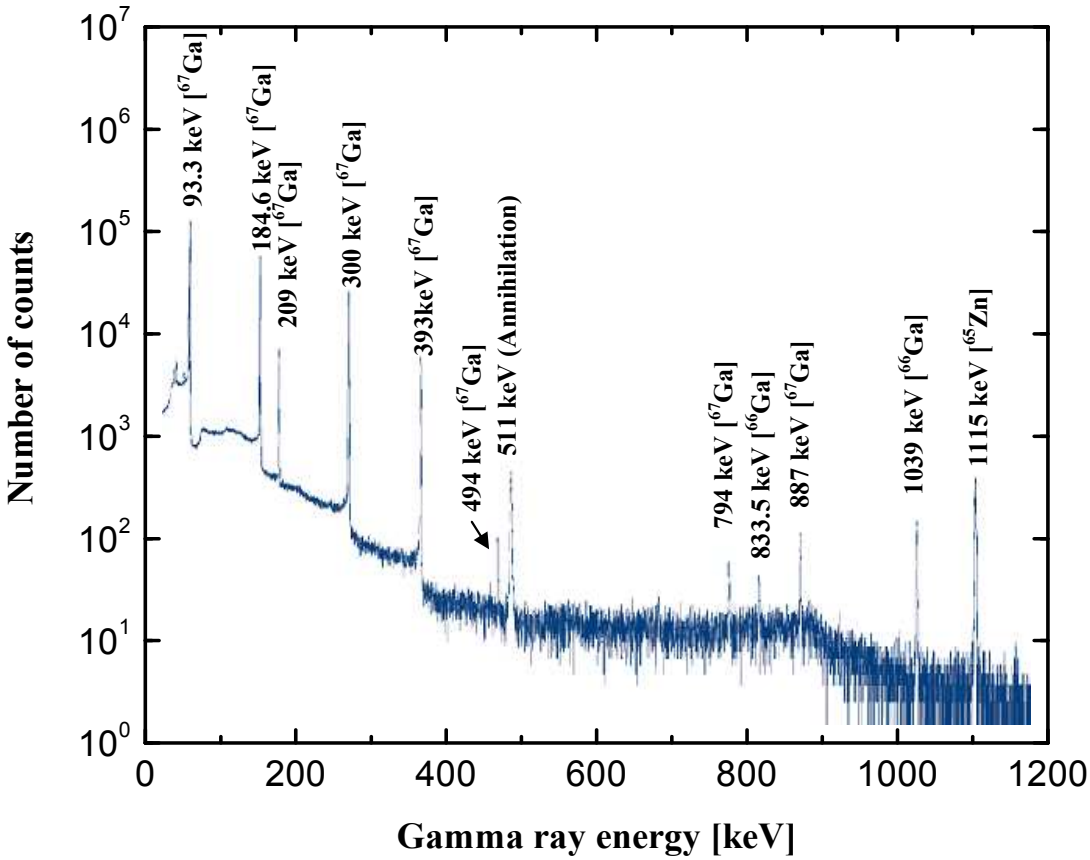

Fig. 4.15: Gamma-ray spectrum of electroplated zinc target irradiated with 17 MeV protons after some decay of ^{66}Ga.

4.3.1 Anion and Cation Exchange Studies

4.3.1.1 Effect of hydrochloric acid concentration on the anion exchange process

The effect of HCl concentration (1-12 M) on the adsorption behaviour of ^{67}Ga and Zn on the anion exchange resin Amberlite CG-400-II (Cl^- form) is represented in Fig. 4.16. Radiogallium was adsorbed on the resin and its adsorption increased with the increasing HCl concentration. In contrast, zinc was only partly adsorbed, and at all HCl concentrations the value remained nearly constant.

At low HCl concentrations the distribution coefficient of radiogallium was low due to the formation of cationic species Ga^{3+}. At higher concentrations of HCl radiogallium begins to form anionic species like $[GaCl_4]^-$. The Zn occurs as Zn^{2+} and $ZnCl^+$ at low concentrations of the acid but forms $[ZnCl_4]^{2-}$ at higher HCl concentrations (Marcus, 1967).

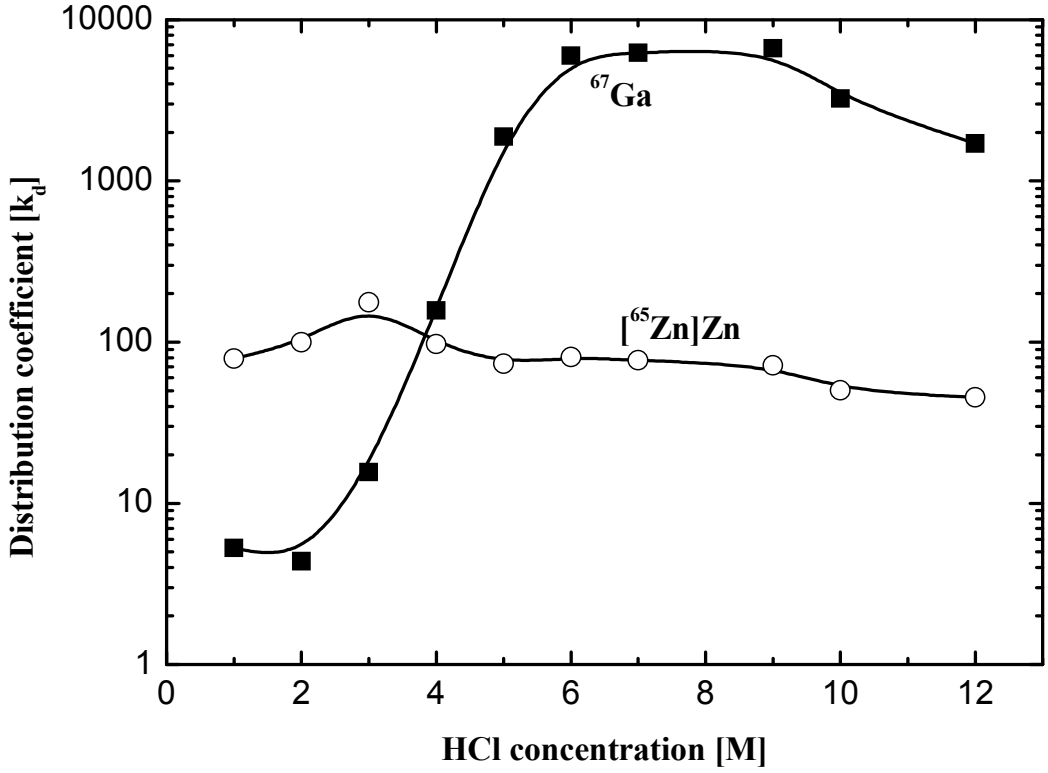

Fig. 4.16: Distribution coefficients of radiogallium and zinc at various concentrations of HCl on anion exchange resin Amberlite CG-400-II, Cl^- form.

4.3.1.2 Effect of hydrochloric acid concentration on cation exchange process

The absorption behaviour of ^{67}Ga and Zn on the cation exchanger resin Dowex 50Wx8 (H^+ form) at various HCl concentrations was investigated. The results are summarized in Fig. 4.17. It was observed that both of them are adsorbed at very low concentration of HCl, and this adsorption decreased with the increasing HCl concentration up to 2 M HCl. This can be attributed to the formation of cationic species of both Ga and Zn at a low concentration of HCl (see 4.3.1.1). The adsorption behaviour of radiogallium at low acid concentration is stronger than in case of zinc, which could be concluded from the distribution coefficient values [K_d]. At HCl range 2-12 M, radiogallium and zinc were not retained on the cation exchanger resin used, because both of them form anionic species at high HCl concentrations as explained in section 4.3.1.1.

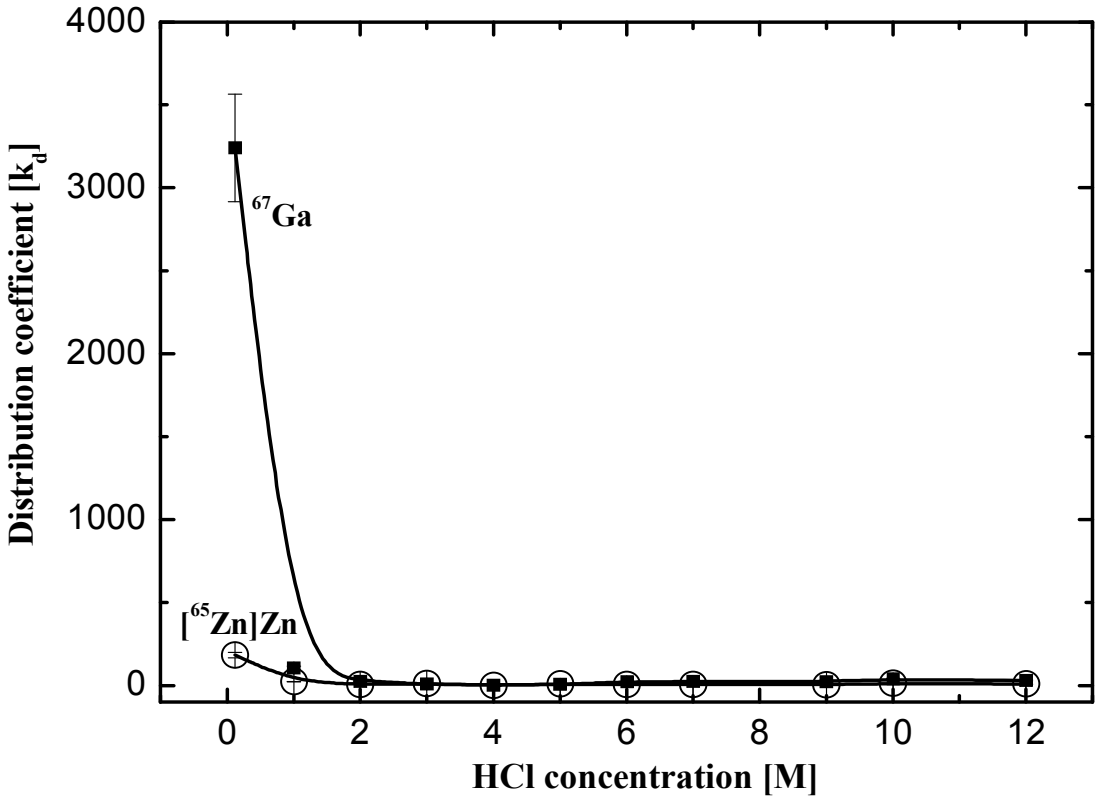

Fig. 4.17: Distribution coefficients of radiogallium and zinc at various concentrations of HCl on the cation exchange resin Dowex 50Wx8, H^+ form.

From the investigation described above, it is clear that both radiogallium and zinc are strongly retained on the cation exchange resin, while in case of anion exchange resin used the adsorption of radiogallium was high but that of zinc was lower. However, the amounts of remaining zinc on the resin were still significant. Thus the separation of radiogallium and zinc by the two exchange resins used is not possible.

4.3.2 Solvent Extraction Studies

The solvent extraction process was studied for the separation of ^{67}Ga from irradiated zinc using diisopropylether. Various parameters were investigated to determine the optimum conditions for the extraction process.

The distribution of radiogallium between ether and aqueous phase for various concentrations of hydrochloric acid is shown in Fig. 4.18. It was found that the K_d value of ^{67}Ga increased with the HCl concentration up to 7-8 M, and then decreased by further increase of HCl.

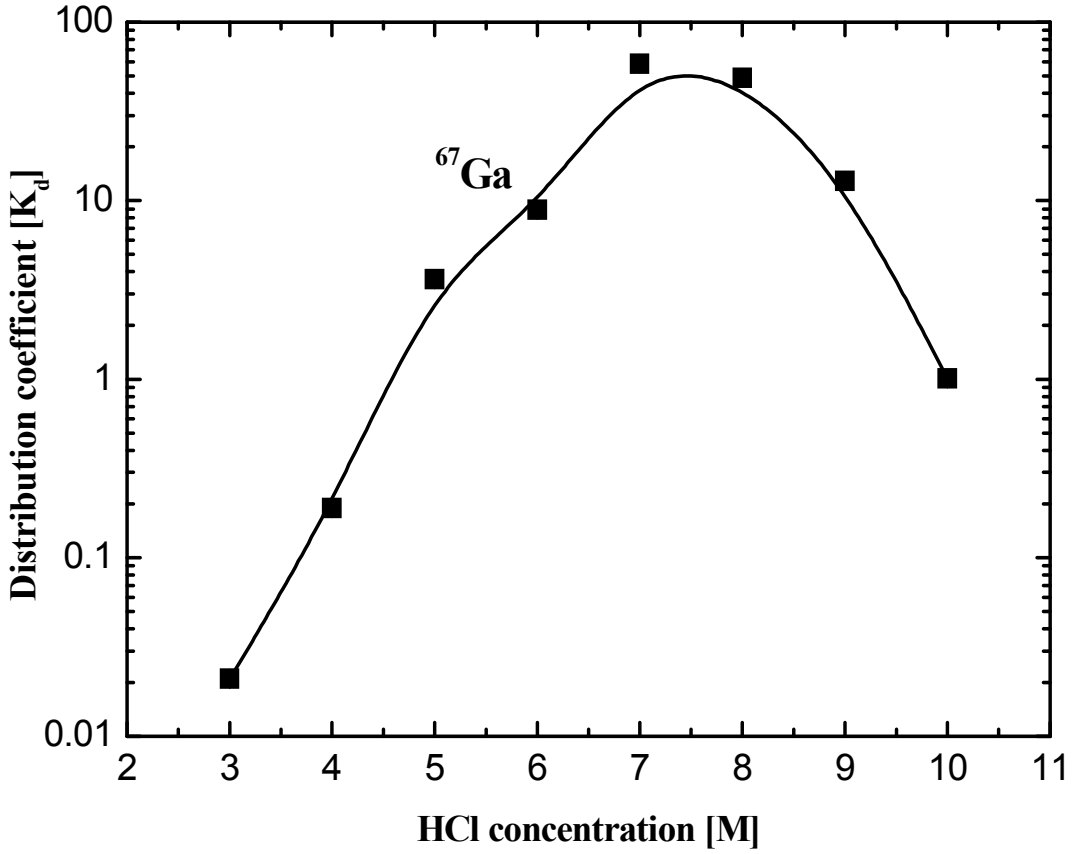

Fig. 4.18: Distribution coefficient of radiogallium in solvent extraction with diisopropylether at various HCl concentrations.

These results agree with those of other authors (e.g. Nachtrieb and Fryxell 1949; Brown, 1971). It has long been recognized that radiogallium is readily extracted from strongly acidic chloride solutions. The presence of HCl promotes the formation of $HGaCl_4$ extracted by solvation but, above 6 M acidity, competition with acid extraction reduces the recovery of gallium (Mihaylov and Distin, 1992). Depending on gallium and chloride levels, a third phase may be formed at 8-9 M acid, which is related to the solubility of the gallium complex in isopropylether. No ^{65}Zn was detected over the HCl concentration range studied except at 3 and 4 M HCl, where about 1 % was detected in the organic phase. This may be due to the formation of $ZnCl_2$ species.

4.3.3 Optimized Method for Separation of Radiogallium

No-carrier-added ^{67}Ga was separated from a proton irradiated zinc target using diisopropylether at 7 M HCl. Under these conditions n.c.a ^{67}Ga was extracted by 98.3 % while Zn remained in the aqueous phase. Fig. 4.19 shows the flow sheet of the separation method of ^{67}Ga from an irradiated zinc target. In the final product, the absence of ^{65}Zn was confirmed by γ-spectrometry. The n.c.a. ^{67}Ga was back-extracted from the organic phase to water very easily. The aqueous solution was evaporated and dissolved again in water. It contained pure no-carrier-added ^{66,67}Ga. After a decay time of about 3 days, the only radioactive isotope was ^{67}Ga.

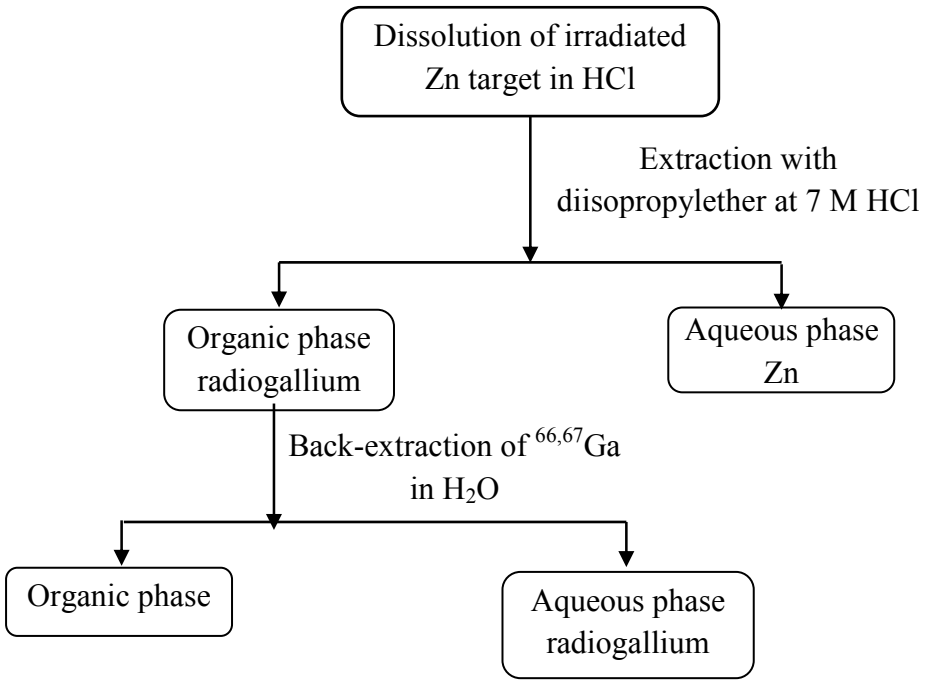

Fig. 4.19: Flow sheet of the separation method of ^{66,67}Ga from an irradiated zinc target.

The results obtained in this section provided more confidence to the methods used for the separation of the radiotracer ^{67}Ga of the required quality. Furthermore, some comparative studies established the superiority of the solvent extraction technique.

4.4 Separation of ^{68}Ga from Parent ^{68}Ge

Several ^{68}Ge/^{68}Ga generator systems have been developed over the past few years. The systems available today are not necessarily optimal [section 1.8.3.2]. So further investigations appear to be useful.

The separation of radiogallium from radiogermanium was studied using anion exchange chromatography and liquid-liquid extraction method. Various parameters were investigated to optimize the separation process. The studies were performed using the radiotracers ^{69}Ge and ^{67}Ga. About 500 µL of the separated n.c.a. ^{68}Ge/^{69}Ge solution and 200 µL of ^{67}Ga solution were used in each experiment. The ^{68}Ge/^{69}Ge (n.c.a.) solution was obtained by separation from an irradiated Ga_2O_3 target using toluene (see section 4.2), while ^{67}Ga solution was obtained by separation from a proton irradiated zinc target using solvent extraction (see section 4.3). The optimized separation method was then applied for the separation of ^{68}Ga from parent ^{68}Ge.

4.4.1 Optimization Studies on the Separation via Solvent Extraction

A series of solvent extraction experiments using Aliquat 336 (trioctylmethylammonium chloride) as liquid anion exchanger were conducted to determine the optimum conditions for the separation of radiogallium from radiogermanium.

4.4.1.1 Effect of HCl concentration

The influence of various HCl concentrations on the extraction of radiogallium and radiogermanium by Aliquat 336 (trioctylmethylammonium chloride) in o-xylene was investigated and the results are given in Fig. 4.20. The extraction of radiogallium and radiogermanium increased by increasing the HCl concentration, reaching a plateau at 2 M and 7 M, respectively. Thus an efficient extraction of radiogallium with 0.1 M Aliquat 336 in o-xylene requires an acid concentration of at least 2 M. It was extracted as tetrachlorogallate $[GaCl_4]^-$ into quaternary ammonium salt by anion exchange (Mihaylov and Distin, 1992) according to:

$$GaCl_4^- + R_3R'NCl_{Org} \leftrightarrow R_3R'NGaCl_{4,org} + Cl^- \qquad 4.3$$

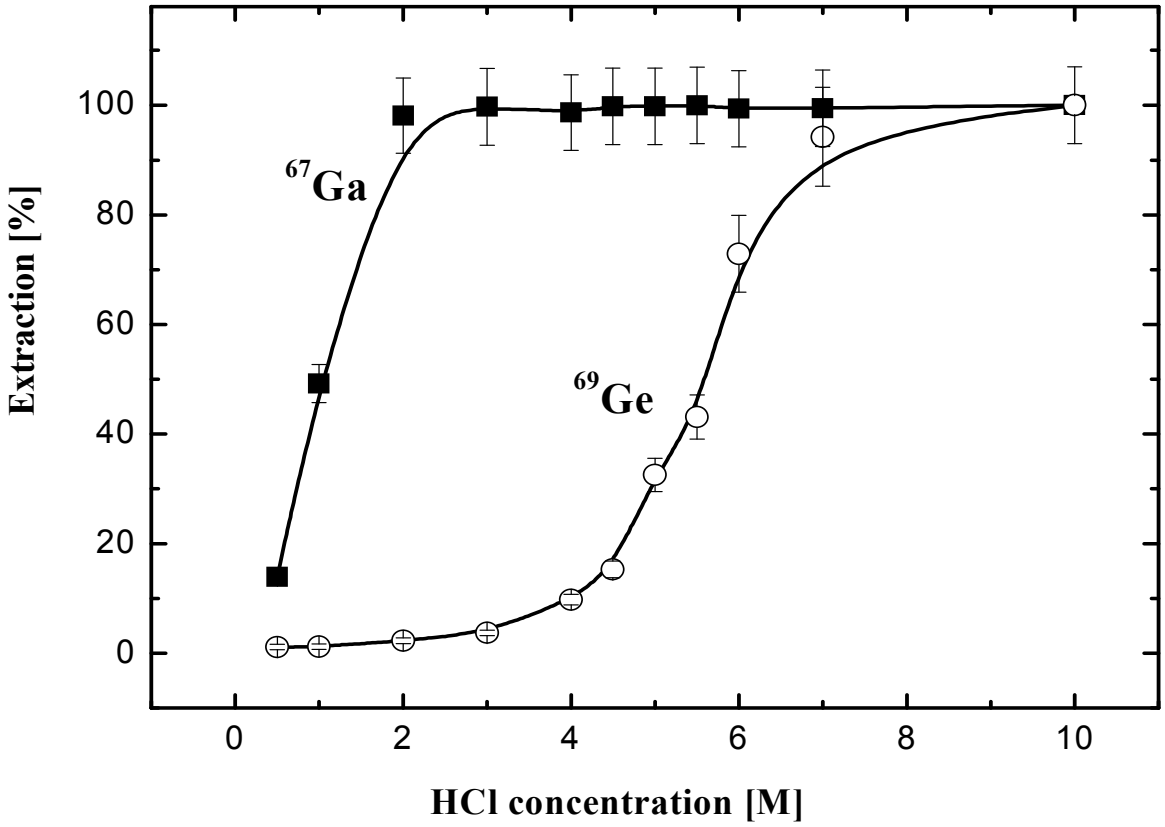

Fig. 4.20: Effect of HCl concentration on the extraction of radiogallium and radiogermanium using 0.1 M Aliquat 336 in o-xylene.

The extraction of radiogermanium increased with increase in HCl concentration, since germanium forms anionic chloro-complexes at high concentrations of hydrochloric acid (Mirzadeh and Lambrecht, 1996).

In general, a negatively charged metal complex can be extracted according to the equation;

$$ML_n^{-p} + pRNH^+L^-(org) \leftrightarrow (RNH^+)_p^{p+}ML_n^{-p}(org) + pL^- \qquad 4.4$$

where M = gallium or germanium

A priori, it must be assumed that the aqueous phase contains all the stepwise complexes ML_n^{z-n}. Thus the distribution ratio is

$$D_M = \frac{[(RNH)_p^{+p}ML_n^{-p}]_{org}}{\sum[ML_n^{z-n}]} = K_{ex}\frac{\beta_p[L^-]^p[RNHL]_{org}^p}{1+\sum\beta_p[L^-]^p} \qquad 4.5$$

The distribution of the compared M depends on both the free amine salt in the organic phase and the concentration of free L^- in the aqueous phase, until all elements in the aqueous phase are bound in the ML_n^{-p} complex

The results of this work suggest that the optimum condition for the separation of radiogallium from radiogermanium is an HCl concentration of 3 mol/L; at this acid concentration the extraction of radiogallium was 98.7±2 % and the co-extraction of radiogermanium about 3.2±0.5 %.

4.4.1.2 Effect of diluents

Various organic solvents, namely o-xylene, carbon tetrachloride, benzene, n-hexane, and cyclohexanone were tested to study the effect of varying nature of the organic diluent on the separation of radiogallium and radiogermanium with Aliquat 336. The organic phase diluents can influence the extraction process because both physical and chemical interactions exist between diluents and extractants. Extraction studies were carried out using 0.1 M Aliquat 336 in one of these solvents as the organic phase and 3 M HCl solution as the aqueous phase; the results are given in Table 4.9.

Table 4.9: Effect of various diluents on the extraction of radiogallium and radiogermanium from 3 M HCl using 0.1 M Aliquat 336.

Organic solvent	Radiogermanium [%]	Radiogallium [%]
o-Xylene	3.2 ± 0.5	98.7 ±1
Carbon tetrachloride	97.2 ± 1	1.7 ± 0.5
Benzene	3 ± 1	99.2 ± 1
n-Hexane	2.8 ± 0.5	98.9 ± 1
Cyclohexanone	14 ± 1	97.3 ± 2

It was observed that in the case of carbon tetrachloride the extraction of radiogallium was very low (about 2 %) while extraction of radiogermanium was about 97 %. It is better to

use CCl_4 for the separation of radiogermanium from gallium. Using cyclohexanone, radiogallium was extracted to about 97 % but with high co-extraction of radiogermanium (about 14 %). As apparent from the data, the extraction of radiogallium is higher (about 99 %) and co-extraction of radiogermanium is lower (about 3 %) and comparable in benzene, o-xylene, and n-hexane. In all other studies o-xylene was used as a diluent throughout the work.

4.4.1.3 Back extraction of radiogallium

After extraction, radiogallium and traces of radiogermanium were back-extracted from the organic phase (0.1 M Aliquat 336 in o-xylene) using different mineral acids and alkalis. Table 4.10 represents the results obtained.

Table 4.10: Effect of different stripping agents on the back-extraction of radiogermanium and radiogallium from Aliquat 336 in o-xylene.

Stripping Agent	Radiogermanium [%]	Radiogallium [%]
0.5 M HCl	98.5 ± 1	18.2 ± 1
3 M HCl	96.4 ± 2	0.1 ± 0.05
4 M HCl	95.4 ± 2	0.01 ± 0.005
0.5 M H_2SO_4	97.1 ± 1	3.6 ± 0.5
0.5 M KOH	96.7 ± 2	98.8 ± 1

Back-extraction experiments involving different concentrations of HCl as stripping solution revealed that the degree of back-extraction of radiogallium increased with the decreasing concentration of HCl. At 3 and 4 M HCl, radiogallium was not back-extracted; only radiogermanium was back-extracted. Sahoo (1991) reported that germanium was separated from gallium by a judicious choice of stripping agents. Both radiogallium and radiogermanium were back-extracted with 0.5 M KOH. From the above investigations, it was concluded that radiogermanium was back-extracted with 3 M HCl with 96.4±2 % yield while radiogallium was still extracted as chloro-complexes in the organic phase, and later back-extracted by 0.5 M KOH with a yield of 98±2 %.

4.4.2 Optimization Studies on the Separation via Cation – Exchange Chromatography

The adsorption behaviours of radiogallium and radiogermanium on the cation- exchange column (Amberlite IR-120) were studied in detail. The dependence of the distribution coefficients (K_d values) for n.c.a. ^{67}Ga and n.c.a. ^{68}Ge/^{69}Ge on the HCl concentrations was investigated and the results obtained are given in Fig. 4.21.

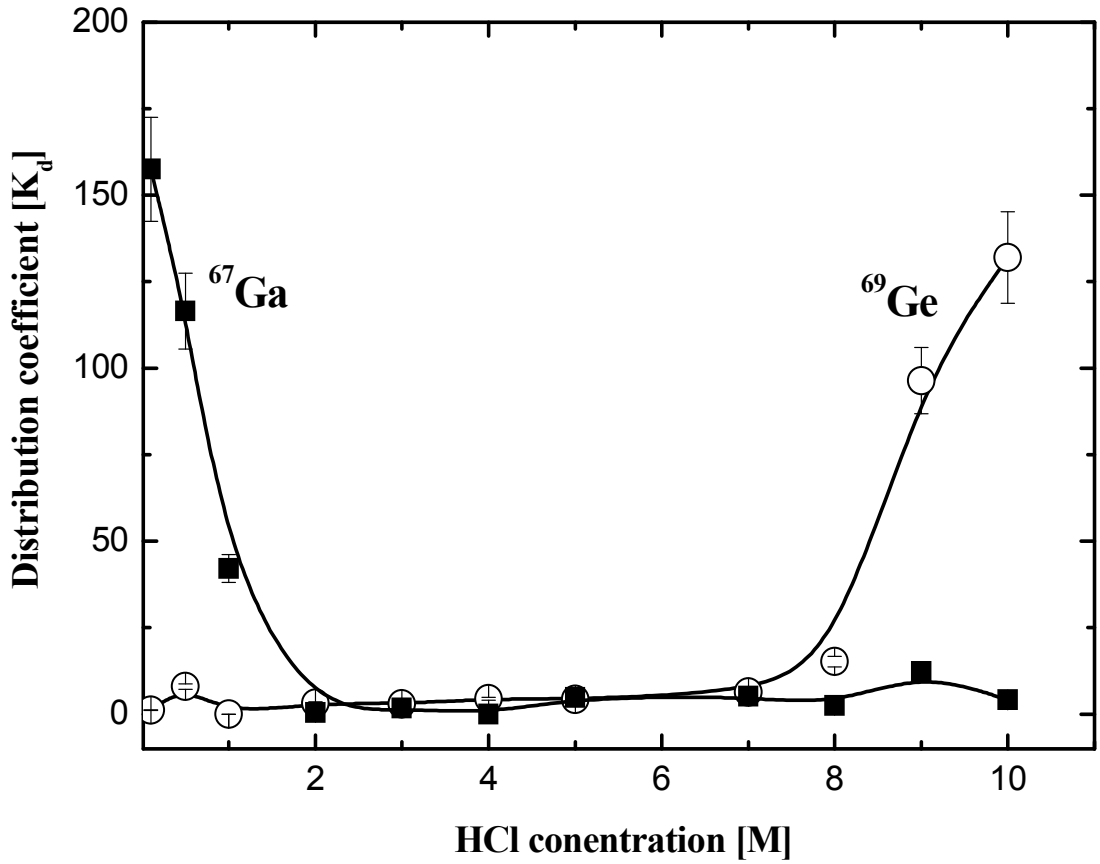

Fig. 4.21: Distribution coefficients of no-carrier-added ^{67}Ga and ^{69}Ge on Amberlite IR-120 as a function of HCl concentration.

The results show that radiogallium is adsorbed on the resin at low HCl concentration (< 1 M) with declining tendency as the HCl concentration increases up to 2 M. This can be attributed to the formation of cationic species of radiogallium at low concentration of HCl (see above). By increasing the concentration of HCl from 2 to 10 M, radiogallium was not retained on the used exchanger, possibly due to the formation of anionic $[^{67}GaCl_4]^-$. On the other hand, radiogermanium is weakly adsorbed at low acid concentration but is retained at high HCl concentration. Ge exists in negatively-charged chlorogermanium complexes which show the expected low absorptivity toward cation exchanger. However, as shown in Fig. 4.21, in stronger HCl solutions, the distribution coefficient of germanium increases rapidly. This is

not unexpected since at high acid concentrations the germanium distribution constant is hampered by the serious loss of volatile germanium chloride. Nelson and Michelson (1966) observed nearly the same behaviour in case of germanium with cation exchanger but in HBr medium. The adsorption of negatively charged halocomplexes of germanium on a cation exchanger is a phenomenon that is not clearly understood (Mirzadeh and Lambrecht, 1996).

Depending on the distribution coefficient [K_d] values obtained, the elution profiles of radiogermanium and radiogallium were measured in the column experiment. About 500 µL of the separated n.c.a. $^{68}Ge/^{69}Ge$ solution and 200 µL of ^{67}Ga solution were applied. The mixture was loaded onto a glass column containing Amberlite IR-120 resin after adjusting to 0.5 M HCl. The results are shown in Fig. 4.22. At low HCl of 0.5 M concentration, radiogermanium was instantly eluted and runs through the column during the loading process. Later, about 80 % of the radiogallium activity could be eluted by 80 mL of 3 M HCl. No ^{69}Ge was detected by γ-spectrometry in this eluted solution.

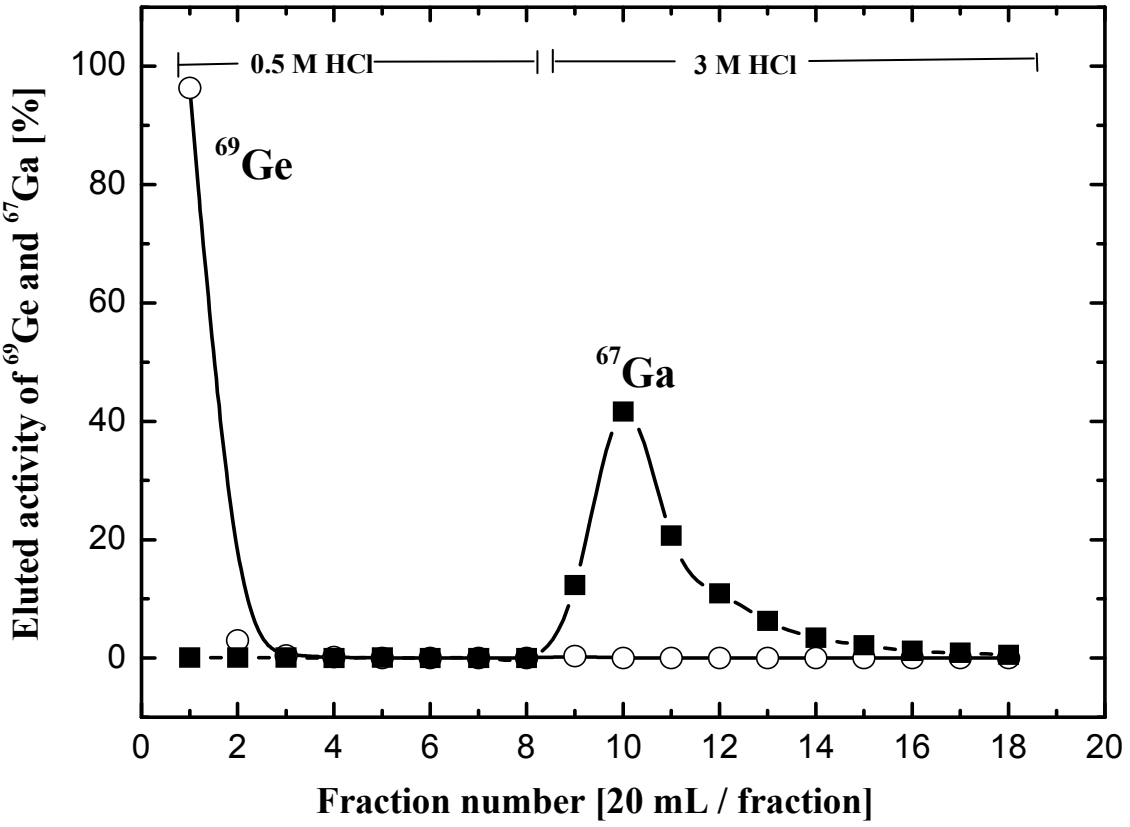

Fig. 4.22: Elution profiles of ^{67}Ga and ^{69}Ge with 0.5 and 3 M HCl from a column packed with Amberlite IR120. Fraction volume, 20 mL; flow rate, 3 mL/min. Elution started directly after loading the activity on the column.

4.4.3 Comparison of Investigated Separation Methods

The data on the separation of radiogallium via solvent extraction and cation exchange methods, obtained under the optimized conditions of the two processes, (sections 4.4.1 and 4.4.2) are summarized in Table 4.11. A comparison of the two methods investigated in this work reveals that the radiochemical separation using 0.1 M Aliquat 336 in o-xylene is advantageous than that using the strong cation-exchanger Amberlite IR120: the efficiency of the separation is higher, the time needed is shorter, and the final volume is smaller.

Table 4.11: Comparison of separation methods for no-carrier-added radiogallium from parent radiogermanium.

Parameter	Aliquat 336 in o-xylene	Amberlite IR120
Efficiency of separation [%]	> 95	80
Time of separation	15 min	2 h
Volume of product solution	10 mL	80 mL
Chemical form of the activity after separation	Hydroxide	Chloride

4.4.4 Application of the Optimized Method to ^{68}Ge / ^{68}Ga Separation

A summary of the radiochemical procedure with the optimized conditions for separation of no-carrier-added radiogallium from parent radiogermanium is schematically presented in Fig. 4.23. The solution containing radiogermanium (parent) was adjusted to 3 M HCl and an extraction using 0.1 M Aliquat 336 in o-xylene was carried out. After shaking for 2 min, 98.7 % of radiogallium was extracted from the parent radiogermanium. About 3.2 % of radiogermanium was co-extracted. To remove these traces of radiogermanium, which co-extracted with the radiogallium, the organic phase was shaken with 3 M HCl solution (two times) and then the radiogallium was back-extracted using 0.5 M KOH with a yield of 99.2 %.

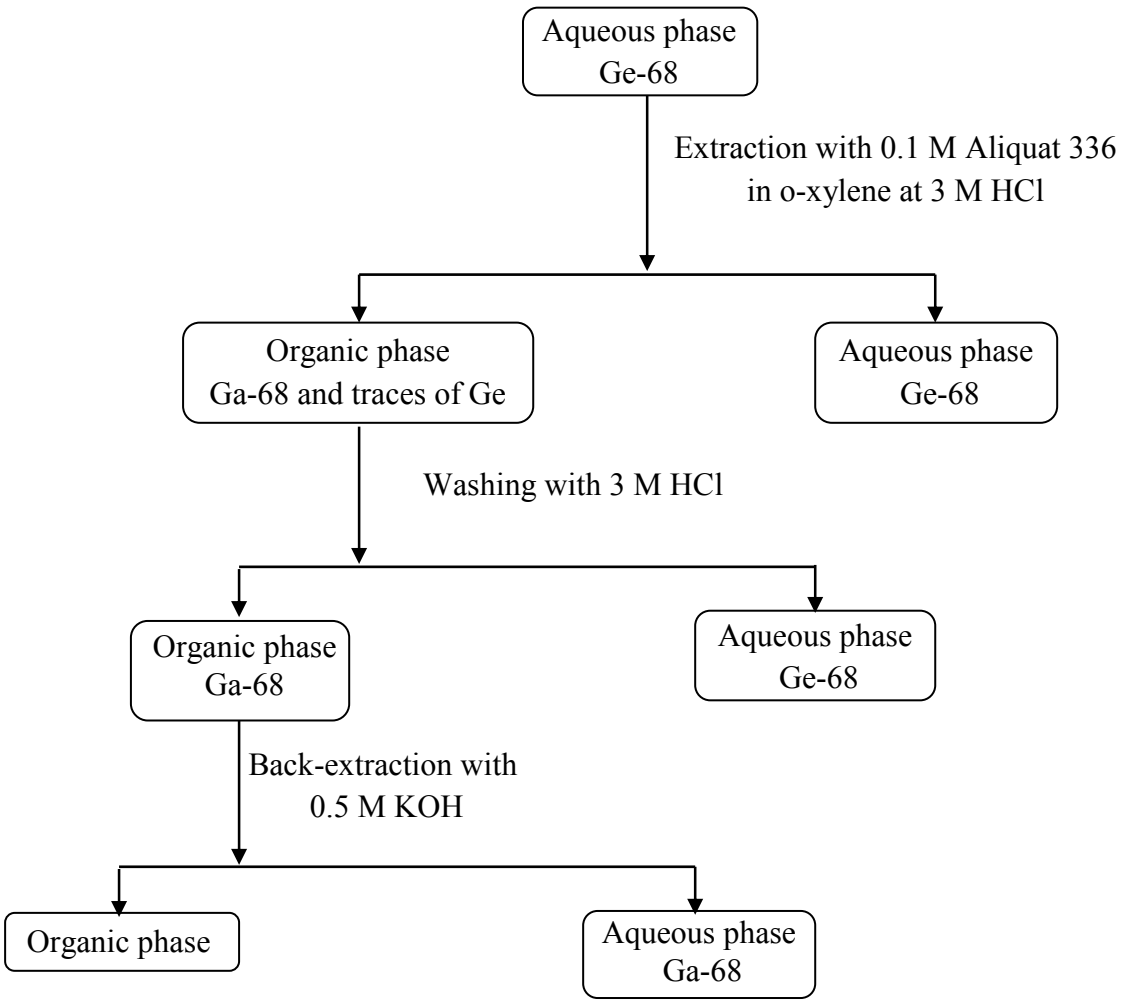

Fig. 4.23: Flow sheet of the separation method of ^{68}Ga from parent ^{68}Ge.

4.4.5 Production and Quality Control of ^{68}Ga

The radiochemical procedure developed leads to the separation of radiochemically pure no- carrier-added ^{68}Ga radionuclide. The recovery yield of ^{68}Ga was found to be 95.2 % with high radionuclidic purity. Less than 0.008 % of ^{68}Ge was detected in the final separated solution via gamma-ray spectrometry. To decrease the amount of ^{68}Ge further, the back-extraction of ^{68}Ge with 3 M HCl solution was repeated two or three times before n.c.a. ^{68}Ga was finally back-extracted with 0.5 M KOH. Fig. 4.24 shows the γ-ray spectrum of ^{68}Ga after separation from the parent ^{68}Ge under optimum conditions.

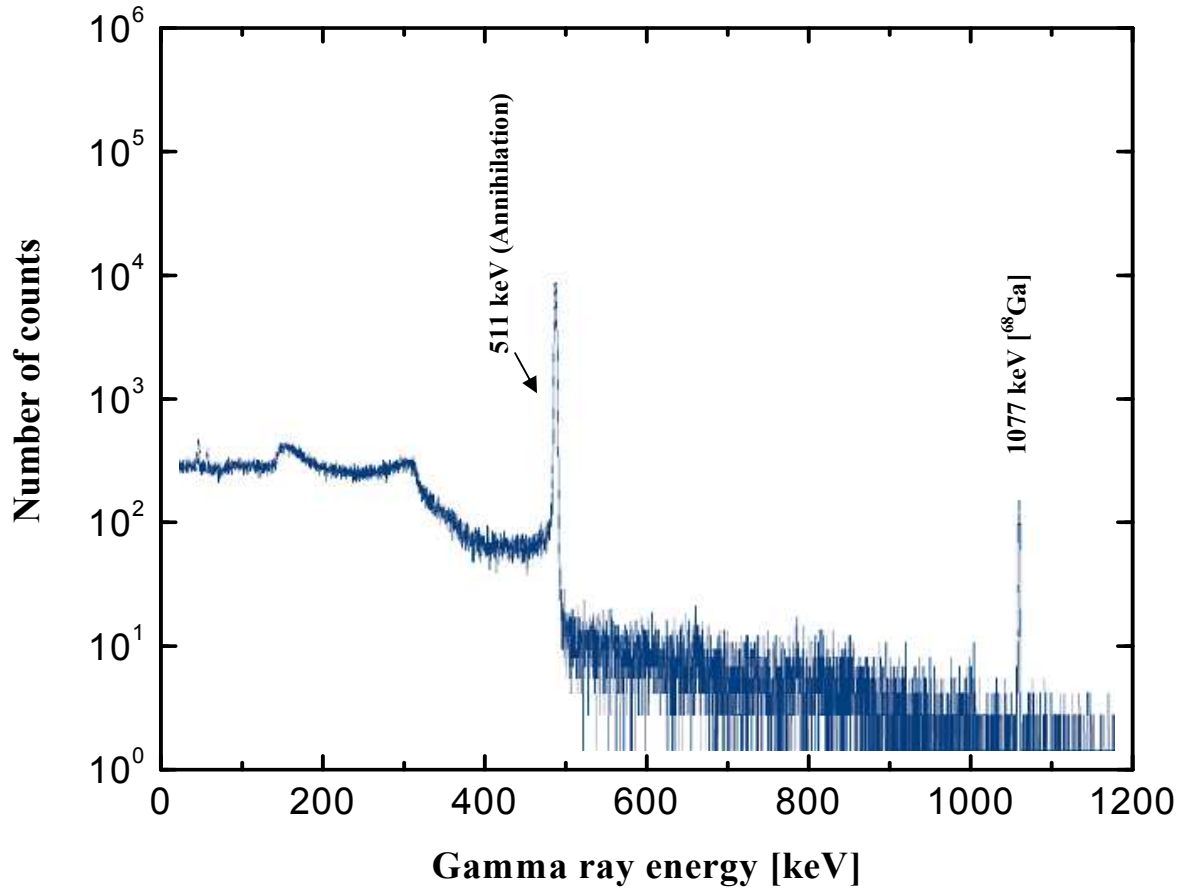

Fig. 4.24: Gamma-ray spectrum of ^{68}Ga after separation from parent the ^{68}Ge.

4.5 Separation of n.c.a. Radiobromine and n.c.a. Radiogallium from Irradiated ZnSe Targets

Several methods for isolation of bromine isotopes are described in the literature but none of those methods make use of ion exchange chromatography [section 1.9.3]. In the present work the separation of no-carrier-added radiobromine and no-carrier-added radiogallium from an irradiated ZnSe target is developed using ion exchange chromatography. ZnSe is a good heat conductor and it is potentially a good target material for producing radiobromine. In this work ZnSe of natural abundance was chosen as material for the developmental studies. Thus bromine and selenium radioisotopes were formed in the interaction of protons with Se and several radioisotopes of gallium and zinc were formed from Zn. Fig. 4.25 reproduces the γ–ray spectrum of ZnSe target irradiated with 45 MeV protons at the injector of COSY. For production of an individual bromine radionuclide in high radionuclidic purity, of course isotopically enriched targets would be needed.

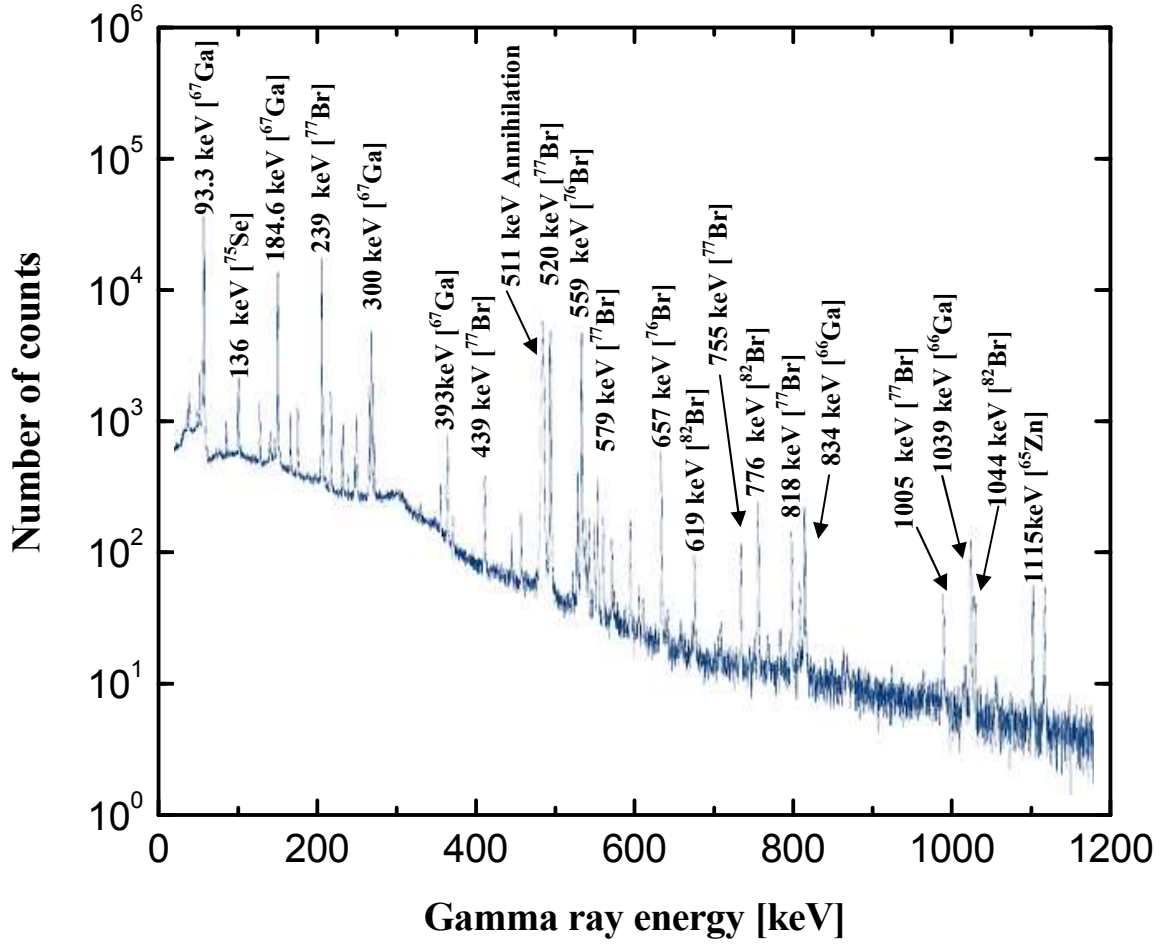

Fig. 4.25: Gamma-ray spectrum of ZnSe target irradiated with 45 MeV protons at injector of COSY.

In order to determine the radiochemical purity of the separation processes, the two radionuclides ^{65}Zn and ^{75}Se were used to analyse the fractions of zinc and selenium target material in each experiment. The radionuclide ^{65}Zn was formed by two nuclear reactions on ^{66}Zn, namely ^{66}Zn(p,pn)^{65}Zn and ^{66}Zn(p,2n)^{65}Ga→^{65}Zn. ^{75}Se was produced by ^{76}Se(p,pn)^{75}Se and ^{76}Se(p,2n)^{75}Br→^{75}Se nuclear reactions. Finally, an optimized procedure for the production of ^{77}Br and ^{67}Ga was developed, and quality control of the products was done.

4.5.1 Cation Exchange Studies

4.5.1.1 Effect of HNO_3 and HCl concentrations

Various concentrations of HNO_3 (0.1 -13 M) and of HCl (0.5-10 M) were used to study the effect of nitric and hydrochloric acid concentrations on the adsorption of n.c.a. radiobromine, n.c.a. radiogallium, zinc and selenium on the cation exchange resin Amberlyst 15, in H^+ form, as described before in section 3.8.2. Figs. 4.26 and 4.27 illustrate the results obtained. There was no significant adsorption of n.c.a. radiobromine and selenium on this resin at any acid concentration studied. This is attributed to the formation of anionic species like bromide and selenide/selenite in case of n.c.a. radiobromine and selenium, respectively, which are not adsorbed on the cation exchange resin. In both acids, i.e. HNO_3 and HCl, n.c.a. radiogallium was strongly adsorbed at very low concentrations <1 M, increasing with decreasing molarity of acid, but its adsorption was stronger in case of nitric acid than in case of hydrochloric acid. After 1 M of HNO_3 or HCl there was no further adsorption of n.c.a. radiogallium with the increasing acid concentration.

The adsorption of n.c.a. radiogallium at low acid concentrations is due to the formation of cationic Ga^{3+} species, while with the increasing acid concentration, n.c.a. radiogallium forms anionic species $[GaCl_4]^-$ in case of hydrochloric acid, and may be $[Ga(NO_3)_4]^-$ in case of nitric acid. Zinc was adsorbed on the resin in HNO_3 and HCl at very low concentrations because it forms cationic Zn^{2+} species. Its adsorption decreased with the increasing concentration of acids due to the formation of anionic species $[ZnCl_4]^{2-}$ with HCl and may be $[Zn(NO_3)_4]^{2-}$ with HNO_3.

From the above results, it is concluded that n.c.a. radiogallium and zinc were adsorbed at very low concentrations of both acids while n.c.a. radiobromine and selenium were not. It is not possible to separate n.c.a. radiogallium using the conditions described above, due to the co-adsorption of traces of zinc with it.

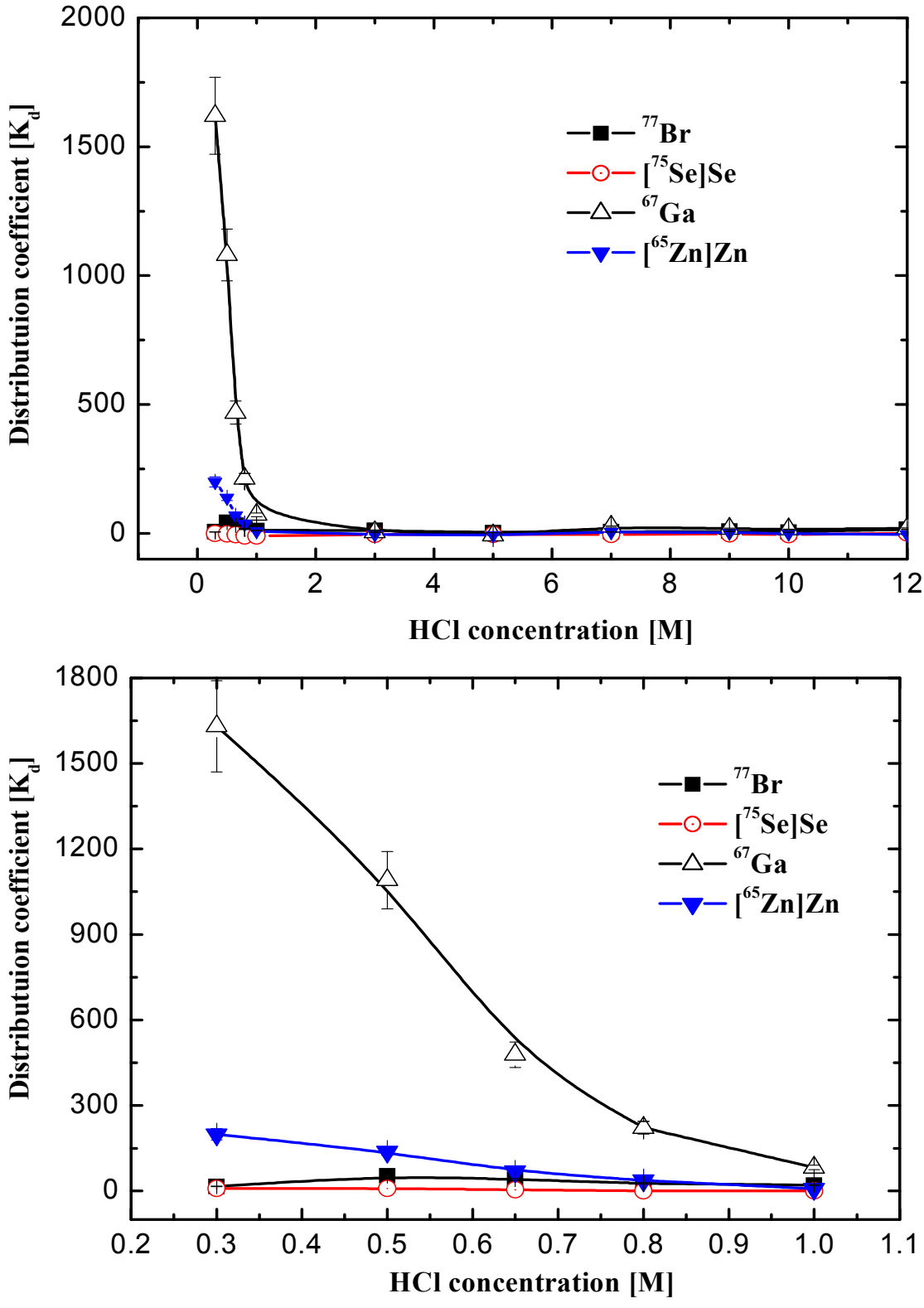

Fig. 4.26: Distribution coefficients of no-carrier-added radiobromine, no-carrier-added radiogallium, zinc and selenium at various HCl concentrations on cation exchange resin Amberlyst 15, H^+ form. The above curve shows the whole HCl range while the lower one from 0.3-1 M HCl.

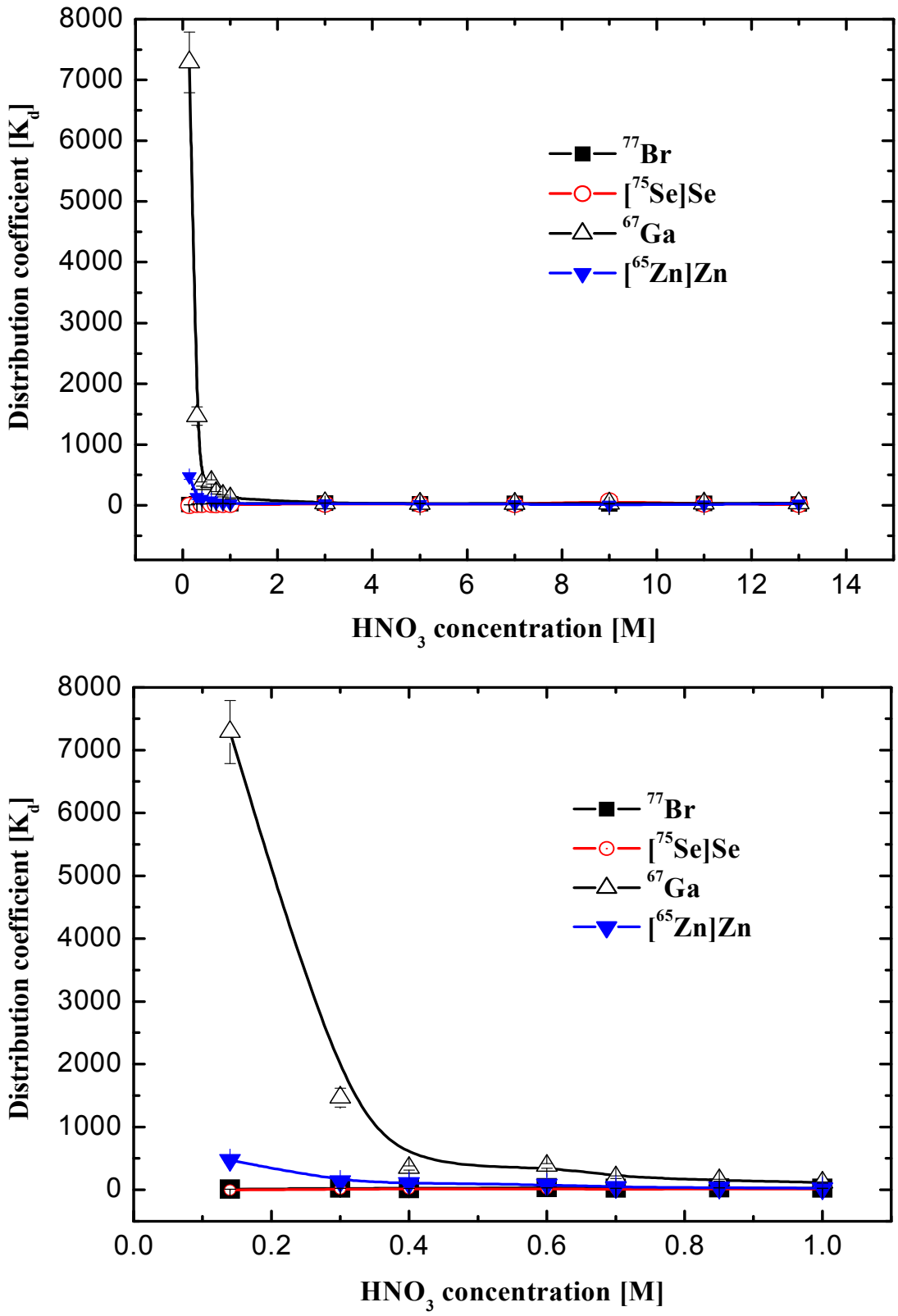

Fig. 4.27: Distribution coefficients of no-carrier-added radiobromine, no-carrier-added radiogallium, zinc and selenium at various HNO_3 concentrations on cation exchange resin Amberlyst 15. The above curve shows the whole HNO_3 range while the lower one from 0.1-1 M HNO_3.

4.5.2 Anion Exchange Studies

The distribution behaviours of no-carrier-added radiobromine, no-carrier-added radio-gallium, zinc and selenium on the anion exchange resin (Dowex 1X10, Cl^- and OH^- form) were investigated under different conditions as described in section 2.8.2.

4.5.2.1 Effect of KOH concentration

The effect of various KOH concentrations (0.1 -10 M) on the adsorption behaviour of the above mentioned elements on the anion exchange resin was studied. Fig. 4.28 illustrates the results obtained. It was observed that the n.c.a. radiobromine is adsorbed at low KOH concentrations. The K_d value was about 400 at 0.1 M; thereafter the adsorption decreased with increasing concentration of KOH up to 1 M and then remained nearly constant. This is due to the fact that bromine occurs as anion species Br^- at low KOH concentrations, while with increasing concentrations hypo-halite ions BrO^- are formed according to the eq. 4.6. Hypo-halite ions in warm concentrated alkaline solution disproportionate to halate $[BrO_3]^-$ and halide ion (Kleinberg and Cowan, 1960).

$$X_2 + 2KOH \leftrightarrow KX + KOX + H_2O \qquad 4.6$$

Radiogallium (n.c.a.) was not adsorbed on the anion exchange resin in KOH over the whole pH range studied. This is attributed to the formation of intermediate activated species such as $K^+Ga(OH)_3.OH^-$ at KOH level below 1 M, or $K^+_2Ga(OH)_3$ at high potassium levels (Mihaylov and Distin, 1992), according to the next equation, valid for low potassium hydroxide concentration,

$$K^+[Ga(OH)_4]^- \underset{K_2}{\overset{K_1}{\leftrightarrow}} K^+[Ga(OH)_3], OH^- \qquad 4.7$$

At higher concentration of potassium hydroxide it is,

$$K^+ + K^+[Ga(OH)_4]^- \underset{k_2}{\overset{k_1}{\leftrightarrow}} K^+.K^+[Ga(OH)_3] + OH^- \qquad 4.8$$

Selenium and zinc were adsorbed at very low concentration and the adsorption decreased with the increasing KOH concentration up to 0.8 M. With further increase, no adsorption of both elements was observed. The adsorption of zinc at low KOH concentrations is based on the formation of $[Zn(OH)_4]^{2-}$. Hirsch and Portock (1970) reported that Zn(II) is one of the cations (at high pH) forming anionic hydroxide complexes which are not absorbed into the anion resin to any great extent. In case of selenium, anion species Se^{2-} and $[SeO_3]^{2-}$ are formed at low KOH concentrations.

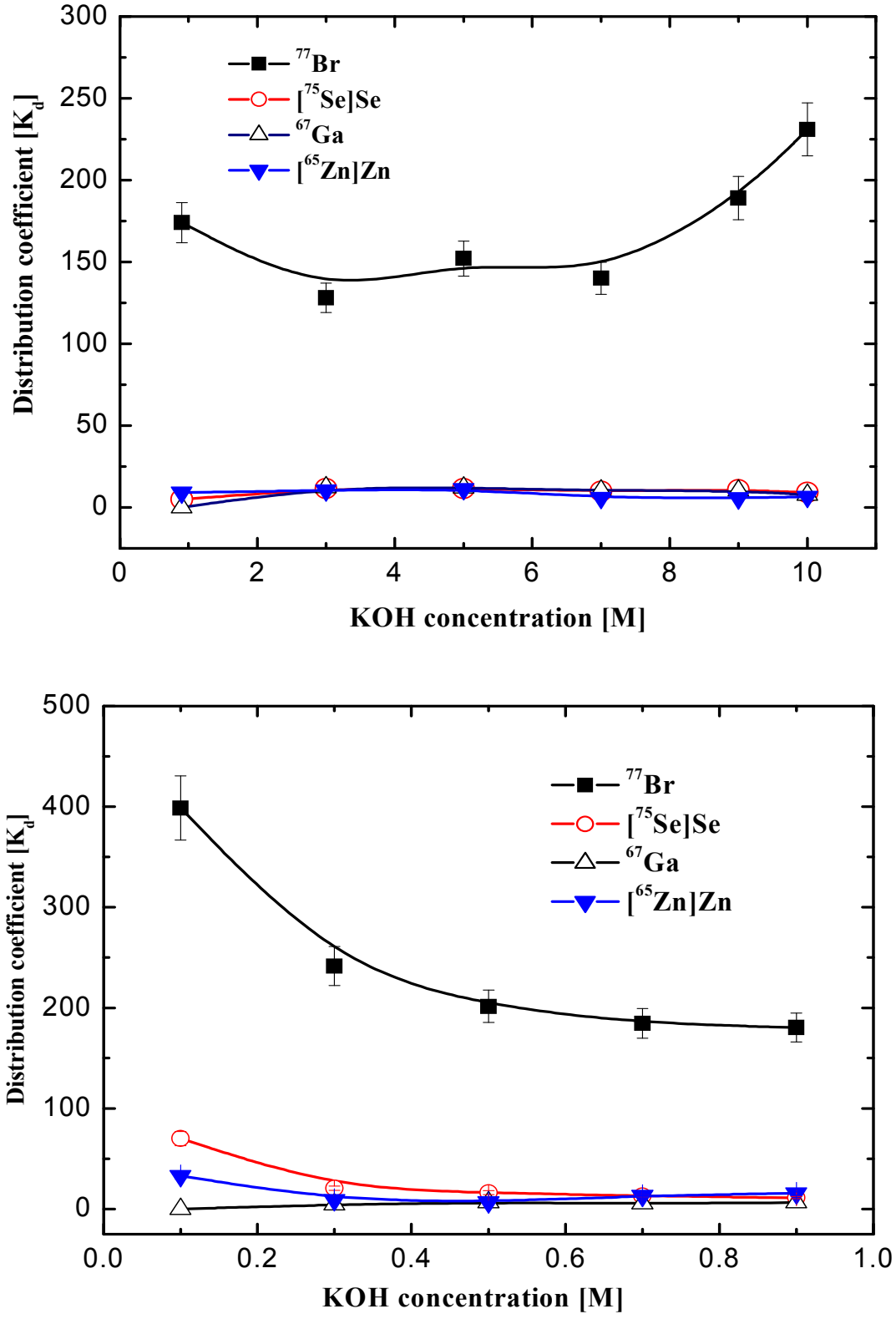

Fig. 4.28: Distribution coefficient of no-carrier-added radiobromine, no-carrier-added radiogallium, zinc and selenium at various concentrations of KOH on anion exchange resin Dowex 1x10. The upper curve shows the 1-10 M KOH range while the lower one the 0.1-1 M KOH range.

By dissolution with excess KOH, selenium was converted to selenide/selenite mixture according to equation 4.9. Nevertheless, both selenide/selenite did not undergo ion exchange reaction with OH^- at high KOH concentrations; thus, no appreciable adsorption was observed.

$$6KOH + 3Se \rightarrow 2K_2Se + K_2SeO_3 + 3H_2O \qquad 4.9$$

4.5.2.2 Effect of HNO_3 concentration

Different concentrations of HNO_3 (0.1 -13 M) were used to study the adsorption of n.c.a. radiobromine, n.c.a. radiogallium, zinc and selenium. Fig. 4.29 shows that at low HNO_3 concentrations, n.c.a. radiobromine is adsorbed significantly less than in case of KOH. The K_d value was about 180 at 0.1 M concentration. Thereafter the adsorption of n.c.a. radiobromine decreased with the increasing HNO_3 concentration. This may be attributed to the competition between bromide and nitrate ions. Radiogallium (n.c.a.) was slightly adsorbed at very low concentration but the adsorption decreased at high concentrations of nitric acid. Zinc was slightly adsorbed at higher concentration of nitric acid. Selenium was not adsorbed from nitric acid. Faris and Buchanan (1964) reported that gallium, zinc and selenium were not adsorbed on strongly basic anion exchanger Dowex 1x10 from 0.1 -14 M HNO_3**.**

4.5.2.3 Effect of HCl concentration

The effect of HCl concentration (0.5-10 M) on the adsorption behaviour of n.c.a. radiobromine and n.c.a. radiogallium and zinc is shown in Fig. 4.30. The n.c.a. radiobromine is not adsorbed from HCl under conditions studied. Radiogallium was strongly adsorbed and its adsorption increased with increasing HCl concentration, due to the formation of anionic species $[GaCl_4]^-$. The zinc adsorption increased with increasing acidity and reached a maximum at about 4 M HCl, then decreasing with higher concentrations. Zinc adsorption from HCl medium is attributed to the formation of strong anionic complexes $[ZnCl_4]^{2-}$ (Marcus, 1967).

From the distribution coefficient (K_d) values investigated in sections 4.5.2.1, 4.5.2.2. and 4.5.2.3, it is concluded that the optimum conditions for n.c.a. radiobromine separation were after dissolution of ZnSe target in KOH. The n.c.a. radiobromine was adsorbed at 1 M KOH using anion exchange Dowex 1x10 while the other elements were not.

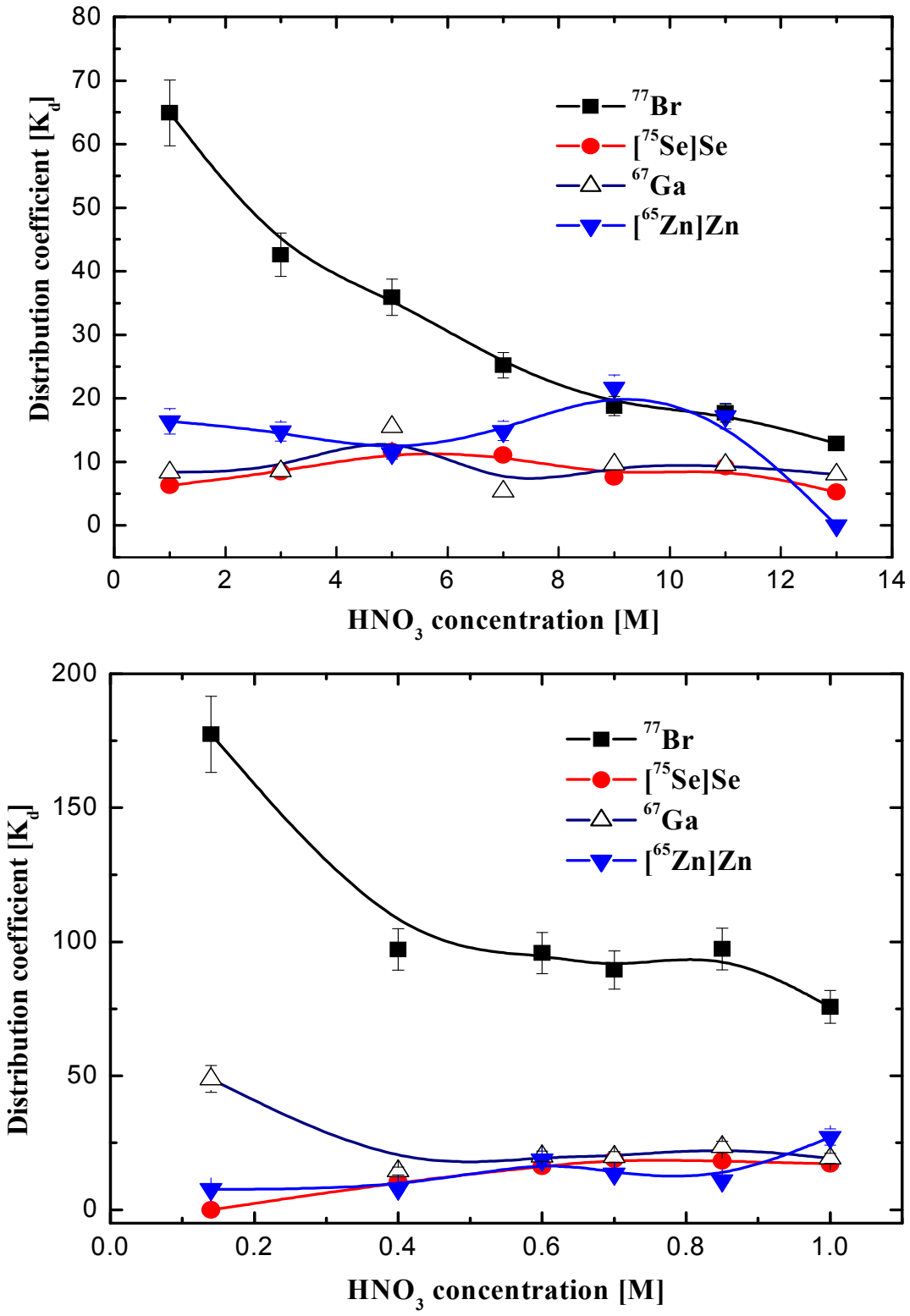

Fig. 4.29: Distribution coefficient of no-carrier-added radiobromine, no-carrier-added radiogallium, zinc and selenium at various concentration of HNO_3 on anion exchange resin Dowex 1x10 , the upper curve shows results for 1-13 M HNO_3 while the lower one for 0.1-1 M HNO_3.

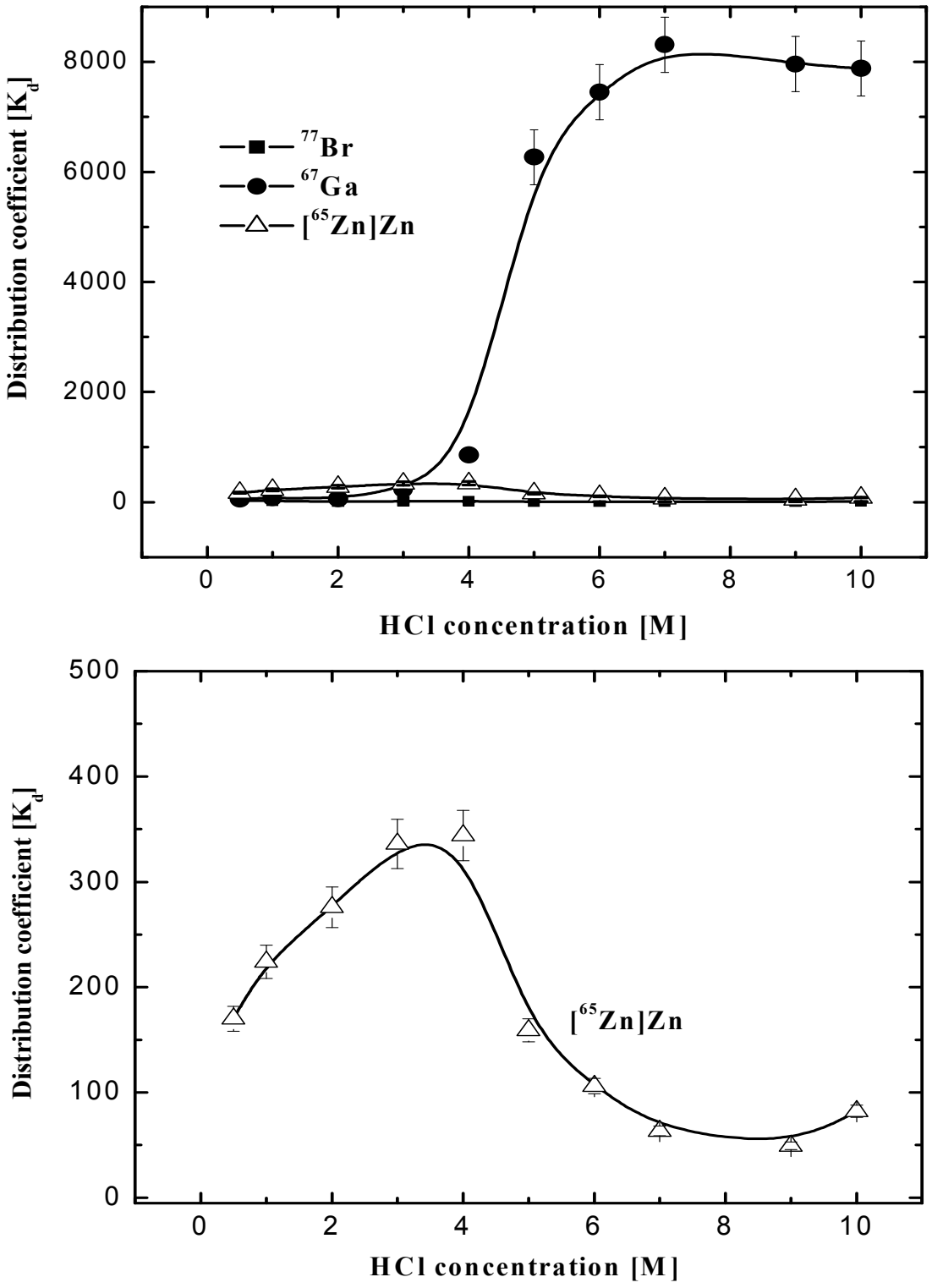

Fig. 4.30: Distribution coefficient of no-carrier-added radiobromine, no-carrier-added radiogallium, zinc and selenium on anion exchange resin Dowex 1x10 at various concentrations of HCl. The above digram shows all elements studied, while the lower one only the Zn adsorption behaviour.

4.5.2.4 Effect of concentration of chloride and sulfate ions

The influence of varying Cl^- and SO_4^{-2} concentrations added to 1 M KOH solution on the K_d values of the investigated elements on the anion exchanger Dowex 1x10 was studied as explained in section 2.8.3 and the results obtained are shown in Figs. 4.31 and 4.32. It is seen that K_d values do not remain constant under the conditions studied; they change depending on the concentrations of Cl^- and SO_4^{-2} ions. The n.c.a. radiobromine was slightly adsorbed at low concentrations of both ions and its adsorption decreased with increasing Cl^- and SO_4^{-2} concentrations. In case of Cl^-, (Fig. 4.31) the distribution coefficient values of n.c.a. radiobromine decrease to reach about 3 while in case of sulfate (Fig. 4.32) the values are still high (around 70) with increasing sulfate ions up to 2 M. The decrease in adsorption was attributed to the competition between bromide and chloride and sulfate anions, which appeared to be more significant in the case of chloride than in the case of sulfate. Zinc and selenium show the same behaviour as the n.c.a. radiobromine but to a lesser extent. Radiogallium (n.c.a.) adsorption increased by increasing both chloride and sulfate anion concentrations. Radiogallium may form with chloride and sulfate complex anions which can be adsorbed on the anion exchanger.

From the results obtained, it is concluded that n.c.a. radiogallium can be separated from the other elements under investigation by increasing the chloride strength using HCl or NH_4Cl.

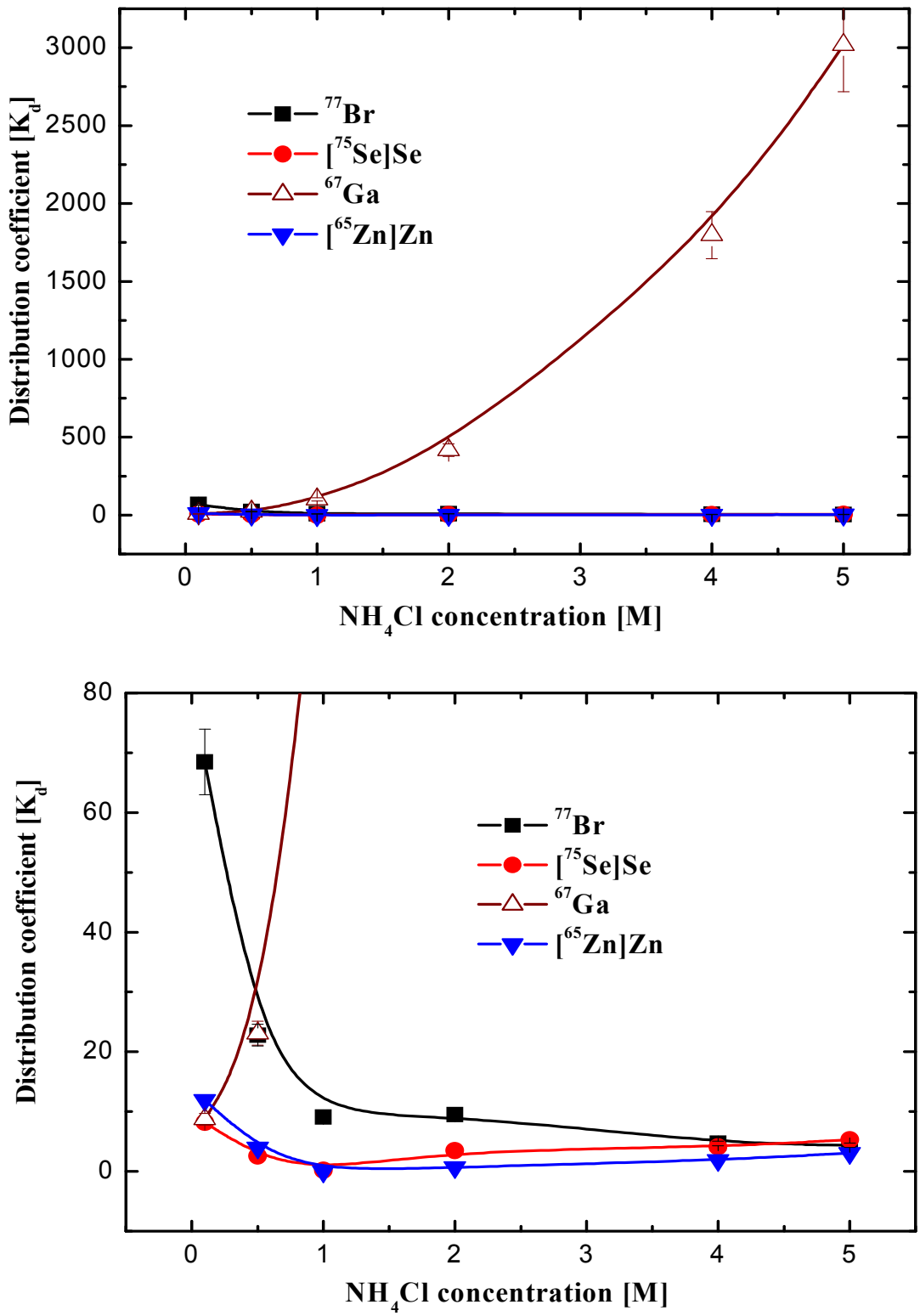

Fig. 4.31: Distribution coefficient of no-carrier-added radiobromine, no-carrier-added radiogallium, zinc and selenium at various concentrations of NH_4Cl on anion exchange resin Dowex 1x10. The above diagram shows the full K_d range while the lower one shows the adsorption behaviour of elements at lower K_d scale.

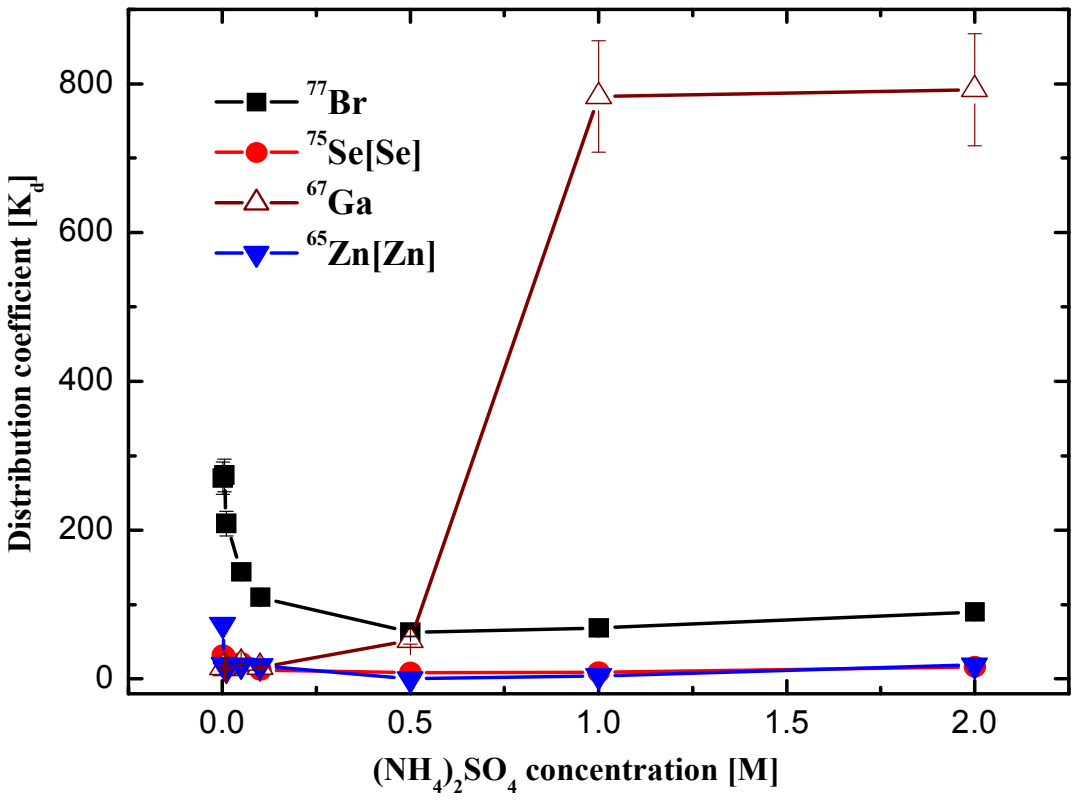

Fig. 4.32: Distribution coefficients of no-carrier-added radiobromine, no-carrier-added radiogallium, zinc and selenium at various concentrations of $(NH_4)_2SO_4$ on anion exchange resin Dowex 1x10.

4.5.3 Elution of n.c.a. Radiobromine

From the above mentioned experiments it is evident that n.c.a. radiobromine is strongly adsorbed on the Dowex 1x10 resin at low KOH concentration (Fig. 4.28), while n.c.a. radiogallium, zinc and selenium are weakly adsorbed and run through the column during the loading process. Several reagents for the elution of n.c.a. radiobromine like tetroctyl methyl ammonium chloride (TOMAC) in o-xylene and 0.2 M H_2SO_4 were used as described in section 2.8.4. The separation profiles are shown in Figs. 4.33 and 4.34. By using 1 M KOH as a mobile phase, n.c.a. radiogallium, zinc and selenium were removed. Some of the selenium got precipitated on the top of the column. In case of tetra octyl methyl ammonium chloride in o-xylene, the elution of n.c.a. radiobromine was about 95±2 % of the loaded sample. The problem in this case was that 12±2 % of the selenium on the top of the column was eluted with the n.c.a. radiobromine.

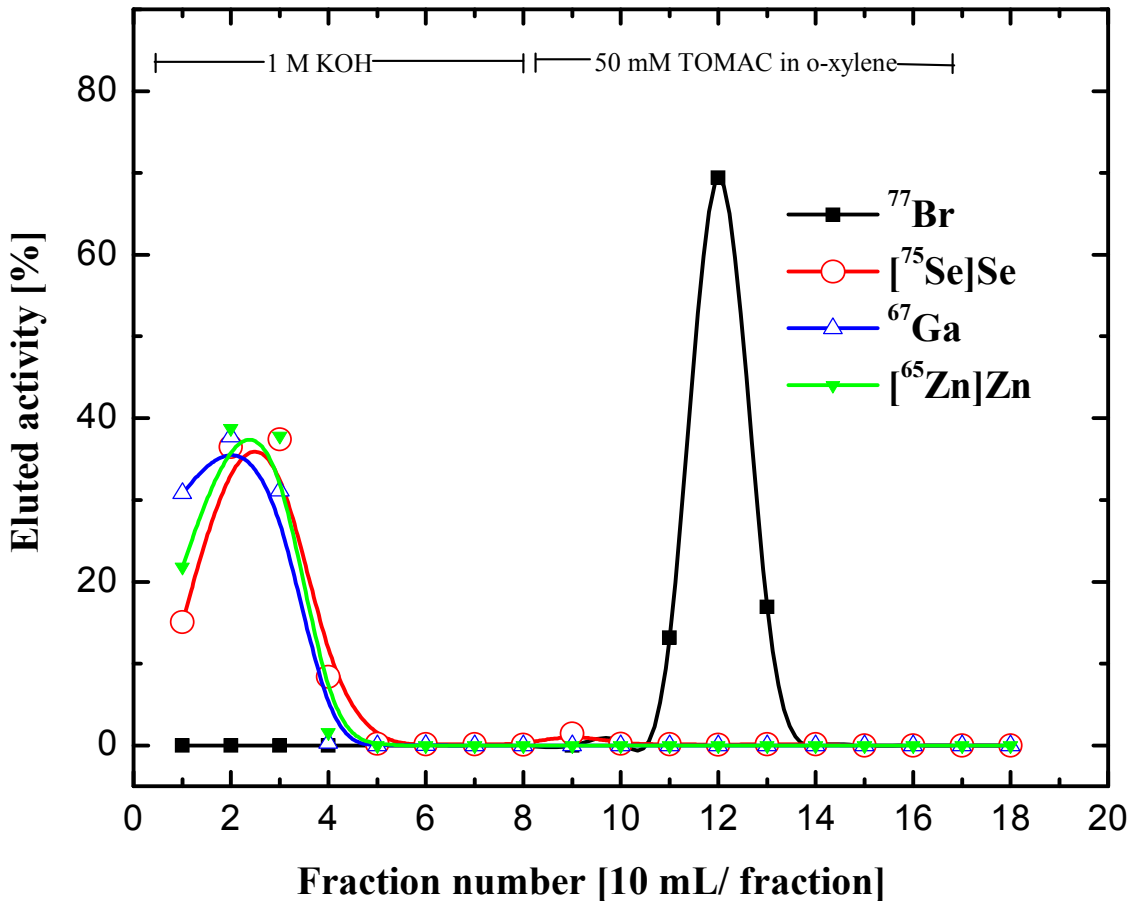

Fig. 4.33: Elution curves for no-carrier-added radiobromine, no-carrier-added radiogallium, zinc and selenium using Dowex 1x10 resin with a flow rate of 1±0.2 mL/min.

When using 0.2 M H_2SO_4 for the n.c.a. radiobromine elution, 50 mL of H_2O were used for washing the column before change from alkaline to acidic. The elution curve of n.c.a. radiobromine is shown in Fig. 4.34. More than 95 ±2 % of n.c.a. radiobromine was obtained in 50 mL of 0.2 M H_2SO_4. Before evaporation, an excess of KOH was added to form K^*Br and to avoid any loss of radiobromine. As described in section 3.8.4, during evaporation process a K_2SO_4 precipitate appeared, resulting in about 1-4 % loss of n.c.a. radiobromine. At the end, K^*Br in high purity was obtained. No ^{67}Ga was found in radiobromine solution. From the above results, it was concluded that 0.2 M H_2SO_4 is the best for the elution. The overall yield of no-carrier-added radiobromine was more than 92 ±2 % with high purity.

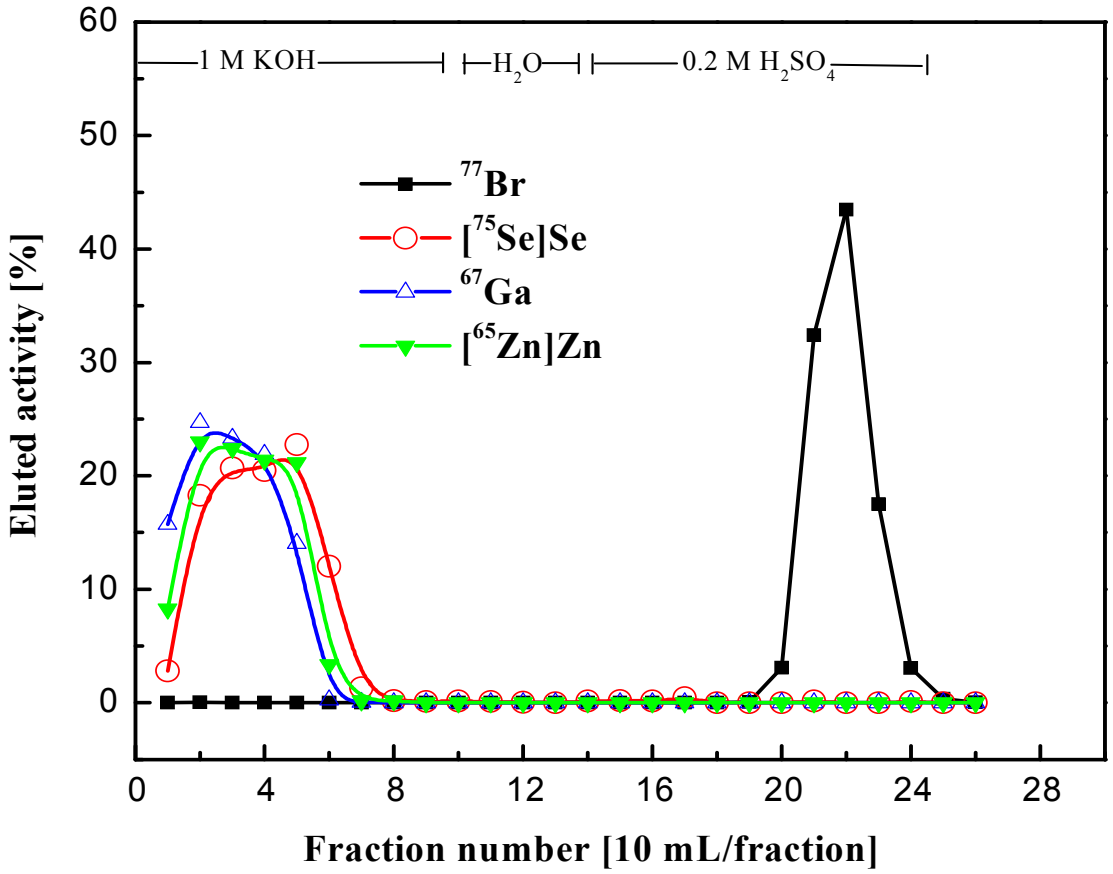

Fig. 4.34: Elution curves for no-carrier-added radiobromine, no-carrier-added radiogallium, and zinc and selenium from Dowex 1x10 resin with flow rate of 1±0.2 mL/min of various eluting agents.

4.5.4 Elution of n.c.a. Radiogallium

After the separation of no-carrier-added radiobromine, the eluted solution in 1 M KOH contains no-carrier-added radiogallium, zinc and selenium. Two methods were used to elute n.c.a. radiogallium; the first by acidifying the solution up to 9 M HCl and passing through a column filled with Dowex 1x10, Cl^- form. The elution profile (Fig. 4.35) shows that with 9 M HCl selenium was eluted completely in 80 mL while n.c.a. radiogallium was adsorbed and zinc is eluted slowly and increased by using conc. HCl. No-carrier-added radiogallium was eluted with 0.5 M HCl. However, the produced n.c.a. radiogallium still contained about 0.3 % of zinc, i.e. it was not of high purity.

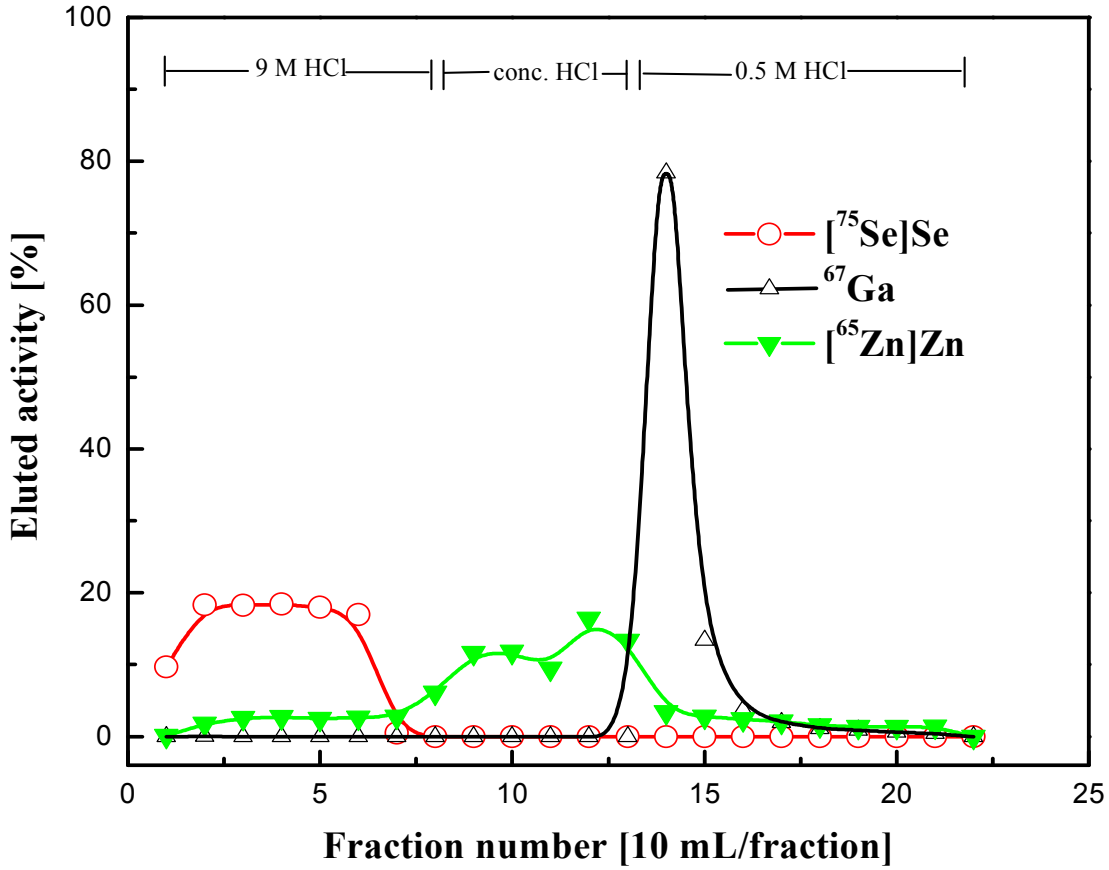

Fig. 4.35: Elution curves for no-carrier-added radiobromine, no-carrier-added radiogallium, zinc and selenium using Dowex 1x10 resin with a flow rate of 1±0.2 mL/min of various eluting agents.

The second method was based on increasing the chloride ion strength by dissolving NH_4Cl in the residue solution (60 mL of 1 M KOH) to reach 4 M after separation of n.c.a. radiobromine. Then the sample was passed through the column filled with Dowex 1x10, Cl^- form. Radiogallium (n.c.a.) was adsorbed while zinc and selenium were eluted by 4 M NH_4Cl solution. Thereafter, radiogallium (n.c.a.) was eluted by 0.1 M HCl. More than 96±3 % of n.c.a. radiogallium loaded on the column was obtained in 40 mL. The radionuclides ^{65}Zn< 0.008 % and ^{75}Se < 0.0004 % were detected in the radiogallium solution. The elution profile is shown in Fig. 4.36.

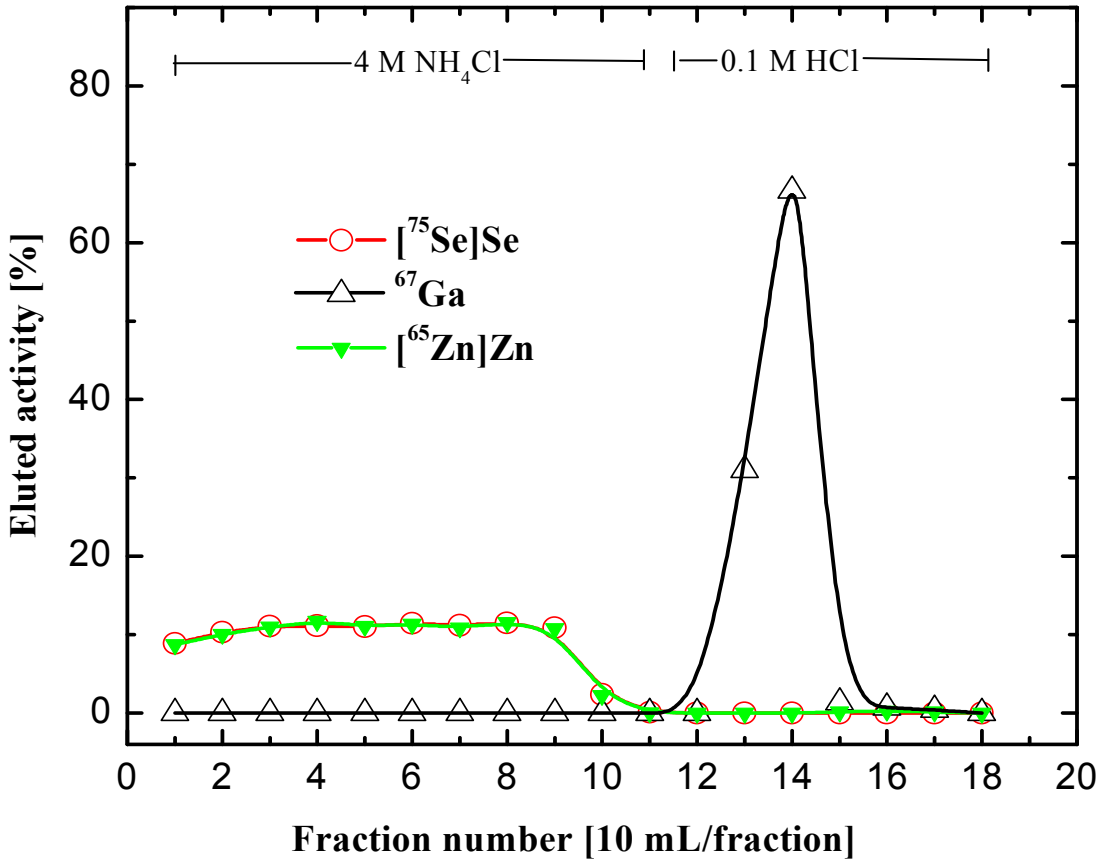

Fig. 4.36: Elution curves for no-carrier-added radiogallium, zinc and selenium on Dowex 1x10 resin, Cl^- form, with a flow rate of 1±0.2 mL/min of two different eluting agents.

4.5.5 Solvent Extraction Studies

A series of solvent extraction experiments on the recovery of n.c.a. radiobromine, n.c.a. radiogallium, zinc and selenium using 0.7 M trioctylamine dissolved in o-xylene with varying concentration of nitric acid, ranging from 0.1 M to 14 M, were conducted to deduce the optimum conditions (see section 3.8.5). The species formed upon equilibration of an amine solution with nitric acid is thought to be $R_3NH^+NO_3^-$. Equilibrium of this salt with the ion solution then extracts anion which replaces the nitrate ion. Fig. 4.37 represents the effect of HNO_3 concentration on the extraction process. The extraction of radiobromine decreased from about 84 % to 40 % on increasing the concentration of HNO_3 to 14 M. This was attributed to the competition with nitric acid extraction. The nitric acid tends to dissolve in the organic phase formed by the amine dissolved in o-xylene, the ratio $(HNO_3)_{org}/(TOA)_{org}$ being more than one at relatively low aqueous HNO_3 concentrations (Bertocci and Rolandi,

1961). This ratio increases linearly with HNO_3 concentration and is independent of the organic amine concentration. Equally, there are changes in the organic phase conditions at high acidities because of the formation of the $[H(NO_3)_2]^-$ ion, so that the n.c.a. radiobromine-amine equilibrium may be in competition with the extraction of excess acid into the organic phase by the process

$$R_3NH.NO_{3(org)} + HNO_{3(aq)} \Leftrightarrow R_3NH.H(NO_3)_{2(org)} \qquad 4.9$$

Zinc and gallium were not extracted under these conditions whereas a very small amount of selenium (around 1 %) was extracted.

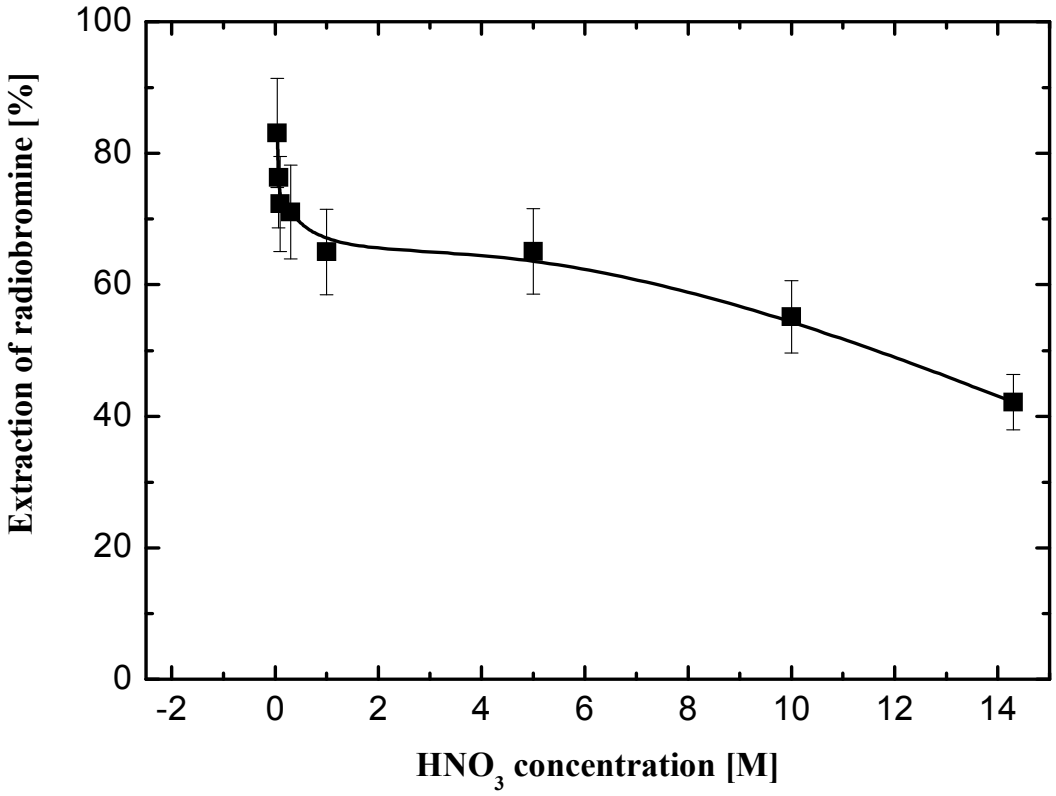

Fig. 4.37: Extraction yield of no-carrier-added radiobromine into TOA in o-xylene at various concentrations of HNO_3.

Back-extraction of n.c.a. radiobromine from organic phase was investigated with 0.5 and 1 M KOH; about 92.6 and 89.1 % of the activity, respectively, was obtained.

The effect of various concentrations of TOA in o-xylene was studied at 1 M HNO_3. The results obtained are shown in Fig. 4.38. Apparently, the TOA concentration in o-xylene has no effect on the extraction of no-carrier-added radiobromine. A molarity of 0.5 M of TOA in o-xylene was considered to be optimum for the no-carrier-added radiobromine extraction.

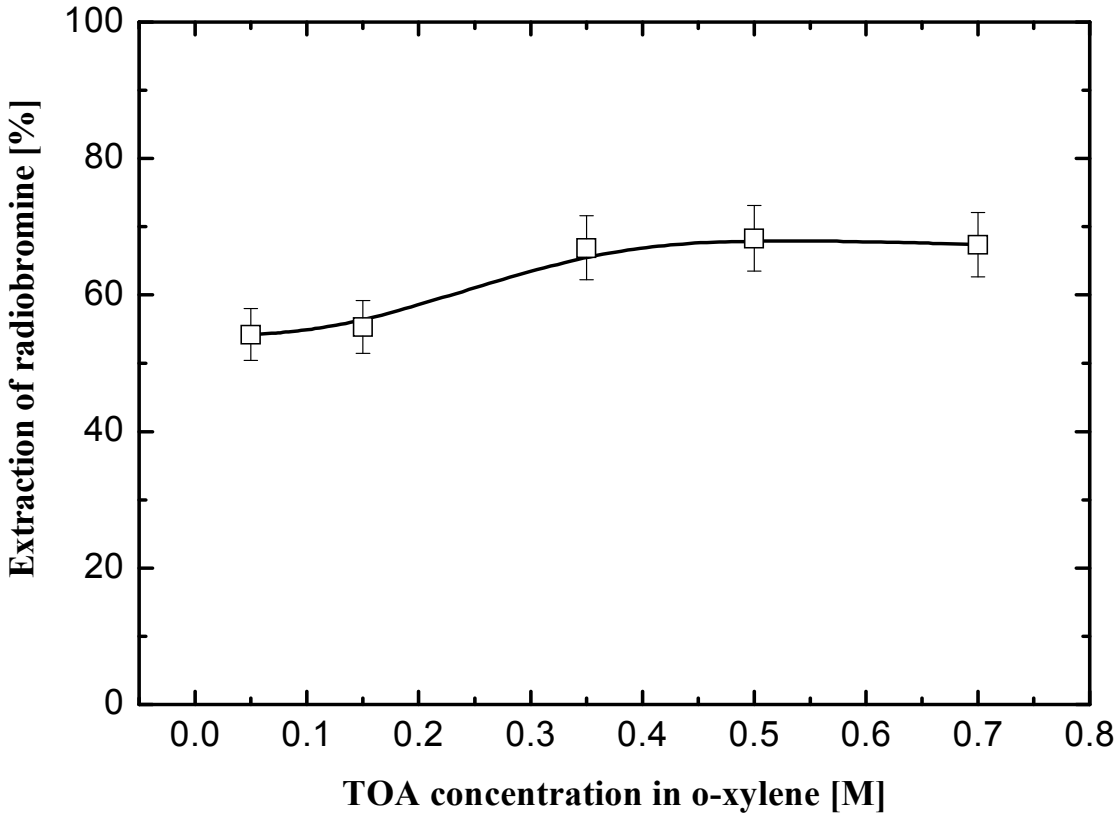

Fig. 4.38: Extraction yield of no-carrier-added radiobromine using various concentrations of TOA in o-xylene at 1 M HNO_3.

The optimum separation conditions were thus 1 M HNO_3 and 0.5 M TOA in o-xylene. The overall separation yield of the no-carrier-added radiobromine was about 67 % in combination with 0.5 % co-extracted selenium.

4.5.6 Separation of n.c.a. Radiobromine and n.c.a. Radiogallium via an Optimized Ion Exchange Procedure

The flow sheet of the optimized method of separation of no-carrier-added radiobromine and no-carrier-added radiogallium from a ZnSe target is given in Fig. 4.39. The irradiated ZnSe was dissolved in 10 KOH, diluted to 1 M KOH, and then passed through a column filled with Dowex 1x10, OH^- form. Radiobromine (n.c.a.) was adsorbed while n.c.a. radiogallium, zinc and selenium were eluted with 1 M KOH. Radiobromine (n.c.a.) was recovered by 0.2 M H_2SO_4, followed by addition of 1 M KOH, evaporation and filtration (see section 3.8.6). Finally K^*Br solution was obtained containing about 93±3 % of the no-carrier-added radiobromine loaded on to the column.

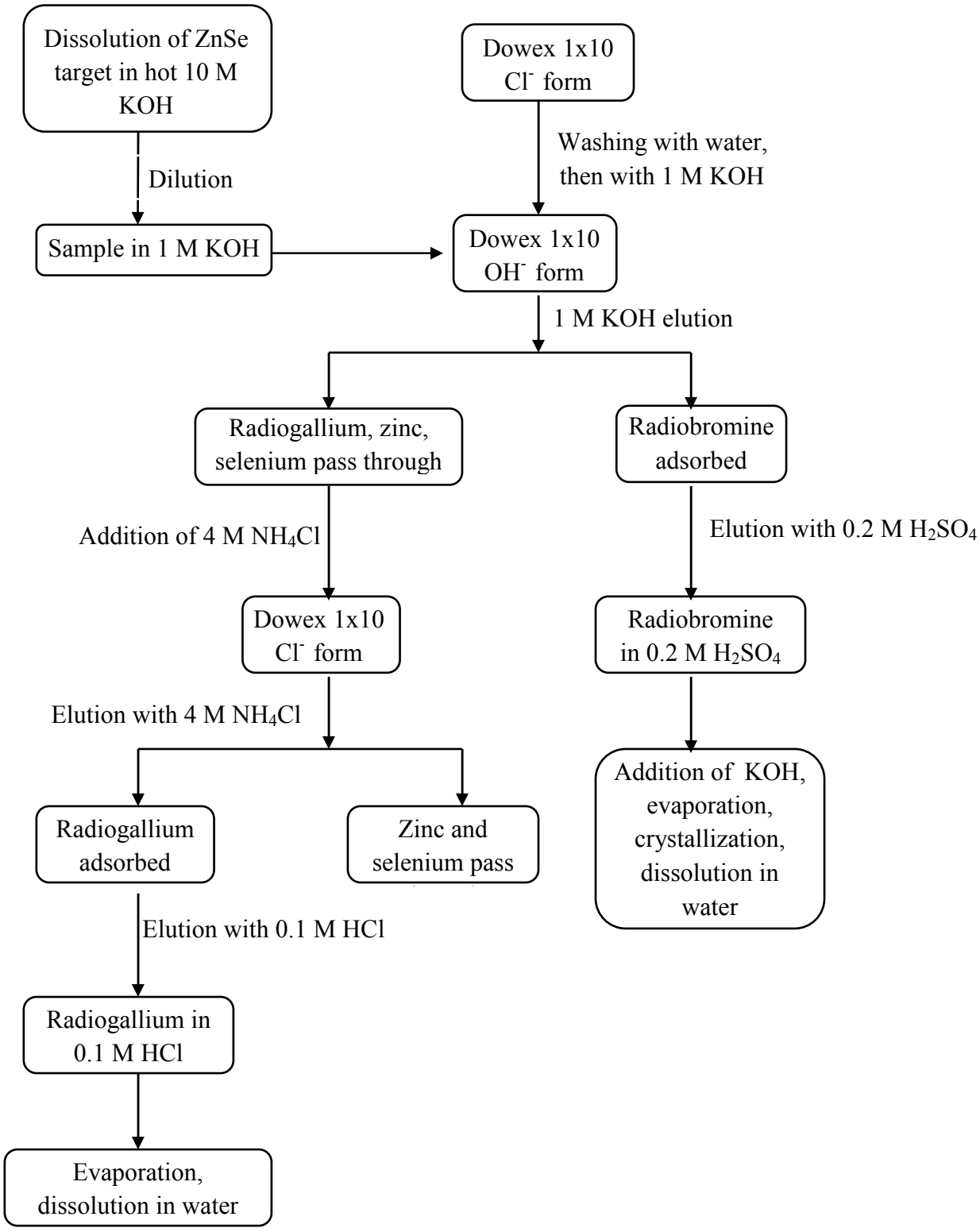

Fig. 4.39: Flow sheet of method of separation of no-carrier-added radiobromine and no-carrier-added radiogallium from the irradiated ZnSe target.

The chloride strength in the solution residue, which contained no-carrier-added radiogallium, zinc and selenium, was increased to 4 M by adding NH_4Cl, and then loaded on to Dowex 1x10, (Cl^- form) column. Radiogallium (n.c.a.) was adsorbed while zinc and selenium were eluted with 4 M NH_4Cl. About 94±2 % of the no-carrier-added radiogallium loaded on the column was then eluted with 0.1 M HCl. This eluate was evaporated and finally dissolved in H_2O.

4.5.7 Quality Control of n.c.a. Radiobromine and n.c.a. Radiogallium

The production and quality control of no-carrier-added radiobromine and no-carrier-added radiogallium were investigated with the emphasis to show that both radionuclides are suitable for use in nuclear medicine. For that propose, 250 mg of ZnSe was pressed to a pellet and irradiated at the Baby Cyclotron with 17 MeV protons at 1 μA current. The optimized separation method elaborated above was applied in the production of ^{76}Br, ^{77}Br, ^{66}Ga and ^{67}Ga via the $^{nat}Se(p,x)^{76,77}Br$ and $^{nat}Zn(p,x)^{66,67}Ga$ nuclear reactions, respectively. ^{75}Br and ^{80m}Br were not determined because both of them have short half-lives and decayed out before the separation was done.

A comparison of the practical yield with the theoretical yield was done. We calculated the thick target yields of ^{76}Br, ^{77}Br, ^{66}Ga and ^{67}Ga from a ZnSe target for the respective energy ranges used in the experiments based on the corresponding cross-sections given by El-Azony et al. (2009) for radiobromine and Al-Saleh et al. (2007) for radiogallium. The experimental yields of ^{76}Br, ^{77}Br amounted to 80±4 % of the theoretical values while for ^{66}Ga and ^{67}Ga they amounted to 78±3 % of the theoretical values.

The radionuclidic purity of the finally isolated no-carrier-added radiobromine and no-carrier-added radiogallium was checked by high-resolution Ge(Li) detector γ-ray spectroscopy. Table. 4.12 shows a summary of production results of ^{76}Br, ^{77}Br, ^{66}Ga and ^{67}Ga as well as the associated radionuclidic and chemical impurities, after separation from a proton irradiated ZnSe target. The radionuclides ^{65}Zn (< 0.002 %) and ^{75}Se (< 0.0007 %) were detected in the case of n.c.a. radiobromine while ^{65}Zn (< 0.008 %) and ^{75}Se (< 0.0004 %) were detected in n.c.a. radiogallium. The inactive impurities were Zn and Se at a level of < 2 μg and < 1 μg, respectively, in radiobromine solution and at a level of < 9 μg and < 0.5 μg, respectively, in ^{67}Ga solution.

Table 4.12: Thick target yields of ^{76}Br, ^{77}Br, ^{66}Ga and ^{67}Ga and associated radionuclidic impurities, after separation from a proton irradiated ZnSe target.

Energy range [MeV]	Radionuclide	Theoretical yield of radionuclide at EOB [MBq/μAh]	Experimental yield of radionuclide at EOB [MBq/μAh]	Experimental yield [%]	Radionuclidic impurities [%]	Chemical impurity
17 →10	^{76}Br	17.3	13.4	77.5	^{65}Zn< 0.002*	Zn < 2 μg
	^{77}Br	7.5	6.1	81.3	^{75}Se < 0.0007	Se < 1 μg
	^{67}Ga	4.2	3.3	78.6	^{65}Zn< 0.008** ^{75}Se < 0.0004	Zn < 9 μg Se< 0.5 μg

* No ^{67}Ga was detected in radiobromine fraction.

** No radiobromine was detected in radiogallium fraction.

4.6 Study of the $^{80}Se(p,n)^{80m}Br$ Nuclear Reaction

^{80m}Br ($T_{1/2}$ = 4.4 h) can be produced in small amounts via the $^{79}Br(n,\gamma)$ reaction in a nuclear reactor, but the specific activity is very low. Owing to its potential in nuclear medicine, especially in Auger electron therapy, the nuclear reaction cross section for its formation in no-carrier-added form was determined as a function of proton energy using enriched ^{80}Se targets. Several authors determined its cross section previously but only in a small energy range or using natural selenium. Thin samples were irradiated in the stacked-foil arrangement, covering an energy range up to 18 MeV. The radioactivity of ^{80m}Br was determined by counting the weak 37 keV γ-ray using a special low-energy γ-ray spectrometer. The possible thick target yield was calculated. The ground state ^{80}Br ($T_{1/2}$ = 17.6 min) is a β^- emitter and is not of much interest. Its formation was investigated by some other authors and its excitation function is almost as that of ^{80m}Br (Blaser et al., 1951; Levkovskij, 1991), but it was not determined in this work.

4.6.1 Excitation Function of the Reaction $^{80}Se(p,n)^{80m}Br$

The measured cross section data are given in Table 4.13, together with their corresponding uncertainties. The excitation function for the formation of ^{80m}Br using enriched ^{80}Se target material is given in Fig. 4.40.

Table 4.13: Measured cross sections for the formation of ^{80m}Br via the $^{80}Se(p,n)^{80m}Br$ reaction.

Proton energy [MeV]	Cross section [mb]
7.4 ± 0.4	203 ± 31
8.7 ± 0.4	320 ± 48
10.1 ± 0.4	384 ± 58
11.3 ± 0.3	356 ± 53
11.7 ± 0.3	431 ±65
13.1 ± 0.3	253 ± 38
13.3 ± 0.3	306 ± 46

14.4 ± 0.3	172 ± 26
15.2 ± 0.3	99 ± 15
15.7 ± 0.3	147 ± 22
16.8 ± 0.3	66 ± 10
18.5 ± 0.3	72 ± 11

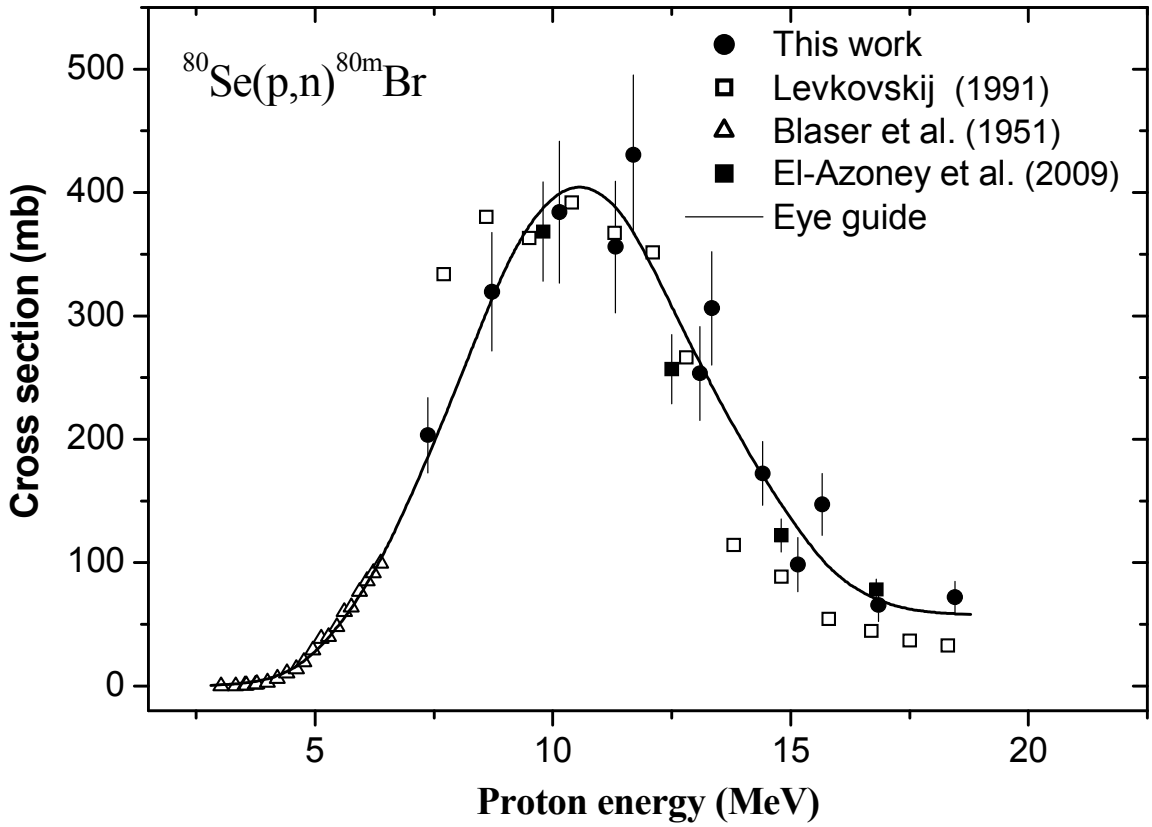

Fig. 4.40: Experimentally determined reaction cross sections for the formation of ^{80m}Br using enriched ^{80}Se target material together with the data from the literature.

In the low energy range up to about 7 MeV some old cross section data (Blaser et al., 1951) were found; the newest, however, are the data reported by Levkovskij in 1991, which are shown in Fig. 4.40 after downwards adjustment by 20 % according to the study of Takács et al., (2002), who showed that those results were based on incorrect cross sections of the used Mo monitor foils. In fact, no measurement detail has been given in that work, so that the authenticity of data cannot be ascertained. Our cross section values, nonetheless, agree rather well with Levkovskij's data: only a slight deviation at higher energies is observed. The data

of El-Azony et al. (2009), which were obtained using natural material, also agree with our new measurements if normalized to a theoretical 100 % enrichment. A possible contribution resulting from the (p,3n) reaction on ^{82}Se (9.4 %) can be neglected within the investigated energy range. In the low energy range up to 6.5 MeV the data of Blaser et al. (1951), obtained using a Geiger counter, show a remarkably good agreement with our results. Our results on enriched ^{80}Se, if normalized to ^{nat}Se as target agree well with the recently published measurement of El-Azony et al. on the ^{nat}Se(p,n)^{80m}Br reaction.

4.6.2 Integral Yield and Radionuclidic Purity

Based on the excitation function presented in this work, the yields for the production of ^{80m}Br using enriched Se target were calculated. The numerical values of the differential and integral yields are given in Table 4.14. Fig. 4.41 represents the calculated integral yield as a function of projectile energy.

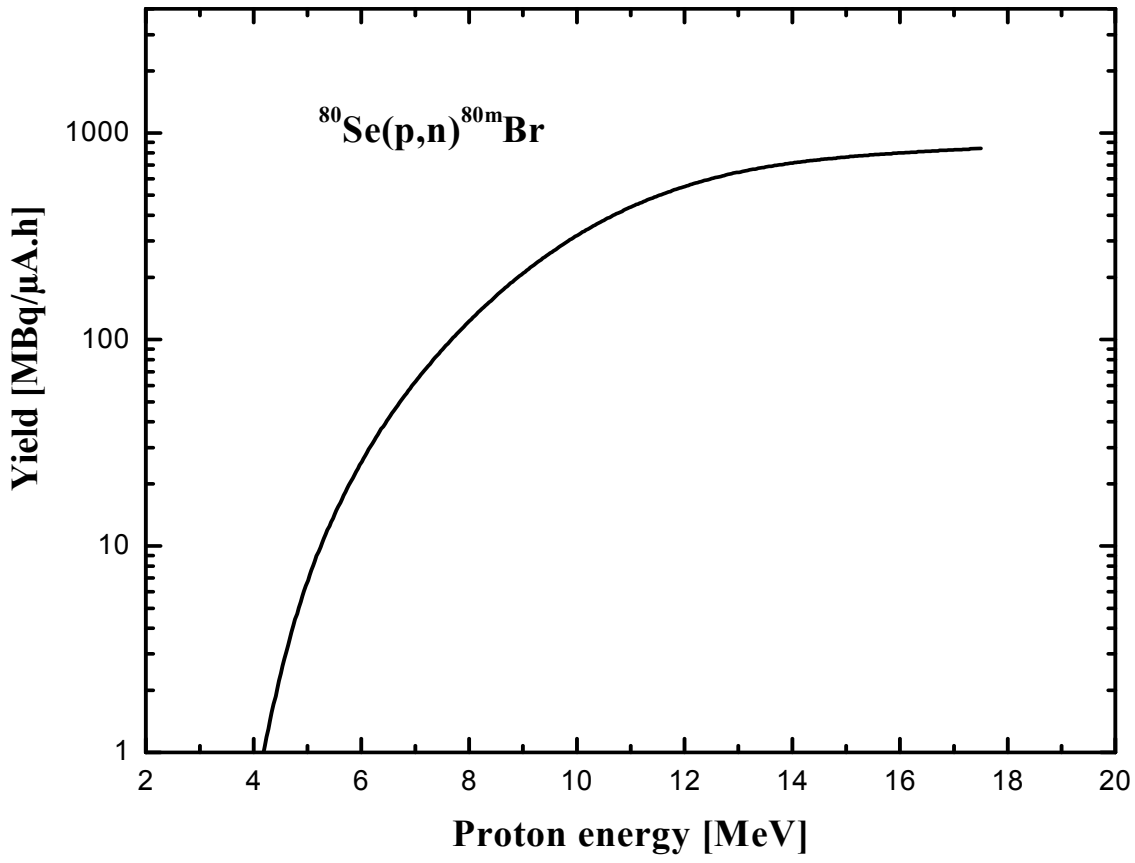

Fig. 4.41: Calculated integral yield of ^{80m}Br based on the determined excitation function (eye guide) of the proton induced nuclear reaction presented in this work.

Table 4.14: Calculated Differential and Integral Yield for the formation of ^{80m}Br via the ^{80}Se(p,n)^{80m}Br reaction.

Proton energy [MeV]	Differential Yield [MBq/µA h]	Integral Yield [MBq/µA h]
17.50	25.3 ± 3.8	841.8 ± 126.3
16.50	30.2 ± 4.5	816.5 ± 122.5
15.50	39.6 ± 5.9	786.3 ± 117.9
14.50	56.8 ± 8.5	746.7 ± 112.0
13.50	80.3 ±12.0	689.9 ± 103.5
12.50	106.9 ± 16.0	609.6 ± 91.4
11.50	118.4 ± 17.8	502.7 ± 75.4
10.50	117.7 ± 17.7	384.4 ± 57.7
9.50	99.8 ± 15.0	266.7 ± 40.0
8.50	75.2 ± 11.3	166.9 ± 25.0
7.50	48.1 ± 7.2	91.7 ± 13.7
6.50	28.1 ± 4.2	43.6 ± 6.5
5.50	12.2 ± 1.8	15.5 ± 2.3
4.50	3.2 ± 0.5	3.3 ± 0.5
3.50	0.1 ± 0.0	0.1 ± 0.0

The possible radionuclide yield amounts to about 800 MBq $\mu A^{-1}h^{-1}$ using an incident proton energy of 16 MeV. Furthermore, the measurements have shown that this nuclear reaction is ideally suitable for production at a small cyclotrons, which by now can be found in many medical facilities; allowing an efficient production of this promising radionuclide. If enriched ^{80}Se is used as target material, no relevant radioactive co-products are produced via this production route. El-Azony et al. calculated a production yield of about 450 MBq $\mu A^{-1}h^{-1}$ in the energy range of up to 15 MeV. By extrapolating the yield from ^{nat}Se to 100 % ^{80}Se, this value agrees with the ^{80}Se(p,n)^{80m}Br reaction yield obtained in this work using enriched target material.

5. Summary

Radionuclides are widely used as radiotracers for online investigations in many fields. For instance, radiotracers are applied in diagnostic medicine, clinical chemistry, molecular biology, technological and industrial processes, and in research in natural and life sciences. Radionuclides are also used as pure radiation sources. Each radionuclide application sets its requirements as to source strength, radiation type, associated energies, half-life and/or character as a chemical element. The production of radionuclides is carried out using nuclear reactors as well as cyclotrons. The reactor-produced radionuclides are generally neutron excess nuclides. They mostly decay by ß$^-$ emission. The cyclotron produced radionuclides are often neutron deficient and decay mainly by EC or β^+ emission. They are especially suitable for diagnostic studies. In this work the production methods of some radionuclides ($^{71, 72, 73, 74}$As, ^{68}Ge/^{68}Ga, ^{76,77,80m}Br) were studied and optimized. The emphasis was on radiochemical separations.

A method for the separation of no-carrier-added arsenic radionuclides from bulk amounts of irradiated germanium oxide (GeO_2) target was developed. After dissolution of the target the ratio of As(III) to As(V) was determined by thin layer chromatography (TLC) in a mixture of $NaHC_4H_4O_6/CH_3OH$ in the ratio of 3/1 and using a Si-60 phase thin layer plate. The extraction of radioarsenic by different organic solvents from acid solutions containing alkali iodide was then studied and optimized. The influence of the concentration of various acids (HCl, $HClO_4$, HNO_3, HBr, H_2SO_4) as well as of KI was studied using cyclohexane. The extraction of radioarsenic with various organic solvents (chloroform, toluene, heptane, diethyl ether) was investigated at 1 M KI and different HCl concentrations, with and without precipitation of the bulk of germanium. The optimum separation of radioarsenic was achieved using cyclohexane with 4.75 M HCl and 0.5 M KI and its back-extraction with a 0.1 % H_2O_2 solution. The extraction leads to high purity radioarsenic containing no radiogallium, with an overall radiochemical yield of 93 ± 3 %. From the irradiated germanium, 0.001 % was found to be co-extracted with the radioarsenic. The practical application of the optimized procedure in the production of ^{71}As and ^{72}As, via the ^{nat}Ge(p,xn)-reactions at 45 MeV proton enegy, was demonstrated and batch yields achieved were in the range of 75 to 84 % of the theoretical values.

A method was developed for the radiochemical separation of n.c.a. ^{68}Ge from proton irradiated Ga_2O_3 via liquid-liquid extraction using H_2SO_4-HCl/ toluene system. The irradiated Ga_2O_3 was dissolved in H_2SO_4 and various parameters affecting the extraction of

radiogermanium were studied. The effect of sulfuric acid and hydrochloric acid concentration on the extraction process was also investigated. For comparision the extraction of radiogermanium by chloroform was also studied. The 8 M H_2SO_4 – 0.4 M HCl / toluene solvent extraction system was successfully used for the no-carrier added separation of ^{68}Ge from Ga_2O_3. The optimized separation method was used practically in the production of n.c.a. ^{68}Ge of high radionuclidic purity via the ^{nat}Ga(p,x) ^{68}Ge reaction. It was advantageous to carry out the separation of ^{68}Ge after one month so that ^{69}Ge and ^{67}Ga had decayed out. No radiogallium and ^{65}Zn were detected in the separated solution. The experimental yield of ^{68}Ge amounted to 83 ± 4 % of the theoretical value.

For optimization studies on the separation of n.c.a. ^{68}Ga from the ^{68}Ge generator system, a suitable tracer for germanium and a longer lived tracer of gallium were needed. The germanium tracer used was ^{69}Ge ($T_{1/2}$= 1.63 d) and it was prepared via the same method as described above for ^{68}Ge. The radionuclide ^{67}Ga ($T_{1/2}$ =3.26 d) was used as tracer for gallium. It was produced by the ^{nat}Zn(p.x)^{67}Ga nuclear reaction on natural zinc. The separation of n.c.a. ^{67}Ga from a proton irradiated zinc target was studied using anion exchange and solvent extraction processes. The distribution coefficients of radiogallium and zinc on the anion exchange resin Amberlite CG-400-II (Cl^- form) and the cation exchange resin Dowex 50Wx8 (H^+ form) were determined. Both radiogallium and zinc were strongly retained on the two resins and a separation was not possible. So the emphasis was shifted to solvent extraction studies using diisopropylether. Various parameters were investigated. Thus, no-carrier-added ^{67}Ga was separated from a proton irradiated zinc target after 3 days using diisopropylether at 7 M HCl. The extraction yield of n.c.a ^{67}Ga was 98.3 % while Zn remained in the aqueous phase. The n.c.a. ^{67}Ga was back-extracted from the organic phase into water very easily. The aqueous solution was evaporated and dissolved again in water. It contained pure no-carrier-added ^{67}Ga.

The radiochemical separation of n.c.a. radiogallium (^{67}Ga) from n.c.a. radiogermanium (^{69}Ge) was studied using ion exchange chromatography (Amberlite IR-120) and solvent extraction (Aliquat 336 in o-xylene). A series of solvent extraction experiments using Aliquat 336 (trioctylmethylammonium chloride) as liquid anion exchanger were conducted. The influence of various HCl concentrations on the extraction of radiogallium and radiogermanium by Aliquat 336 (trioctylmethylammonium chloride) in o-xylene was investigated. It was found that the separation using Aliquat 336 in o-xylene is better than that using Amberlite IR-120 (cation-exchanger): the efficiency of separation is higher, the time needed is shorter, the final volume smaller. In actual practice, the solution containing

radiogermanium (parent) and radiogallium (daughter) in equilibrium, was adjusted to 3 M HCl and extraction using 0.1 M Aliquat 336 in o-xylene was carried out. After shaking for 2 min, 98.7 % of radiogallium was extracted from the parent radiogermanium. About 3.2 % of radiogermanium was co-extracted. To remove these traces of radiogermanium the organic phase was shaken with 3 M HCl solution (two times) and then the radiogallium was back-extracted using 0.5 M KOH with a yield of 99.2 %. The radiochemical procedure developed leads to a satisfactory separation of the generator-produced no-carrier-added ^{68}Ga. The recovery yield of ^{68}Ga was found to be 95.2 % with high radionuclidic purity. Less than 0.008 % of ^{68}Ge was detected in the final separated solution via gamma-ray spectrometry. To decrease the amount of ^{68}Ge further, the back-extraction of ^{68}Ge with 3 M HCl solution was repeated two or three times before n.c.a. ^{68}Ga was finally back-extracted with 0.5 M KOH.

The separation of no-carrier-added radiobromine and no-carrier-added radiogallium from an irradiated ZnSe target was also studied. The adsorption behaviours of n.c.a. radiobromine, n.c.a. radiogallium, zinc and selenium towards the cation-exchange resin Amberlyst 15, in H^+ form, and towards the anion-exchange resin Dowex 1x10 in Cl^- and OH^- forms, were investigated and the elution of n.c.a. radiobromine and n.c.a. radiogallium was studied using different solvents. Additionally separation of n.c.a. radiobromine was also done via solvent extraction using TOA in o-xylene.

The radiobromine was strongly adsorbed on the Dowex 1x10 resin at a low KOH concentration, while n.c.a. radiogallium, zinc and selenium were weakly adsorbed and ran through the column during the loading process. Several reagents for the elution of n.c.a. radiobromine like tetroctyl methyl ammonium chloride in o-xylene and 0.2 M H_2SO_4 were used. After the separation of no-carrier-added radiobromine, the eluted solution in 1 M KOH contained no-carrier-added radiogallium, zinc and selenium. Two methods were used to separate n.c.a. radiogallium; the first by acidifying the solution up to 9 M HCl and passing through a column filled with Dowex 1x10, Cl^- form. The second method was based on increasing the chloride ion strength by dissolving the residue in 4 M NH_4Cl after separation of n.c.a. radiobromine. Then the sample was passed through the column filled with Dowex 1x10, Cl^- form. The optimized methods of separation of no-carrier-added radiobromine and no-carrier-added radiogallium were then applied in the real practice. The irradiated ZnSe was dissolved in 10 KOH, diluted to 1 M KOH, and then passed through a column filled with Dowex 1x10, OH^- form. Radiobromine (n.c.a.) was adsorbed while n.c.a. radiogallium, zinc and selenium were eluted. The radiobromine (n.c.a.) was then recovered by 0.2 M H_2SO_4, followed by addition of KOH, evaporation and filtration. Finally K^*Br solution was obtained

containing about 93±3 % of the no-carrier-added radiobromine loaded onto the column. The chloride strength in the solution residue, which contained no-carrier-added radiogallium, zinc and selenium, was thereafter increased to 4 M by adding NH_4Cl, and then loaded onto Dowex 1x10, Cl^- form, column. Radiogallium (n.c.a.) was adsorbed while zinc and selenium were not. About 94±2 % of the no-carrier-added radiogallium loaded on the column were then eluted with 0.1 M HCl. This eluate was evaporated and finally dissolved in H_2O. Using this method no-carrier-added radiobromine and no-carrier-added radiogallium could be obtained in high purity. The optimized separation method elaborated above was applied in the production of ^{76}Br, ^{77}Br, ^{66}Ga and ^{67}Ga via the $^{nat}Se(p,x)^{76,77}Br$ and $^{nat}Zn(p,x)^{66,67}Ga$ nuclear reactions, respectively. The experimental yield of ^{76}Br and ^{77}Br amounted to 80±4 % of the theoretical value while that of ^{66}Ga and ^{67}Ga was found to be 78±2 % of the theoretical value. The radionuclides ^{65}Zn (< 0.002 %) and ^{75}Se (< 0.0007 %) were detected in the case of n.c.a. radiobromine while ^{65}Zn (< 0.008 %) and ^{75}Se (< 0.0004 %) were detected in n.c.a. radiogallium.

The nuclear reaction cross section for the formation of the Auger electron emitting radionuclide ^{80m}Br ($T_{1/2}$=4.4 h) was determined as a function of proton energy using enriched ^{80}Se targets. Thin ^{80}Se samples were prepared by the sedimentation technique and irradiated with incident protons of energies up to 18 MeV in a stacked-foil arrangment. The induced radioactivity was measured using a special low-energy γ-ray spectrometer. The measurements allowed the determination and extension of the excitation function of the $^{80}Se(p,n)^{80m}Br$ reaction. The possible thick target yield was then calculated. The production of ^{80m}Br via the $^{80}Se(p,n)$ process can be done with good efficiency and high purity at a small cyclotron. The yield of ^{80m}Br amounts to about 800 MBq μA^{-1} h^{-1} using an incident proton energy of 16 MeV.

6. References

Aardaneh, K. and Shirazi, B. (2005) "Radiochemical separation of ^{67}Ga from Zn and Cu using the adsorbent resin Amberlite XAD-7", J. Radioanal. Nucl. Chem. **265**:47.

Aardaneh, K. and Van der Walt, T. N. (2006) "Ga_2O for target, solvent extraction for radiochemical separation and SnO_2 for the preparation of a ^{68}Ge/^{68}Ga generator", J. Radioanal. Nucl. Chem. **268**:25.

Alfassi, Z. B. and Helus, F. (1983) "Simple method for carrier free separation of ^{77}Br from metallic selenium", J. Radioanal. Chem. **76**:325.

Al-Saleh, F. S., Al Mugren K. S. and Azzam, A. (2007) "Excitation function measurements and integral yields estimation for ^{nat}Zn(p,x) reactions at low energies", Appl. Radiat. Isot. **65**:1101.

Ambe, S., (1988) "^{68}Ge-^{68}Ga generator with alpha-ferric oxide support", Appl. Radiat. Isot. **39**:49.

Anderson, K. C., Leonard, R.C. F., Cannellos, C. P., Skarin, A. T. and Kaplan, W. D., (1983) "High-dose gallium imaging in lymphoma", Am. J. Med. **75**:327.

Azarez, J., Moneo, P., Vidad J. C. and Palacios, F., (1985) "Extraction spectrophotometric determination of germanium with phenylfluorone in N,N-dimethylformamide", Analyst **110**:747.

Ballaux, C., Dams, R. and Hoste, J., (1967) "Neutron activation analysis of high purity selenium, Part I. Determination of bromine", Anal. Chim. Acta **37**:164.

Barong, B. and Yinsong, W., (1992) Nucl. Sci. Tech. **3**:202.

Basile, D., Birattari, C., Bonardi, M., Goetz, L., Sabbioni E. and Salomone, A., (1981) "Excitation functions and production of arsenic radioisotopes for environmental toxicology and biomedical purpose", Int. J. Appl. Radiat. Isot. **32**:403.

Beard, H. C. and Cuninghame, J. G., (1965) "Radiochemistry of arsenic", Nuclear Science Series, National Academy of Sciences-National Research Council, United States Atomic Energy Commission, NAS-NS-3002.

Beard, H. C. and Lyerly, L. A., (1961) "Separation of arsenic from antimony and bismuth by solvent extraction", Anal. Chem. **33**:1781.

Bertocci, U., and Rolandi, G. (1961) "Equilibria between tri-octylamine and some mineral acids", J. Inorg. Nucl. Chem. **23**:323.

Billinghurst, M. W., Abrams D. N. and Cantor, S., (1990) "Separation of radioarsenic from a germanium dioxide target", Appl. Radiat. Isot. **41**:501.

Blaser, J. P., Treves, S., Wolf, A. P. and Lambrecht, R. M. (1951)"Anregungsfunktionen und Wirkungsquerschnitte der (p,n)-Reaktion (II)", Helv. Phys. Acta **24**:441.

Blessing, G. and Qaim, S. M., (1984) "An improved internal Cu_3As-Alloy cyclotron target for the production of ^{75}Br and ^{77}Br and separation of the by-product ^{67}Ga from the matrix activity" Appl. Radiat. Isot. **35**:927.

Blessing, G., Weinreich, R., Qaim S. M. and Stöcklin, G., (1982) "Production of ^{75}Br and ^{77}Br via the $^{75}As(^{3}He,3n)^{75}Br$ and $^{75}As(\alpha,2n)^{77}Br$ reactions using Cu_3As-alloy as a high-current target material", Appl. Radiat. Isot. **33**:333.

Bokhari, T. H., Mushtaq A. and Khan, I. U., (2009) "Concentration of ^{68}Ga via solvent extraction" Appl. Rad. Isot. **67**:100.

Bonardi, M. and Birattari, C. (1983) "Optimization of irradiation parameters for ^{67}Ga production from $^{nat}Zn(p,xn)$ nuclear reactions", J. Radioanal. Chem. **76**:311-318.

Brits, R. J. N. and Strelow, F. W., (1990) "^{67}Ga/Zn separation with an organic adsorbent", Appl. Radiat. Isot. **41**:575.

Broden, K. and Skarnemark, G., (1981) "Rapid continuous separation procedures for zirconium, niobium, technetium, bromine and iodine from complex reaction product mixtures", J. Inorg. Nucl. Chem. **43**:765.

Brown, L. C., (1971) "Chemical processing of cyclotron-produced ^{67}Ga", Int. J. Appl. Radiat. Isot. **22**:710.

Byrne, A. R. and Gorenc, D., (1972a) "The toluene extraction of some elements as iodides from sulfuric acid-potassium iodide media. Application to neutron activation analysis", Anal. Chim. Acta **59**:81.

Byrne, A. R., (1972b) "The toluene extraction of some elements as iodides from sulfuric acid-potassium iodide media. Application to neutron activation analysis", Anal. Chim. Acta **59**:91.

Carlton, J. E. and Hayes, R. L., (1971) "Rapid separation of generator produced gallium-68 from EDTA elute", Int. J. Appl. Radiat. Isot. **22**:44.

Chappell, J., Chiswell B. and Olszowy, H., (1995) "Speciation of arsenic in a contaminated soil by solvent extraction", Talanta **42**:323.

Chattopadhyay, S., Pal, S., Vimalnath, K. V. and Das, M. K., (2007) "A versatile technique for radiochemical separation of medically useful no-carrier-added radioarsenic from irradiated germanium oxide targets", Appl. Radiat. Isot. **65**:1202.

Cheng, W., Jao, Y., Lee, C. and Lo, A., (2000) "Preparation of ^{68}Ge/^{68}Ga generator with a binary Ga/Ag electrodepositions as solid target", J. Radioanal. Nucl. Chem. **245:** 25.

Choppin, G. R., Liljenzin, J. and Rydberg, J. (2002) "Radiochemistry and Nuclear Chemistry", Oxford: Butterworth Heinemann, Oxford, UK.

Coenen, H. H., (1986) "New radiohalogenation methods: An overview", in: Progress in Radiopharmacology (Cox, P. H.., Mather, S. J., Sampson, C. B., Lazarus, C. R., eds.) Martinus Nijhoff Publishers, Dordrecht, 196.

Coenen, H. H., Moerlein S. M. and Stöcklin, G., (1983) "No-carrier-added radiohalogenation methods with heavy halogens", Radiochim. Acta **34**:47.

Das, M. K., Chattopadhayay, S., Sarkar B. R. and Ramamoorthy, N., (1997) "A cation exchange method for separation of ^{111}In from inactive silver, copper, traces of iron and radioactive gallium and zinc isotopes", Appl. Radiat. Isot. **48**:11.

Dmitriev, P. P., Krasnov, N. N., Molinans, G. A. and Panarin, M. V., (1972), "Yields of ^{68}Ge in irradiation of gallium by protons and deuterons and irradiation of zinc by α-particles", translated from Atomnya Energiya **33**:774.

Donaldson, E. M. and Wang, M., (1986) "Methyl isobutyl ketone extraction of iodide complexes from sulfuric acid- potassium iodide media and back-extraction into aqueous phase", Talanta **33**:35.

Egamediev, S. Kh. and Khujaev, S., (2001) "Production of carrier free germanium-68 by alpha particle bombardment of zinc cyclotron target", CP 600, Cyclotrons and their Applications 2001, Sixteenth International Conference, edited by F. Marti, American Institute of Physics 0-7354-0044-X/01.

Egamediv, S. Kh., Khujaev S. and Mamathazina, A. Kh., (2000) "Influence of preliminary treatment of aluminum oxide on the separation of ^{68}Ge-^{68}Ga radionuclide chain", J. Radioanal. Nucl. Chem. **246**:593.

Ehrhardt, G. J. and Welch, M. J., (1978) "A new germanium-68/gallium-68 generator'', J. Nucl. Med. **19**:925.

El-Azony, K. M., Ferig Kh. and Saleh, Z. A., (2003) "Direct separation of ^{67}Ga citrate from zinc and copper target materials by anion exchange", Appl. Radiat. Isot. **59,** 329.

El-Azony, K. M., Suzuki, K., Fukumura, T., Szelecsényi F. and Kovács, Z., (2009) "Excitation functions of proton induced reactions on natural selenium up to 62 MeV", Radiochim. Acta **97**:71.

Ellis, B. L. and Sharma, H. L. (1999) "Co, Fe and Ga chelates for cell labeling: a potential use in PET imaging", J. Nucl. Med. Commun. **20**:1017.

Faris, J. P. and Buchanan, R. F., (1964) "Anion exchange characteristics of elements in nitric acid medium", Anal. Chem. **36**:1157.

Fassbender, M., Arzumanov, A., Jamriska, D. J., Lyssukhin, S. N., Trellue H. and Waters, L. S., (2007) "Proton beam simulation with MCNPX: gallium metal activation estimates below 30 MeV relevant to the bulk production of ^{68}Ga and ^{65}Zn", Nucl. Instr. Meth. Phys. B **261**:742.

Fassbender, M., Jamriska, D. J., Hamilton, V. T., Nortier F. M. and Philips, D. R., (2005) "Simultaneous ^{68}Ge and ^{88}Zr recovery from proton irradiated Ga/Nb capsules (LA-UR#03-2319) ", J. Radioanal. Nucl. Chem. **263**:497.

Firestone, R. B. and Ekström L. P. (2004) LBNL Isotopes Project - LUNDS Universitet, Version 2.1, January, http://ie.lbl.gov/toi.

Fombkins, E. R. and Mayer, S. W., (1947) "Ion exchange as a separation method", J. Am. Chem. Soc. **69**:2859.

Forehand, T. J., Dupuy, A. E., Jr., and Tal, H., (1976) "Determination of arsenic in sandy soils", Anal. Chem. **48**:999.

Gallano, E. and Tilbury, R. S., (1998) "The cyclotron production of carrier free ^{77}Br via the ^{79}Br(p,3n)^{77}Kr→^{77}Br reaction using a liquid target and on-line extraction", Appl. Radiat. Isot. **49**:105.

Gleason, G. I., (1960) "A positron cow", Int. J. Appl. Radiat. Isot. **8**:90.

Grant, P. M., Whipple, R. E., Barnes, J. W., Bentley, G. E., Wanek P. M. and O'Brien, H. A., (1981) "The production and recovery of ^{77}Br at Los Alamos for nuclear medicine studies", J. Inorg. Nucl. Chem. **41**:2217.

Green, M. A., and Welch, M. J., (1989) "Review of gallium radiopharmaceutical chemistry", Nucl. Med. Biol. **16**:435.

Greene, M. W. and, Tucker, W. D., (1961) "An improved gallium-68 cow", Int. J. Appl. Radiat. Isot. **12**:62.

Guin, R., Das, S. K., and Saha S. K. (1998) "Separation of carrier free arsenic from germanium", J. Radioanal. Nucl. Chem. **227**:181.

Gul, K., (2001) "Calculation for the excitation functions of 3-26 MeV proton reactions on ^{66}Zn, ^{67}Zn and ^{68}Zn", Appl. Radiat. Isot. **54**:311.

Hermanne, A., Szelecsényi, F., Sonck, M., Takács, S., Tárkányi F. and Van der Winkel, P., (1999) "New cross section data on ^{68}Zn(p,2n)^{67}Ga and ^{nat}Zn(p,xn)^{67}Ga nuclear reactions for the development of a reference data base", J. Radioanal. Nucl. Chem. **240**:623.

Hassan, H.E., Qaim, S. M., Shubin, Yu., Azzam, A., Morsy M. and Coenen, H. H., (2004) "Experimental studies and nuclear model calculations on proton-induced reactions on ^{nat}Se, ^{76}Se and ^{77}Se with particular reference to the production of the medically interesting radionuclides ^{76}Br and ^{77}Br", Appl. Radiat. Isot. **60**:899.

Helus, F., (1970) "Preparation of carrier free bromine-77 for medical use", Radiochem. Radioanal. Lett. **3**:45.

Hirsch, R. F. and Portock, J. D., (1970) "Anion-exchange equlibria in alkaline media", Anal. Chim. Acta **49**:473.

Hnatowich, D. J., Kulprathipanja, S., Evans, G. and Elmaleh, D., (1979) "A comparison of positron-emitting blood pool imaging agents", Int. J. Appl. Radiat. Isot. **30**:335.

Horiguchi, H., Kumahora, H., Inoue, H. and Voshizawa, Y., (1983) "Excitation functions of Ge(p,xnyp) reactions and production of ^{68}Ge", Int. J. Appl. Radiat. Isot. **34**:1531.

Hubert, A. E., (1983) "Determination of arsenic in geological materials by X-ray fluorescence spectrometry after solvent extraction and deposition on a filter", Talanta **30**:967.

Jahn, M. (2009)" Nicht-geträgerte Radioarsenisotope: Herstellung, Abtrennung und Markierung von Proteinen" Doctoral Dissertation, Johannes Gutenberg-Universität, Mainz.,

Jahn, M., Radchenko, V., Filosofov, D., Hauser, H., Eisenhut, M., Röch, F. and Jennewein, M., (2010) "Separation and purification of no-carrier-added arsenic from bulk amounts of germanium for use in radiopharmaceutical labelling", Radiochim. Acta **98**:807.

Janssen, A. G., van den Bosch, R. L. P., de Goeij J. J. M. and Theelen, H. M. J., (1980) "The reactions ^{77}Se(p,n) and ^{78}Se(p,2n) as production routes for ^{77}Br", Int. J. Appl. Radiat. Isot. **31:**405.

Jennewein, M., Constantinescu, A., Bergner, O., Lewis, M., Zhao, D., Selioutine, S., Slavine, N., O'kelly, S., Maus, S., Qaim, S. M., Tsyganov, E., Antich, P. P., Rösch, F., Mason R. P., Thorpe, Na P. E., (2004a) "Molecular imaging of the vascular targeting antibody vatuximab in rat prostate cancer", Eur. J. Nucl. Med. Mol. Im. **31**:259.

Jennewein, M., Qaim, S. M., Hermanne, A., Jahn, M., Tsyganov, E., Slavine, N., Seliounie, S., Antich, P. A., Kulkarni, P.V., Thorpe, P.E., Mason, R.P. and Rösch, F., (2005)

"A new method radiochemical separation of arsenic from irradiated germanium oxide", Appl. Radiat. Isot. **63:**343.

Jennewein, M., Schmidt, A., Novgorodov, A. F., Qaim S. M. and Rösch, R., (2004b) "A no-carrier- added ^{72}Se/^{72}As radionuclide generator based on distillation", Radiochim. Acta **92**:245.

Jong, D. De., Kooiman H. and Veenboer, J. Th., (1979) "^{76}Br and ^{77}Br from decay of cyclotron produced ^{76}Kr and ^{77}Kr", Int. J. Appl. Radiat. Isot. **30**:786.

Kakavand, T., Sadeghi, M., Mokhtari L. and Majdabadi, A., (2010) "Zinc electrodeposition on copper substrate using cyanide bath for the production of ^{66,67,68}Ga", J. Radioanal. Nucl. Chem. **283**:197.

Kleinberg, J. and Cowan, G. A., (1960), "The radiochemistry of fluorine, chlorine, bromine and iodine", Nuclear Science Series, National Academy of Sciences, United States Atomic Energy Commission NAS-NS3005.

Konstantin, P., Zhernosekov, D. V., Filosofov, R. P., Baum, P. A., Heiner, B., Antoli, A. R., Markus, J., Mark, J., Rösch, F., (2007) "Processing of generator produced ^{68}Ga for medical application", J. Nucl. Med. **48**:1741.

Kopecky, P., (1990) "Cross sections and production yields of ^{66}Ga and ^{67}Ga for proton reactions in natural zinc", Appl. Radiat. Isot. **41**:606.

Kopecky, P., Mudrova B. and Svoboda, K., (1973) "The study of conditions for the preparation and utilization of ^{68}Ge-^{68}Ga generator", Int. J. Appl. Radiat. Isot. **24**:73.

Korkisch, J. and Feik, F., (1967) "Anion-exchange separation of germanium from arsenic (III) and arsenic (V) and other elements in hydrochloric acid- acetic acid medium", Separation Science **2**:1.

Környel, J., Szirtes, L. and Kecskes, F. (1986) "Radio-paperchromatographic determination of different chemical forms of Ga ", J. Radioanal. Nucl. Chem. **103**:313.

Kovács, Z., Blessing, G., Qaim, S. M. and Stöcklin, G., (1985) "Production of ^{75}Br via the ^{76}Se(p,2n)^{75}Br reaction at a compact cyclotron", Int. J. Appl. Radiat. Isot. **36**:632.

Lahiri, S., Banerjee S. and Das, N. R., (1997) "Simultaneous production of carrier free ^{65}Zn and ^{66,67,68}Ga in alpha particles activated copper target and their application with TOA", App. Radiat. Isot. **48**:15.

Lambrecht, R. M., (1983) "Radionuclide generators", Radiochim. Acta **34**:9.

Leonard, A., (1991) "Metals and their compounds in the environment: occurence, analysis and biological relevance", VCH, Weinheim- NewYork-Basel-Cambridge, 751

Levkovskij, V. N. "Activation cross sections for nuclides of average masses (A=40-100) by protons and alpha-particles with average energies (E=10-50 MeV)", Inter Vesi, Moscow, 1991.

Lieser, K. H., (2001) "Nuclear and Radiochemistry: Fundamentals and Applications", Weinheim : VCH Verl. Ges., 2001.

Loc'h, C., Maziere, B., Comar, D. and Knipper, R., (1982) "A new preparation of germanium-68", Int. J. Appl. Radiat. Isot. **33**:267

Loveland, W. D., Morrissey, D. J., Seaborg, G. T., (2006) "Modern Nuclear Chemistry" New York, NY: Wiley.

Madhusudhan, C. P., Treves, S., Wolf, A. P. and Lambrecht, R. M., (1979) "Cyclotron isotopes and radiopharmaceuticals: XXXI. Improvement in ^{77}Br production and radiochemical separation from enriched ^{78}Se", J. Radioanal. Chem. **53**:299-305

Magill, J., Pfennig, G., and Galy, J. "Chart of the Nuclides" Edition 2006, revised printing 2007, European Commission Joint Research Centre, Institute for Transuranium Elements, Karlsruhe, Germany.

Maher, W. A. (1981) "Determination of inorganic and methylated arsenic species marine organisms and sediments", Anal. Chim. Acta **126**:157.

Maki, Y. and Murakami, Y., (1974) "The separation of arsenic-77 in a carrier free state from the parent nuclide germanium-77 by a thin-layer chromatographic method", Radioanal. Chem. **22**:5.

Marcus, Y., (1967) "Metal chloride complexes studied by ion exchange and solvent extraction methods", Coordin. Chem. Rev. **2**:257.

Maziere, B. and Loc'h, C., (1986) "Radiophamaceuticals labeled with bromine isotopes", Appl. Radiat. Isot. **37**:703.

McElvany, K. D., Hopkins, K. T. and Welch, M. J., (1984), "Comparison of ^{68}Ge/^{68}Ga generator systems for radiopharmaceutical production", Appl. Radiat. Isot. **35,** 521.

Mease, R. C., Dejesus, O. T., Gatley, S. J., Harper, P. V., Desombre, E. R., and Friedman, A. M., (1991) "Production of no-carrier -added ^{80m}Br for investigation of auger electron toxicity", Appl. Radiat. Isot. **42**:57.

Meinken, G. E., Kurezak, S., Mausner, L. F., Kolsky, K. L. and Srivastava, S. C., (2005) "Production of high specific activity ^{68}Ge at Brookhaven National Laboratory", J. Radioanal. Nucl. Chem. **263**:553.

Mihaylov, I. and Distin, P. A., (1992) "Gallium solvent extraction in hydrometallurgy: An overview", Hydrometallurgy **28**:13.

Mirzadeh, S. and Lambrecht, R. M., (1996) "Radiochemistry of germanium", J. Radioanal. Nucl. Chem. **202**:7.

Mirzadeh, S., Kahn, M., Grant P. M. and O'Brien, H.A., (1981) "Studies of the chemical behavior of carrier-free ^{68}Ge", Radiochim. Acta **28**:47

Mushtaq, A. and Qaim, S. M. (1990) "Excitation functions of α- and ^{3}He-particle induced nuclear reactions on natural germanium: Evaluation of production routes for ^{73}Se", Radiochim. Acta **50**:27.

Nachtrieb, N. H. and Fryxell, R. E., (1949) "The extraction of gallium chloride by isopropyl ether", J. Am. Chem. Soc., **71**:4035.

Nagame, Y., Nakahara, H., and Furukawa, M., (1989) "Excitation functions for alpha and ^{3}He particles induced reactions on zinc", Radiochim. Acta **29**:5.

Nagame, Y., Unno, M., Nakahara H. and Murakami, Y., (1978) "Production of ^{67}Ga by alpha bombardment of natural zinc", Int. J. Appl. Radiat. Isot. **29**:615.

Naidoo, C., van der Walt, T. N. and Raubenheimer, H. G., (2002) "Cyclotron production of ^{68}Ge with a Ga_2O target", J. Radioanal. Nucl. Chem. **253**:221.

Nakayama, M., Haratake, M., Koiso, T., Ishibashi, O., Harada, K., Nakayama, H., Sugii, A., Yahara, S. and Arano, Y., (2002) "Separation of ^{68}Ga from ^{68}Ge using a macroporous organic polymer containing n-methylglucamine groups", Anal. Chim. Acta **453**:135.

Nakayama, M., Haratake, M., Ono, M., Koiso, T., Harada, K., Nakayama, H., Yahara, S., Ohmomo, Y., Arano, Y., (2003) "A new ^{68}Ge/^{68}Ga generator system using an organic polymer containing n-methylglucamine groups as adsorbent for ^{68}Ge", Appl. Radiat. Isot. **58**:9.

Nayak, D. and Lahiri, S., (2001) "Alternative methods for the production of carrier-free ^{66,67}Ga" Appl. Radiat. Isot. **54**:189.

Neirinckx, R. D., Layne, W. W., Sawan, S. P. and Davis, M. A., (1982) "Development of an ionic ^{68}Ge-^{68}Ga generator III. Chelate resins as chromatographic substrates for germanium", Int. J. Appl. Radiat. Isot. **33**:259.

Neirinckx, R. D. and Davis, M. A., (1980) "Potential column chromatography for ionic Ga-68. II: Organic ion exchanges as chromatographic supports", J. Nucl. Medicine **21**:81.

Nelson, F. and Michelson, D.C. (1966) " Ion-exchange procedures: IX. Cation exchange in HBr solutions", J. Chromatogr. **25**:414.

Neves, M., Kling A. and Lambrecht, R. M., (2002) "Radionuclide production for therapeutic radio-pharmaceuticals", Appl. Radiat. Isot. **57**:657.

Norton, E. F., Kondo, K., Karlstrom, K., Lambrecht, R. M., Wolf, A. P. and Treves, S., (1978) "Cyclotron isotopes and radiopharmaceuticals: XXVI. A carrier-free separation of ^{77}Br from Se", J. Radioanal. Chem. **44**:207.

Nozaki, T., Iwamoto, M. and Itoh, Y., (1979) "Production of ^{77}Br by various nuclear reactions", Int. J. Appl. Radiat. Isot. **30**:79.

Nunn, A. D. and Waters, S. L. (1975) "Target materials for the cyclotron production of carrier-free ^{77}Br", Int. J. Appl. Radiat. Isot. **26**:731.

Pacey, G. E. and Ford, J. A., (1981) "Arsenic speciation by ion exchange separation and graphite-furance atomic absorption spectrophotometry", Talanta **28**:935.

Palanivelu, K., Balasubramanian N. and Ramakrishna, T. V., (1992) "A chemical enhancement method for the spectrophotometric determination of trace amounts of arsenic", Talanta **39**:555.

Pao, P. J., Silvester, D. J. and Waters, S. L., (1981) "A new method for the preparation of ^{68}Ga-generators following proton bombardment of gallium oxide targets", **64**:267.

Papardells, T., Vourvoroulos G. and Paleodimopoulos, E., (1984) "The production of gallium-67 with a tandem accelerator", J. Radioanal. Nucl. Chem. **84**:263.

Porile, N. T., Tanaka, H., Amano, H., (1963) "Nuclear reactions of ^{69}Ga and ^{71}Ga with high energy protons", Nucl. Phys. **43**:500.

Qaim, S. M. and Weinreich, R., (1981) "Production of ^{75}Br via the ^{75}Kr precursor: excitation function for the deuteron induced nuclear reaction on bromine", Int. J. Appl. Radiat. Isot. **32**:823.

Qaim, S. M., (1986) "Recent developments in the production of ^{18}F, ^{75,76,77}Br and ^{123}I", Appl. Radiat. Isot. **37**:803.

Qaim, S. M., (2001a) "Nuclear data for medical applications. An overview", Radiochim. Acta, **89**:189.

Qaim, S. M., (2001b) "Nuclear data relevant to the production and application of diagnostic radionuclides", Radiochim. Acta, **89**:223.

Qaim, S. M., (2001c) "Therapeutic radionuclides and nuclear data", Radiochim. Acta, **89**:297.

Qaim, S. M., (2003) "Cyclotron production of medical radionuclides", Handbook of Nuclear Chemistry- Vol.**4**, (F. Rösch, Editor), 47-79, Kluwer Academic Publishers, Dordrecht, The Netherlands.

Qaim, S. M., (2004) "Use of cyclotrons in medicine", Radiation Physics and Chemistry, **71**:917.

Qaim, S. M., (2010) "Radiochemical determination of nuclear data for theory and applications", J. Radioanal. Nucl. Chem., **284**:489-505

Qaim, S. M., and Stöcklin, G., (1993) "Excitation functions of ^{74}Se(d,xn)^{75,74m}Br reactions: comparative evaluation of possible routes for the production of ^{75}Br at a small cyclotron", Appl. Radiat. Isot. **44**:1443-1447

Qaim, S. M., Stöcklin, G. and Weinreich, R., (1977) "Excitation functions for the formation of neutron deficient isotopes of bromine and krypton via high-energy deuteron induced reactions on bromine: Production of ^{77}Br, ^{76}Br and ^{79}Kr", Int. J. Appl. Radiat. Isot. **28**:947-953

Qaim, S. M., Tárkányi, F., Takács, S., Hermanne, A., Nortier, M., Oblozinsky, P., Scholten, B., Shubin, Yu. N., Gul, K. and Zhuang Youxiang, (2001), "Charged particle cross-section data base for medical radioisotope production: Diganostic radioisotopes and monitor reactions" IAEA-TECDOC-1211, Vienna 2001

Rashid, M., Bari, A. and Ejaz, M., (1992) "Radiochemical studies on the extraction of arsenic(III) by trilaurylamine oxide and benzene from aqueous iodide solutions and its determination in water samples by spectrometry", J. Radioanal. Chem. **157**:193-202

Rösch, F. and Knapp, F. F. (2003) "Radionuclide generators" Handbook of Nuclear Chemistry.Vol.**4**, (F. Rösch, Editor), 81-118, Kluwer Acadamic Publishers, Dordrecht, The Netherlands.

Rösch, F. and Filosofov, D. V. (2010) "Production, radiochemical processing and quality evaluation of ^{68}Ge"' IAEA Radioisotopes and Radiopharmaceuticals Series No.2, "Production of Long Lived Parent Radionuclides for Generators: ^{68}Ge, ^{82}Sr, ^{90}Sr and ^{188}W", IAEA Vienna 2010, STI/PUB/1436

Rösch, F., Qaim, S. M., and Stöcklin, G., (1993) "Nuclear data relevant to the production of the positron emitting radioisotope ^{86}Y via ^{86}Sr(p,n) and ^{nat}Rb(^{3}He,xn)-processes", Radiochim. Acta **61**:1

Rösch, F., Zhernosekov, K., Filosofov, D., Jahn, M., Jennewein, M., Baum R. and Bihl, H., (2006) "Processing of ^{68}Ge/^{68}Ga generator eluates for labeling of biomolecules via bifunctional chelators" J. Nucl. Med. **47,** 162P

Sabet, M., Rowshanfarzad, P., Jalilian, A. R., Ensaf, M. R. and Rajamand, A. A., (2006) "Production and quality control of ^{66}Ga radionuclide", Nukleonika **51**:147-154

Sadeghi, M. and Mokhtari, L., (2010) "Rapid separation of ^{67,68}Ga from ^{68}Zn target using precipitation technique", J. Radioanal. Nucl. Chem. **284**:471–473

Sadeghi, M., Kakavand, T., Rajabifar, S., Mokhtari, L. and Nezhad, A. R., (2009) "Cyclotron production of ^{68}Ga via proton induced reaction on ^{68}Zn target", Nukleonika **54**:25.

Sahoo, S. K., (1991) "Reversed phase extraction chromatographic separation of germanium with Aliquat 336S from citric acid", Bull Chem. Soc. Jpn. **64**:2484.

Schönfeld, E., Schötzig, U., Günther, E. and Schrader, H., (1994) "Standardization and decay data of ^{68}Ge/^{68}Ga", Appl. Radiat. Isot. **45**:955.

Schumacher, J. and Maier-Borst, W., (1981) "A new ^{68}Ge/^{68}Ga radioisotope generator system for production of ^{68}Ga in dilute HCl", Int. J. Appl. Radiat. Isot. **32**:31.

Shanthly, N. and Thakur, M. L., (2006) "Application of Radiotracers in Chemical, Environmental and Biological Science", S. Lahiri, D. Nayak and A. Mukhopadhyay (Eds.), vol. 1, Saha Institute of Nuclear Physics, Kolkata, p. 23.

Spahn, I., Steyn, G. F., Kandil, S. A., Coenen H. H. and Qaim, S. M., (2007b) "New data for the production of ^{73}As, ^{88}Y and ^{153}Sm: Important radionuclides for environmental and medical applications", International Conference on Nuclear Data for Science and Technology, DOI:10.1051/ndata:07351, p. 1363, Nice, France, 22 -27 April, 2007.

Spahn, I., Steyn, G. F., Notier, F. M., Coenen, H. H., Qaim, S. M., (2007a) "Excitation functions of ^{nat}Ge(p,xn)^{71,72,73,74}As reactions up to 100 MeV with a focus on the production of ^{72}As for medical and ^{73}As for environmental studies", Appl. Radiat. Isot. **65**:1057.

Spahn, I., Steyn, G. F., Vermeulen, C., Kovács, Z., Szelecsenyi, F., Coenen H. H. and Qaim, S. M., (2009) "New cross measurements for production of the positron emitters ^{75}Br and ^{76}Br via intermediate energy proton induced reactions", Radiochim. Acta **97**:535.

Spahn, I., Steyn, G. F., Vermeulen, C., Kovács, Z., Szelecsényi, F., Shehata, M. M., Spellerberg, S., Scholten, B., Coenen, H. H., and Qaim, S. M., (2010) "New cross section measurements for production of the Auger electron emitters ^{77}Br and ^{80m}Br", Radiochim Acta **98**:749.

Suzuki, N., Satoh, K., Shoji H. and Imura, H., (1986) "Liquid-Liquid extraction behaviour of arsenic(III), arsenic(V), methylarsonate and dimethylarsine in various systems", Anal. Chim. Acta **185**:239.

Szelécsényi, F., Boothe, T. E., Takács, S., Tárkányi, F. and Tavano, E., (1998) "Evaluated cross section and thick target yield data bases of Zn+p processes for practical applications", Appl. Radiat. Isot. **49**:1005.

Szelécsényi, F., Kovács, Z., van der Walt, T. N., Steyn, G. F., Suzuki, K. and Okada, K., (2003) "Investigation of the $^{nat}Zn(p,x)^{62}Zn$ nuclear process up to 70 MeV: A new $^{62}Zn/^{62}Cu$ generator", Appl. Radiat. Isot. **58**:377.

Takács, S. Tárkányi, F., Sonck, M. and Hermanne, A., (2002) "Investigation of the $^{nat}Mo(p,x)^{96mg}Tc$ nuclear reaction to monitor proton beams: New measurements and consequences on the earlier reported data", Nucl. Instr. Meth. Phys. Res. **B198**:183.

Tanaka, K. and Takagi, N., (1969) "Extraction and spectrophotometric determination of tin, arsenic and germanium as their iodides", Anal. Chim. Acta **48**:357.

Tárkányi, F., Ditroi, F., Csikai, J., Takács, S., Uddin, M. S., Hagiwara, M., Baba, M., Shubin, Yu. N. and Dityuk, A. I., (2005) "Activation cross-sections of long-lived products of proton induced nuclear reactions on zinc", Appl. Radiat. Isot. **62**:73.

Tárkányi, F., Kovács Z. and Qaim, S. M., (1993) "Excitation functions of proton induced nuclear reactions on highly enriched ^{78}Kr: Relevance to the production of ^{75}Br and ^{77}Br at a small cyclotron", Appl. Radiat. Isot. **44**:1105.

Tárkányi, F., Szelecsenyi, F. and Kovács, Z., (1990) "Excitation functions of proton induced nuclear reactions on enriched ^{66}Zn, ^{67}Zn and ^{68}Zn", Radiochim. Acta **50**:19.

Tolmachev, V., Lövqvist, A., Einarsson, L., Schultz, J. and Lundqvist, H., (1998) "Production of ^{76}Br by a low-energy cyclotron", Appl. Radiat. Isot. **49**:1537.

Tolmachev, V., Lundqvist, H., (2001) "Separation of arsenic from germanium oxide targets by dry distillation", J. Radioanal. Nucl. Chem. **247**:61.

Tombkins, E. R. and Mayer, S. W., (1947) "Ion exchange as a separation method. III Equilibrium studies of the reactions of rare earth complexes with synthetic ion exchange resin", J. Am. Chem. Soc. **69**:2859.

Uddin, M. S., Khandaker, M. U., Kim, K. S., Lee, Y. S. and Kim, G. N., (2007) " Excitation functions of the proton induced nuclear reactions on ^{nat}Zn up to 40 MeV", Nucl. Instr. Meth. Phys. Res. B **258**:313.

Vaalburg, W., Paans, A. M. J., Terpstra, J. W., Wiegman, T., Dekens, K., Rijskamp A. and Woldring, M. G., (1985) "Fast recovery by dry distillation of ^{75}Br induced in reusable metal selenide targets via $^{76}Se(p,2n)^{75}Br$ reaction", Int. J. Appl. Radiat. Isot. **36**:961.

Velikyan, I., Beyer, G. J., Langstörm, B. (2004), "Microwave-supported preparation of ^{68}Ga bioconjugates with high specific radioactivity", Biconjugate Chem. 15:554.

Vibhute, C. P. and Khopkar, S. M., (1986a) "Solvent extraction separation of gallium, indium, and thallium with high relative molecular mass amine from citrate solutions", Analyst **111**:435.

Vibhute, C. P. and Khopkar, S. M., (1986b) "Solvent extraction separation of germanium with Aliquat 336S from citric acid solution", Bull Chem. Soc. Jpn. **59**:3229.

Wachsmuth, M., Eichler, B., Tobler, L., Jost, D.T., Gäggeler H. W. and Ammann, M., (2000) "On-line phase separation of short-lived bromine nuclides from precursor selenium" Radiochim. Acta **88**:873.

Wachter, J. A., Miranda, P. A., Cancino, S. A., Morales J. R. and Dinator, M. I., (2008) "Production yields of $^{nat}Zn(p,x)^{67}Ga$ reaction in the energy range of 1.6 to 2.5 MeV", J. Phys.: conference series **134**:12.

Wakui, Y., Ebina, T., Matsunaga, H. and Suzuki, T. M., (2002) "Solvent extraction of arsenic(V) with dispersed ultrafine magnetite particles", Anal. Sci. **18**:793.

Ward, T. E., Swindle, D. L., Wright R. J. and Kuroda, P. K., (1970) "Radiochemical procedure for arsenic and germanium", Radiochim. Acta, **14**:70.

Waters, S. L., Nunn, A. D. and Thakur, M. L., (1973) "Cross-section measurements for the $^{75}As(\alpha,2n)^{77}Br$ reaction", J. Inorg. Nucl. Chem. **35**:3411.

Weinreich, R., Schult O. and Stöcklin, G., (1974) "Production of ^{123}I via the $^{127}I(d,6n)^{123}Xe(\beta^{+},EC)^{123}I$ process", Int. J. Appl. Radiat. Isot. **25**:535.

Williamson, C: F., Boujot, J. P. and Picard, J., (1966) "Tables of Range and Stopping Power of Chemical Elements for Charge Particles of Energy 0.5 to 500 MeV", Report CEA-R 3042. p.1

Zalutsky, M. R., (2003) "Radionuclide therapy", Handbook of Nuclear Chemistry, Vol.**4**, (F. Rösch, Editor) 315-342, Kluwer Academic Publishers, Dordrecht, The Netherlands.

Acknowledgements

The research work presented in this thesis has been performed in the Institut für Neurowissenschaft und Medizin, INM-5, Nuklearchemie; Forschungszentrum Jülich GmbH, Germany, under the general guidance of Prof. Dr. H. H. Coenen, the director of the Instiute. I would like to express my gratitude to him for his meaningful interest in this work, for encouragement and for providing excellent working conditions.

My warm thanks are due to Prof. Dr. Dr. h.c. mult. S. M. Qaim for suggesting the interesting topic of this thesis, for supervising this work and for sharing his wide knowledge and experience during my whole stay in Jülich.

I also wish to show my gratitude to all the other colleagues in the laboratory, especially Dr. B. Scholten and Dr. I. Sphan for their co-operation, encouragement, help in experiments and technical discussions. Mr. S. Spellerberg I thank for the co-operation in preparing samples and irradiations.

Furthermore, I thank the operators of COSY and Baby Cyclotron for carrying out numerous irradiations, which were the basis of this experimental work.

I am indebted to my Country (Egypt) for granting me scholarship and financial support for the whole period of study in Germany. In addition, I am grateful to the Accelerators and Ion Sources Department, Nuclear Reaserch Center, Atomic Energy Authority, Cairo, Egypt for granting me leave of absence to complete my PhD research work in Germany.

Finally yet importantly, I would like to thank all my family members and colleagues for their moral support.

Jülich, May 2011 Mohamed M. Shehata

Ich versichere, dass ich die von mir vorgelegte Dissertation selbständig angefertigt, die benutzten Quellen und Hilfsmittel vollständig angegeben und die Stellen der Arbeit- einschließlich Tabellen, Karten und Abbildungen-, die anderen Werken im Wortlaut oder dem Sinn nach entnommen sind, in jedem Einzelfall als Entlehnung kenntlich gemacht habe, dass diese Disseration noch keiner anderen Fakultät oder Universität zur Prüfung vorgelegen hat; dass sie abgesehen von unten angegeben Teilpublikationen noch nicht veröffentlicht worden ist sowie, dass ich eine solche Veröffentlichung vor Abschluss des Promotionsverfahrens nicht vornehmen werde. Die Bestimmungen der Promotionsordnung sind mir bekannt. Die von mir vorgelegte Dissertation ist von Prof. Dr. Dr. h.c. mult. Syed M. Qaim betreut worden.

Jülich, im Mai 2011

Teilveröffentlichungen

- I. Spahn, G. F. Steyn, C. Vermeulen, Z. Kovács, F. Szelecsényi, **M. M. Shehata**, S. Spellerberg, B. Scholten, H. H. Coenen and S. M. Qaim, (2010) "New cross section measurements for production of the Auger electron emitters ^{77}Br and ^{80m}Br", Radiochim Acta **98**:749.

- **M. M. Shehata**, B. Scholten, I. Spahn, H. H. Coenen and S. M. Qaim, (2011) "Radiochemical separation of radioarsenic in the production of ^{71}As and ^{72}As ", J. Radioanal. Nucl. Chem. **287**:435.

- **M. M. Shehata**, B. Scholten, I. Spahn, S. M. Qaim and H. H. Coenen, (2011) "Radiochemical studies relevant to the separation of ^{68}Ga and ^{68}Ge", J. Radioanal. Nucl. Chem. *In press*.